

PHOSPHOGENESIS IN COASTAL UPWELLING SYSTEMS

—

BACTERIALLY-INDUCED PHOSPHORITE FORMATION

Dissertation

zur Erlangung des Doktorgrades in den Naturwissenschaften

– Dr. rer. nat. –

vorgelegt im

Fachbereich Geowissenschaften der Universität Bremen

von

Dipl. Geowissenschaftlerin Esther Arning

Bremen, September 2008

Gutachter: Prof. Dr. Jörn Peckmann

Prof. Dr. Heide Schulz-Vogt

Tag des Promotionskolloquiums: 8.12.2008

Prüfer: PD Dr. Matthias Zabel

Prof. Dr. Wolfgang Bach

*Gib jedem Tag die Chance,
der schönste deines Lebens zu werden.*

Mark Twain

PREFACE

The work presented in this thesis was funded by the Deutsche Forschungsgemeinschaft in the research area “Biogeochemical processes” as part of the project “Bacterial control of phosphorite formation in coastal upwelling systems” of the Excellence Cluster MARUM at the University of Bremen. This work was prepared from September 2005 until September 2008 in the Geobiology Group, University of Bremen and has been supervised by Prof. Dr. Jörn Peckmann.

With this thesis, it is my goal to demonstrate the importance of microorganisms in phosphorite formation in coastal upwelling systems. To elucidate this, recent phosphogenic sediments from upwelling areas (paper 1, published in *Geomicrobiology Journal*) as well as authigenic phosphorite crusts from the upwelling area off Peru (papers 2 and 3, both submitted to international journals) were studied. In addition, the thesis comprises one manuscript (paper 4, draft, not yet submitted), which examines microbial processes in the formation of dolomites from the Miocene Monterey Formation, a prominent phosphorite deposit in the Miocene. The scientific framework of the manuscripts and a general introduction into the subject of phosphorite formation is given in chapter I. In the “Concluding remarks and perspectives” the main results are summarized, remaining open questions are addressed, and perspectives for potential future work are proposed. References to the literature for chapter I and for the “Concluding remarks and perspectives” are given at the end of this thesis.

TABLE OF CONTENTS

Abstract	II
Kurzfassung	V
CHAPTER I: Scientific Background of the Thesis	1
1. Introduction	2
1.1 Motivation and main objectives	2
1.2 General aspects of phosphorite formation	3
1.3 The phosphorus cycle in the ocean	6
1.4 The sediment-water interface as important site of phosphorite formation	9
1.5 Coastal upwelling systems – aspects for phosphorite formation	11
2. Tools to decipher microbial involvement in phosphorite formation	15
CHAPTER II: Case Studies – Phosphogenesis in Upwelling Systems and the Importance of Microorganisms	17
Paper 1: Lipid biomarker patterns of phosphogenic sediments from upwelling regions	18
Paper 2: Genesis of phosphorite crusts off Peru	50
Paper 3: Formation of phosphatic laminites off Peru	84
Paper 4: Methanogenic archaea involved in dolomite formation in phosphorite dominated strata	109
Concluding Remarks and Perspectives	126
References	130
Danksagung	136

ABSTRACT

The burial of phosphorus and the formation of phosphorites (phosphogenesis) in marine sediments represent an important sink in the global phosphorus cycle. Numerous basin-scale phosphorite deposits were formed in the geological past, for example the Miocene Monterey Formation in California. Phosphogenesis is not only an ancient phenomenon, however, it has been observed in recent suboxic to anoxic marine sediments of ocean upwelling regions, for example off the coast of Namibia, Chile, and Peru where it occurs near the sediment-water interface.

Phosphorites and their distribution on the ocean floor, in particular close to the sediment-water interface, have been frequently studied. So far, neither the phosphate source of massive phosphorite deposits nor the enrichment mechanisms resulting in supersaturation of pore water with respect to carbonate fluorapatite have been fully recognized. In particular, the importance and function of microorganisms in phosphogenesis has been widely not understood. However, phosphate enrichment in pore water and the subsequent precipitation of carbonate fluorapatite is the initial step in phosphorite formation. In order to obtain insights into the involvement of microorganisms in recent and ancient phosphorite formation of upwelling areas, various biogeochemical and petrographic analyses were performed in this thesis on (1) Modern phosphogenic sediments from the coastal upwelling regions off Namibia, Peru, and Chile and on (2) Miocene to Pleistocene phosphorite crusts from the shelf off Peru (9°40'S to 13°30'S). In addition, dolomites of the Miocene Monterey Formation were analyzed; however this study is only marginally linked with phosphorite formation.

A powerful tool to identify an involvement of bacteria is the analysis of molecular biomarkers. This thesis represents the first molecular biomarker studies on phosphorites. The additional measurements of stable sulfur isotopes of different sulfur species provide insights into the sulfur cycle during phosphogenesis and reveal the involvement of bacterial processes. Furthermore, geochemical analyses of trace elements and rare earth elements help to characterize the geochemical environment during phosphorite formation. Petrographic studies on thin sections of the phosphorite crusts support the biogeochemical analyses.

In most sediments of upwelling areas, the degradation of organic matter via sulfate reduction is the predominant anaerobic oxidation process. In addition, a striking feature of the major modern upwelling regions is the abundance of large colorless, nitrate-storing sulfide-oxidizing bacteria on the seafloor. Sediments of upwelling regions off Namibia, Peru, and Chile contain dense populations of large sulfide-oxidizing bacteria, *Thiomargarita*,

Beggiatoa, and *Thioploca*, which are known to be able to liberate phosphate during metabolic processes. In these sediments, increased contents of monounsaturated C₁₆ and C₁₈ fatty acids were measured especially when a high density of sulfide oxidizers in the sediments was observed. Monounsaturated C₁₆ and C₁₈ fatty acids are known to be produced by the sulfide oxidizers but are not specific enough to be used unequivocally to indicate these bacteria. The distribution of molecular biomarkers attributed to sulfate-reducing bacteria (10MeC_{16:0} fatty acid, *ai*-C_{15:0} fatty acid, and mono-*O*-alkyl glycerol ethers) reveals that the distribution of sulfate-reducing bacteria reflects that of various large sulfide-oxidizing bacteria, known from cell counts. This association indicates a close association between these bacteria.

Furthermore, the distribution of mono-*O*-alkyl glycerol ethers, 10MeC_{16:0} fatty acid, and *ai*-C_{15:0} fatty acid shows that sulfate-reducing bacteria are critical for organic matter remineralization in upwelling sediments populated by large sulfide-oxidizing bacteria. A connection between sulfate-reducing bacteria and phosphate enrichment in the pore water is suggested by the correlation of high contents of the corresponding biomarkers in the sediments with high phosphate concentrations in the pore water. This phosphate enrichment in pore waters due to high mineralization rates favors precipitation of phosphate minerals.

The information obtained from the analyses of modern phosphogenic sediments provides the basis to study authigenic phosphorite crusts from the shelf off Peru (9°40'S to 13°30'S). The phosphorite crusts consist of a phosphooid facies and a later phosphatic laminite. The Peruvian phosphorites have been formed episodically over an extended period of time lasting from Middle Miocene to Pleistocene. In the Middle Miocene, phosphooids formed, while the authigenic laminite precipitated during the Pleistocene. Calcium isotopes, rare earth element patterns, and redox-sensitive element distribution indicate phosphogenesis in suboxic sediments in the vicinity of the sediment-water interface. High contents of chalcophilic elements, as well as abundant sulfides in phosphooid layers and laminite point to sulfate reduction and episodic anoxia in the course of phosphogenesis. Erosional surfaces of the ooids and positive Europium anomalies in the phosphooid facies indicate their formation on the inner shelf as a result of episodic suspension and shifting redox conditions. During episodic high-energy conditions phosphooids were later transported to the outer shelf, where subsequent authigenic laminite formation was favored under lower energy conditions.

The authigenic phosphatic laminite consists of carbonate fluorapatite layers, which contain abundant sulfide minerals including pyrite (FeS₂) and sphalerite (ZnS). Molecular

biomarkers are excellently preserved as molecular fossils in the laminite. Molecular biomarkers of sulfate-reducing bacteria such as short chain branched fatty acids, mono-*O*-alkyl glycerol ethers, and di-*O*-alkyl glycerol ethers are not only highly concentrated in the laminite, but also tightly bound to the mineral lattice. Thus, the molecular biomarker pattern, similar to the ones identified in recent phosphogenic sediments, reveals the importance of sulfate-reducing bacteria in the formation of authigenic phosphatic laminites in the upwelling region off Peru. The sulfide minerals pyrite and sphalerite, which can be produced due to the activity of sulfate-reducing bacteria were formed simultaneously with carbonate fluorapatite. The low $\delta^{34}\text{S}$ values of pyrite (average: -28.8‰) confirm a bacterial origin. $\delta^{34}\text{S}$ values of carbonate fluorapatite-bound sulfate are significantly lower than $\delta^{34}\text{S}$ values of seawater sulfate, suggesting the bacterial reoxidation of sulfide by large sulfide-oxidizing bacteria. This supports the scenario that the combined activities of closely associated sulfide-oxidizing bacteria and sulfate-reducing bacteria have the potential to drive phosphogenesis in marine sediments below high productivity zones. Model calculations indicate that organic matter degradation by sulfate-reducing bacteria is able to liberate sufficient phosphate to form the Peruvian phosphatic laminites.

Unfortunately, molecular biomarkers in pristine phosphorites of the Miocene Monterey Formation are not well preserved. However, dolomites, frequently present in the Monterey Formation, have a good preservation potential for molecular biomarkers. Molecular biomarker studies of the Monterey dolomites reveal the presence of *sn*-2-hydroxyarchaeol with relatively high $\delta^{13}\text{C}$ values (-25‰) in dolomites enriched in ^{13}C . The detection of relatively heavy *sn*-2-hydroxyarchaeol in the dolomites is the first molecular proof that methanogenic archaea are involved in dolomite formation.

The results presented in this thesis give rise to a new and better understanding of biological processes that are important for phosphogenesis in upwelling areas. The results show the importance of sulfate-reducing and sulfide-oxidizing bacteria in phosphorite formation processes in upwelling areas.

KURZFASSUNG

Die Einlagerung von Phosphor und die Bildung von Phosphoriten (Phosphogenese) in marinen Sedimenten stellt eine wichtige Senke im globalen Phosphor-Kreislauf dar. Im Verlauf der Erdgeschichte haben sich viele beckenweite Phosphoritablagerungen, zum Beispiel die miozäne Monterey Formation, gebildet. Phosphogenese hat jedoch nicht nur in der geologischen Vergangenheit statt gefunden, sondern wird auch in rezenten suboxischen bis anoxischen marinen Sedimenten der ozeanischen Auftriebsgebiete, zum Beispiel vor der Küste von Namibia, Peru und Chile, beobachtet. Hier findet sie dicht an der Sediment-Wasser-Grenze statt.

Phosphorite und ihre Verteilung am Meeresboden, insbesondere dicht an der Sediment-Wasser-Grenze, wurden schon häufig untersucht. Die Herkunft des Phosphats, welches zur Bildung der massigen Phosphoritablagerungen benötigt wird, ist bisher jedoch noch nicht abschließend geklärt. Auch die Mechanismen, die zu einer Anreicherung von Phosphat und zu einer Übersättigung des Porenwassers in Hinsicht auf Carbonatfluorapatit führen und folglich dessen Fällung auslösen, sind nicht vollständig verstanden. Insbesondere die Bedeutung und die Funktion von Mikroorganismen bei der Phosphogenese sind noch unklar. Um einen Einblick in die Beteiligung von Bakterien an der Bildung sowohl von rezenten als auch von fossilen Phosphoriten zu bekommen, wurden in dieser Arbeit verschiedene biogeochemische und petrographische Untersuchungen an (1) rezenten phosphogenen Sedimenten aus den Auftriebsgebieten vor Namibia, Peru und Chile und an (2) miozänen bis pleistozänen Phosphoritkrusten von dem Schelf vor Peru ($9^{\circ}40'S$ bis $13^{\circ}30'S$) durchgeführt. Zusätzlich wurden Dolomite der miozänen Monterey Formation untersucht, auch wenn die Dolomite nicht unmittelbar mit der Bildung von Phosphoriten zusammenhängen.

Ein wichtiges Hilfsmittel zur Erforschung einer möglichen Beteiligung von Bakterien bei der Phosphoritbildung ist die Analyse molekularer Biomarker. Die vorliegende Arbeit zeigt die ersten Studien dieser Art an Phosphoriten. Die Untersuchungen werden durch Messungen stabiler Schwefelisotope von verschiedenen Schwefelspezies unterstützt, welche Einblicke in den Schwefelkreislauf während der Phosphogenese ermöglichen und daran beteiligte bakterielle Prozesse aufdecken können. Des Weiteren wird das geochemische Milieu, das während der Phosphoritbildung vorherrschte, durch Analysen von Spuren- und Seltenerdenelementen rekonstruiert. Die mit Hilfe von Dünnschliffen durchgeführte petrographische Beschreibung der Phosphoritkrusten unterstützt die biogeochemischen Analysen.

In den meisten Sedimenten in Auftriebsgebieten ist Sulfatreduktion der dominierende anaerobe Oxidationssprozess bei der Zersetzung der organischen Substanz. Ein auffälliges Merkmal der bedeutenden rezenten Auftriebsgebiete ist das immense Vorkommen großer, farbloser, nitratspeichernder, sulfidoxidierender Schwefelbakterien am Meeresboden. Die Sedimente der Auftriebsgebiete vor Namibia, Peru und Chile beherbergen große Populationen der Schwefelbakterien *Thiomargarita*, *Beggiatoa* und *Thioploca*, die dafür bekannt sind, Phosphat freisetzen zu können. In diesen Sedimenten wurden besonders dann hohe Gehalte von einfach ungesättigten C₁₆ und C₁₈ Fettsäuren gefunden, wenn auch eine hohe Dichte bei den Schwefelbakterien beobachtet wurde. Einfach ungesättigte C₁₆ und C₁₈ Fettsäuren werden von den großen Schwefelbakterien produziert, sind jedoch zu unspezifisch um als eindeutiger Beweis für das Vorhandensein dieser Bakterien verwendet werden zu können. Die Verteilung von molekularen Biomarkern, die sulfatreduzierenden Bakterien zugeordnet werden (10MeC_{16:0} Fettsäure, *ai*-C_{15:0} Fettsäure und mono-*O*-alkyl Glycerolether), zeigt, dass die Verteilung der sulfatreduzierenden Bakterien die durch Zellauszählungen bestimmte Verteilung der großen Schwefelbakterien widerspiegelt. Demnach besteht eine enge Verbindung zwischen diesen Bakterien.

Die Verteilung von mono-*O*-alkyl Glycerolether, 10MeC_{16:0} Fettsäure und *ai*-C_{15:0} Fettsäure zeigt außerdem, dass sulfatreduzierende Bakterien für die Remineralisierung von organischer Substanz in den von großen Schwefelbakterien besiedelten Sedimenten der Auftriebsgebiete entscheidend sind. Die Korrelation von hohen Gehalten der entsprechenden Biomarker in den Sedimenten mit hohen Phosphatkonzentrationen im Porenwasser zeigt eine Verbindung zwischen sulfatreduzierenden Bakterien und der Anreicherung von Phosphat im Porenwasser an. Diese Anreicherung von Phosphat im Porenwasser auf Grund hoher Remineralisierungsraten begünstigt die Ausfällung von Phosphatmineralen.

Die Informationen, die aus den Analysen der rezenten Sedimente gewonnen wurden, stellen die Grundlage zur Untersuchung authigener Phosphoritkrusten von dem Schelf vor Peru (9°40'S bis 13°30'S) dar. Die Phosphoritkrusten bestehen aus einer Phosphooidfazies und einem später gebildeten phosphatischen Laminit. Die peruanischen Phosphorite haben sich episodisch über einen längeren Zeitraum vom mittleren Miozän bis hin zum Pleistozän gebildet. Während sich die Phosphooidfazies im mittleren Miozän gebildet haben, ist der jüngere phosphatische Laminit während des Pleistozäns entstanden. Calciumisotope, das Verteilungsmuster der Seltenerdenelemente und die Verteilung von redox-sensitiven Elementen zeigen an, dass die Phosphogenese in suboxischen Sedimenten nahe der Sediment-Wasser-Grenze stattfindet. Hohe Gehalte von chalcophilen Elementen und eine Anreicherung

von Sulfidmineralen in den Lagen der Phosphooide sowie des Laminits weisen auf Sulfatreduktion und episodisch auftretende Anoxia während der Phosphoritbildung hin. Erosionsstrukturen an den Oberflächen der Ooide und positive Europiumanomalien in der Phosphooidfazies zeigen eine Bildung der Phosphooide auf dem inneren Schelf, die episodische Suspension der Ooide und sich ändernde Redoxbedingungen an. Die Phosphooide wurden dann während episodisch auftretender hochenergetischer Bedingungen auf den äußeren Schelf transportiert. Hier wurde unter ruhigeren Ablagerungsbedingungen anschließend die Bildung des authigenen Laminits begünstigt.

Der authigene phosphatische Laminite ist aus Lagen von Carbonatfluorapatit aufgebaut, die viele Sulfidminerale, darunter Pyrit (FeS_2) und Sphalerit (ZnS), enthalten. Molekulare Biomarker werden in dem Laminite außerordentlich gut als molekulare Fossilien erhalten. Die Biomarker sulfatreduzierender Bakterien, wie kurzkettige, verzweigte Fettsäuren, mono-*O*-alkyl Glycerolether und di-*O*-alkyl Glycerolether, sind in dem Laminite nicht nur hoch konzentriert, sondern auch an das Mineralgitter gebunden. Das Muster der Biomarker, welches den Mustern der rezenten phosphogenen Sedimente ähnelt, beweist somit eindeutig, dass sulfatreduzierende Bakterien bei der Bildung des authigenen phosphatischen Laminits im Auftriebsgebiet vor Peru eine entscheidende Rolle spielen. Die Sulfidminerale Pyrit und Sphalerit, bekannt dafür durch die Aktivität sulfatreduzierender Bakterien zu entstehen, wurden zeitgleich mit dem Carbonatfluorapatit gebildet. Die niedrigen $\delta^{34}\text{S}$ Werte des Pyrit (um -28.8‰) bestätigen dessen bakterielle Entstehung. $\delta^{34}\text{S}$ Werte von Sulfat, das an Carbonatfluorapatit gebunden ist, sind deutlich geringer als die Werte von dem Sulfat des Meerwassers und weisen auf eine bakterielle Reoxidation von Sulfid durch die großen Schwefelbakterien hin. Diese Ergebnisse bestätigen das Szenario, dass sulfidoxidierende Bakterien und sulfatreduzierende Bakterien eng miteinander assoziiert sind, und dass diese Bakterien durch die Verknüpfung ihrer metabolischen Aktivitäten Phosphogenese in marinen Sedimenten von Hochproduktionsgebieten verursachen können. Modellberechnungen ergeben, dass der Abbau organischer Substanz durch sulfatreduzierende Bakterien ausreichend Phosphat für die Bildung der peruanischen phosphatischen Laminite freisetzen kann.

Pristine Phosphorite der miozänen Monterey Formation sind für die Erhaltung molekularer Biomarker leider ungeeignet. Dolomite hingegen, die in der Monterey Formation häufig sind, weisen ein gutes Erhaltungspotential für molekulare Biomarker auf. Analysen der Biomarker in den Dolomiten der Monterey Formation zeigen, dass *sn*-2-Hydroxyarchaeol mit relativ hohen $\delta^{13}\text{C}$ Werten (-25‰) in ^{13}C angereicherten Dolomiten vorhanden ist. *sn*-2-

Hydroxyarchaeol wird als Biomarker für methanogene Archaeen angesehen. Der Nachweis von relativ schwerem *sn*-2-Hydroxyarchaeol in den Dolomiten ist der erste molekulare Beweis für eine Beteiligung methanogener Archaeen an der Dolomitbildung.

Die Ergebnisse, die in dieser Arbeit vorgestellt werden, führen zu einem neuen und besseren Verständnis der biologischen Prozesse, die bei der Phosphogenese von Bedeutung sind. Sie zeigen, dass sulfatreduzierende und sulfidoxidierende Bakterien bei der Phosphoritbildung in Auftriebsgebieten eine entscheidende Rolle spielen.

CHAPTER I:

SCIENTIFIC BACKGROUND OF THE THESIS

1. INTRODUCTION

1.1 Motivation and main objectives

Phosphorus (in the form of phosphate) is an essential nutrient and energy carrier on many different levels of life. It is believed that phosphate, rather than nitrogen, is the major limiting agent of biological productivity not just in modern ocean environments, but also over geological time scales (Redfield, 1958). By controlling productivity, phosphate interacts with other elements, like carbon, oxygen, sulfur, nitrogen, and iron, which are vital for marine microorganisms. Changes in the oceanic phosphorus will thus have an essential effect on cycles of these elements. Therefore, investigations of the phosphorus cycle, especially of the processes, which remove phosphate from the sea water are important to understand the marine biological cycles.

Many aspects of the phosphorus cycle are still poorly understood. An important sink in the global phosphorus budget is provided by the burial of phosphorus and, especially, by the formation of authigenic phosphorites (phosphogenesis) in marine sediments. Although phosphorites and their distribution on the ocean floor, especially close to the sediment-water interface, have been frequently studied (see Föllmi, 1996 as a review and references therein), the enrichment mechanisms resulting in supersaturation of pore water with respect to carbonate fluorapatite (CFA) and its subsequent precipitation have been poorly understood. In particular, the microbiological and biogeochemical processes responsible for authigenic phosphorite formation have not been fully recognized.

Accordingly, the main goals of this thesis are to

- 1) reveal the importance/involvement of microorganisms in phosphogenesis in upwelling areas
- 2) find signatures typifying microbial phosphorite formation
- 3) define environmental and geochemical conditions of phosphogenesis in upwelling areas
- 4) determine the origin of phosphate in massive phosphorite deposits

In order to elucidate the involvement of microorganisms in phosphogenesis, the environmental conditions of phosphorite formation, and the origin of phosphate in massive phosphorite deposits, I carried out various biogeochemical and petrographic analyses on (1) Modern phosphogenic sediments from the coastal upwelling regions off Namibia, Peru, and Chile, and on (2) Miocene to Pleistocene phosphorite crusts from the shelf off Peru (9°40'S to

13°30'S). All of the investigated areas are prominent for modern and/or ancient phosphorite formation. It was the idea to start in modern phosphogenic sediments to identify diagnostic signatures for microbially induced phosphogenesis (paper 1). Geochemical and environmental conditions of these sediments are well known or can be determined very well. The information obtained from the analyses of modern phosphogenic sediments provides the basis to study authigenic phosphorite formation that occurred in the geological past. Thus, in a second step, the microbial involvement in authigenic phosphorite crust was traced on Pleistocene authigenic phosphorites from off Peru (paper 3). Before, it was necessary to decipher the age and growth history of the Peruvian phosphorite crusts, as well as their geochemical environment of formation (paper 2). Only with this background information it is possible to identify primary microbial signatures with certainty. The results of these studies reveal new insights into the mechanism and the environment of phosphorite formation in association with upwelling, especially concerning the involvement and importance of microorganisms in phosphogenesis.

In the last step, microbial traces in phosphorites of the Monterey Formation, a prominent phosphorite deposit of the Miocene should be found. However, the phosphatic sediments of the Monterey Formation are very soft and porous and inappropriate to preserve microbial signatures. On the other hand, dolomites are frequently present in the Monterey Formation and have a good preservation potential for microbial signatures. Therefore, microbial processes, inducing dolomite formation in the Monterey Formation were investigated (paper 4). Even if this study is only marginally related to the topic of this thesis, it provides important and new insights into microbial processes inducing the formation of authigenic rocks, in this case dolomites.

1.2 General aspects of phosphorite formation

Phosphorites are sediments, which include significant portions of authigenic and biogenic phosphate minerals. Mostly a lower threshold of 18% P_2O_5 is used for their definition (*e.g.* Jarvis *et al.*, 1994). Carbonate fluorapatite (CFA) is suggested to be the thermodynamically stable apatite phase in high carbonate solutions such as sea water (Jahnke, 1984). Therefore, CFA is considered to be the most common phosphate mineral that forms in early diagenetic marine environments and thus is most important in phosphorites (*e.g.* McClellan, 1980; Nathan, 1984; McClellan & van Kauwenbergh, 1990). Its chemical composition is complex,

due to several possible substitutions, but the formula $\text{Ca}_{10-a-b}\text{Na}_a\text{Mg}_b(\text{PO}_4)_{6-x}(\text{CO}_3)_{x-y-z}(\text{CO}_3\cdot\text{F})_y(\text{SO}_4)_z\text{F}_2$ can be seen as a valid approximation (Jarvis *et al.*, 1994).

A rapid (hours to days) precipitation of CFA via an amorphous precursor (either struvite ($\text{NH}_4\text{MgPO}_4\cdot 6\text{H}_2\text{O}$), amorphous calcium phosphate, or octacalcium phosphate ($\text{Ca}_8\text{H}(\text{PO}_4)_6$)) occurs when the pore water is highly supersaturated with respect to CFA (10^{-1} to $2\cdot 10^{-2}$ g l⁻¹ HPO_4^{2-}). At lower levels of supersaturation ($3\cdot 10^{-3}$ to $2\cdot 10^{-2}$ g l⁻¹ HPO_4^{2-}) CFA is precipitated directly, but slowly (months to years), leading to dispersed CFA in sediments outside major upwelling cells. Pore waters of marine sediments show dissolved phosphate concentrations, which are typically higher than those for sea water (approximately $6\cdot 10^{-5}$ g l⁻¹ HPO_4^{2-}). Consequently, supersaturation with respect to CFA is probably the rule (*e.g.* van Cappellen & Berner, 1991). Nevertheless, CFA does not generally precipitate when high phosphate concentrations in the pore water are reached and it also does not precipitate directly from sea water. Direct CFA formation is probably only possible at the sediment-water interface under distinct environmental conditions. Several chemical constituents may favor or inhibit CFA precipitation:

favoring factors

- low levels of interstitial dissolved sulfate (Caraco *et al.*, 1989)
- lowering interstitial pH (van Cappellen & Berner, 1991)
- low alkalinity (Jahnke, 1984; Glenn & Arthur, 1988)

inhibiting factors

- the presence of magnesium (high Mg/Ca ratios) in interstitial water (*e.g.* van Cappellen & Berner, 1991; Jarvis *et al.*, 1994)
- rising alkalinity at greater sediment depth (Jahnke, 1984; Glenn & Arthur, 1988)

Microbiological activity is involved directly or indirectly in most of the chemical changes affecting phosphate content in surface sediments. Relevant for phosphogenesis is also the redox environment. However, suboxic to oxic as well as anoxic environments have been proposed as environments for phosphorite formation. Furthermore, fluctuating redox potentials are also considered to be important (see in Föllmi, 1996 and references therein).

Numerous basin-scale phosphorite deposits were formed in the geological past (Figure 1) and often coincide with the intensification of total phosphorus accumulation in marine

sediments under conditions of intense chemical weathering of rocks on continents and considerable extension of oceanic shelf areas (*e.g.* Trappe, 1998 and references therein).

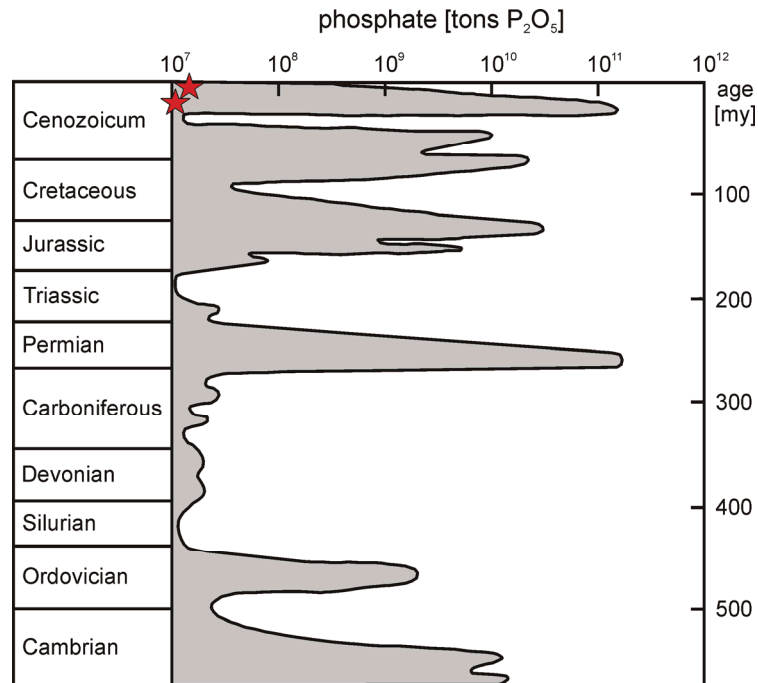


Figure 1 Occurrence of phosphorite deposits through the Phanerozoic. Estimated abundance of phosphate is given on a logarithmic scale in tons P₂O₅ (after Cook & McElhinny, 1979). Red stars indicate the age of phosphorites investigated in this thesis.

Most phosphorus-rich and organic carbon-rich sediments are stratigraphically associated with certain facies in the geological record (*e.g.* Sheldon, 1981; Sandsrom, 1986; Sandsrom, 1990; Föllmi & Garrison, 1991; Glenn *et al.*, 1994; Föllmi, 1996; Föllmi *et al.*, 2005). For instance, the association of phosphorite deposits with strong upwelling systems is very common (Figure 2; Bentor, 1980). All of these areas hold similar sedimentological conditions like a high primary productivity and current dominated sedimentary regimes where sediment reworking processes play a prominent role (Föllmi, 1996). This supports the assumption that biological productivity is predominant in determining regions of intense phosphorite formation. The formation of giant phosphorite deposits would require huge quantities of organic matter, which have been derived from primary producers. However, phosphogenesis is not only found in ancient settings, it is also reported in recent sediments, especially in upwelling regions, as for example off the coast of Namibia, Peru, and Chile (Figure 2).

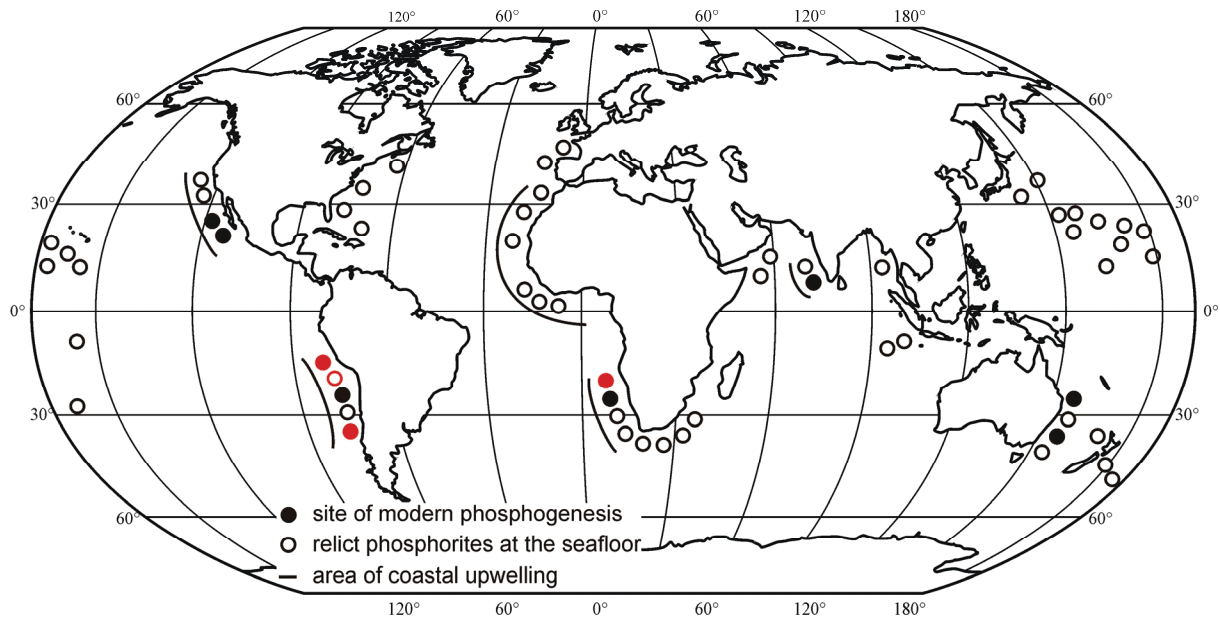


Figure 2 Areas of modern phosphogenesis and relict phosphorites at the sea floor. Areas of coastal upwelling are indicated as well (modified after Baturin, 1982; from Föllmi, 1996). Circles highlighted in red indicate sites explored in this thesis.

The formation of sedimentary phosphate deposits requires two critical conditions: high rates of phosphorus supply to the sea floor, and high retention of phosphate within the uppermost sediment layers. The retention time of dissolved phosphate in the sediment depends on the sediment accumulation rate, irrigation and mixing of the sediment, rate of microbial phosphate uptake, and the precipitation kinetics of phosphates. However, in order to understand the mechanisms, which may be responsible for authigenic phosphorite formation (phosphogenesis) and the still unresolved problems related with phosphorite formation, it is important to have a look at the oceanic phosphorus cycle (section 1.3) and the processes involved in phosphogenesis at the sediment-water interface (section 1.4).

1.3 The phosphorus cycle in the ocean

(Bio-)chemical weathering on continents and subsequent river runoff represents the most important source of bioavailable phosphorus in the form of phosphate into the oceans (Figure 3). In the marine environment, almost all reactive and bioavailable phosphate (organic phosphorus, authigenic phosphorus, loosely sorbed and CaCO_3 -associated phosphorus, and phosphorus associated with iron oxides/hydroxides) from river runoffs and eolian input is incorporated into organic matter of primary producers in the surface zone of the ocean. The

major species of dissolved phosphorus in the marine environment is HPO_4^{2-} . Numbers of estimated phosphorus fluxes and budgets are given in detail in Figure 3.

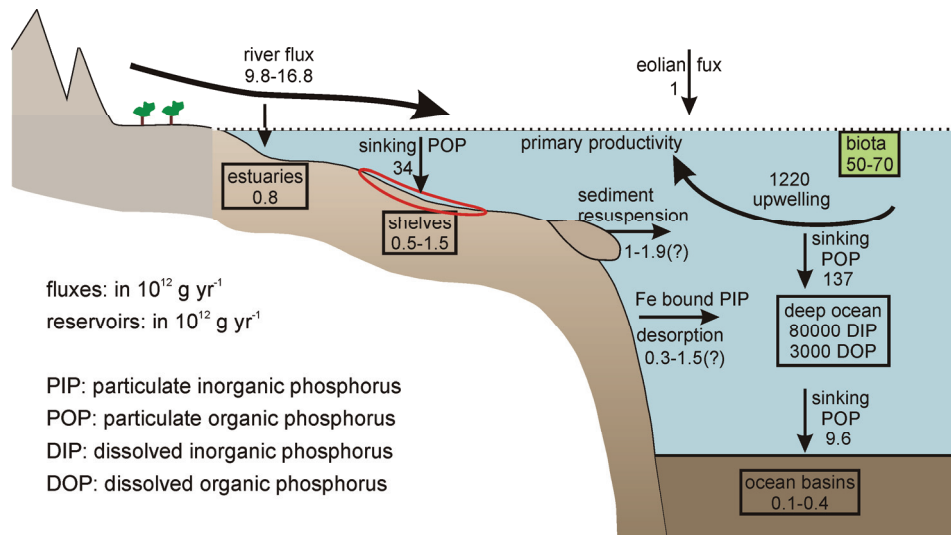


Figure 3 Simplified global, pre-human phosphorus cycle in the ocean, showing the most important fluxes (arrows indicate the direction of the flux) and reservoirs of phosphorus (modified after Compton *et al.*, 2000). Red circle: area of interest addressed in this thesis, detailed processes occurring at this site are outlined in section 1.4 and Figure 5.

Most of the phosphate that was incorporated into the organic matter of primary producers (approximately 95%) is taken up by intermediate and deep water currents and gets reintroduced to the photic zone by upwelling processes, where it is re-utilized by primary producers of the marine ecosystem. Only a small fraction (approximately 5%) is removed from the ocean (Figure 4). Phosphorus from the water column reaches marine sediments in various fractions of inorganic and organic phosphorus. Typically, the phosphorus flux into the sediment is dominated by reactive phosphorus components including ~40% organic phosphorus, ~25% authigenic phosphorus, and ~21% labile phosphorus and/or phosphorus associated with iron oxides/hydroxides. The non-reactive detrital fraction (~13%) is less important (Faul *et al.*, 2005).

As phosphate cannot be used as electron acceptor, there are three major processes that remove phosphate from the water: (1) the biological uptake for the formation of new biomass and as energy carrier (2) the adsorption onto particles or co-precipitation with *in situ*-formed minerals, and (3) the formation of authigenic carbonate fluorapatite (CFA). Therefore, the burial of phosphate and, in particular, the formation of authigenic phosphorites from initially more labile phosphate (*e.g.* organic phosphate) in marine sediments is a major sink for

phosphorus on Earth and removes the phosphate from the nutrient cycle in the water column (e.g. Föllmi, 1996; Compton *et al.*, 2000).

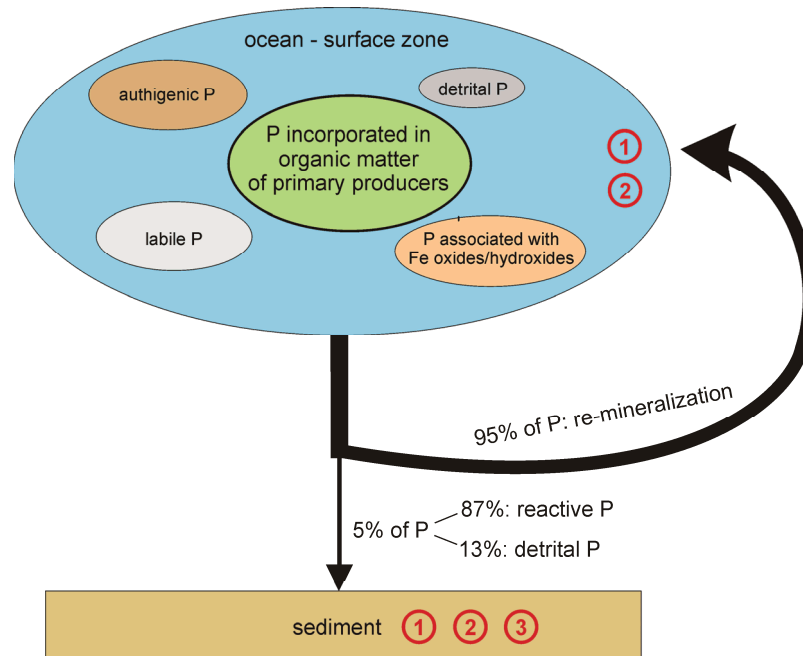


Figure 4 Scheme, illustrating the fate of phosphorus from the surface zone of ocean waters. Numbers in red indicate the processes that remove phosphate from the water (see text). 1: biological uptake, 2: adsorption onto particles, 3: formation of authigenic carbonate fluorapatite.

Numbers for phosphorus sinks and burial budgets differ between different authors and are not yet well known. For example, Ruttenberg (1993) suggests a total phosphorus burial rate of $2.4 \cdot 10^{12}$ to $5.7 \cdot 10^{12}$ g yr⁻¹, which is similar to numbers of Berner & Berner (1996) ($2.9 \cdot 10^{12}$ g yr⁻¹), while the estimate of Filippelli & Delaney (1996) is significantly higher ($6.5 \cdot 10^{12}$ g yr⁻¹). A major cause of uncertainty in estimating the amount of reactive phosphorus burial in marine sediments is the difficulty to distinguish between phosphorus removed from the ocean reservoir in a true sink (e.g. authigenic phosphorites) contrary to phosphorus that bypasses the ocean reservoir but is released into pore water again (e.g. reworked phosphorites; Compton *et al.*, 2000).

1.4 The sediment-water interface as important site of phosphorite formation

In the formation of carbonate fluorapatite (CFA), the first critical step is the transformation of deposited particulate phosphorus into dissolved phosphate. Several processes influence the pore water phosphate concentration in marine sediments close to the sediment-water interface (Figure 5). The major process that liberates phosphate is supposed to be the degradation of phosphate containing organic matter by microbial heterotrophs inhabiting the sediment (Soudry, 2000). Furthermore, benthic microorganism, like microbial mat communities, can have a strong influence on the pore water phosphate concentration by their ability for active uptake and release of phosphate (*e.g.* Gächter *et al.*, 1988; Konhauser *et al.*, 1994; Schulz & Schulz, 2005). Beside microbial processes, the redox dependent desorption and sorption of phosphate associated with iron and manganese oxides/hydroxides also influence the phosphorus cycle in sediments (van Cappellen & Berner, 1988). When sediment gets resuspended, phosphate may be desorbed and released into the water column. A significant portion of phosphate may also diffuse from near surface sediments back into the bottom water (Colman & Holland, 2000).

Dissolved sea water phosphate is an additional source, which may be important in the formation of phosphorites. It can be transferred into the sediments by diffusion, advection, or eddy diffusion (Föllmi & Garrison, 1991). Commonly, phosphate concentrations increase up to several hundred micromolar within centimeters to meters of the sediment-water interface. However, it is still unknown, what percentage of the phosphate in authigenic CFA derives from organic matter degradation or from other sources.

The phosphorus cycle is complex and the involved processes close to the sediment-water interface are not well understood. Uncertainties in the estimations of input and output fluxes between sediment and bottom water are high, as well as in the estimations of amounts of authigenically formed phosphorites. Furthermore, formation mechanisms and phosphate sources of authigenic phosphorites are not known in detail. However, in upwelling regions of the oceans, microorganisms seem to be important in the process of phosphogenesis.

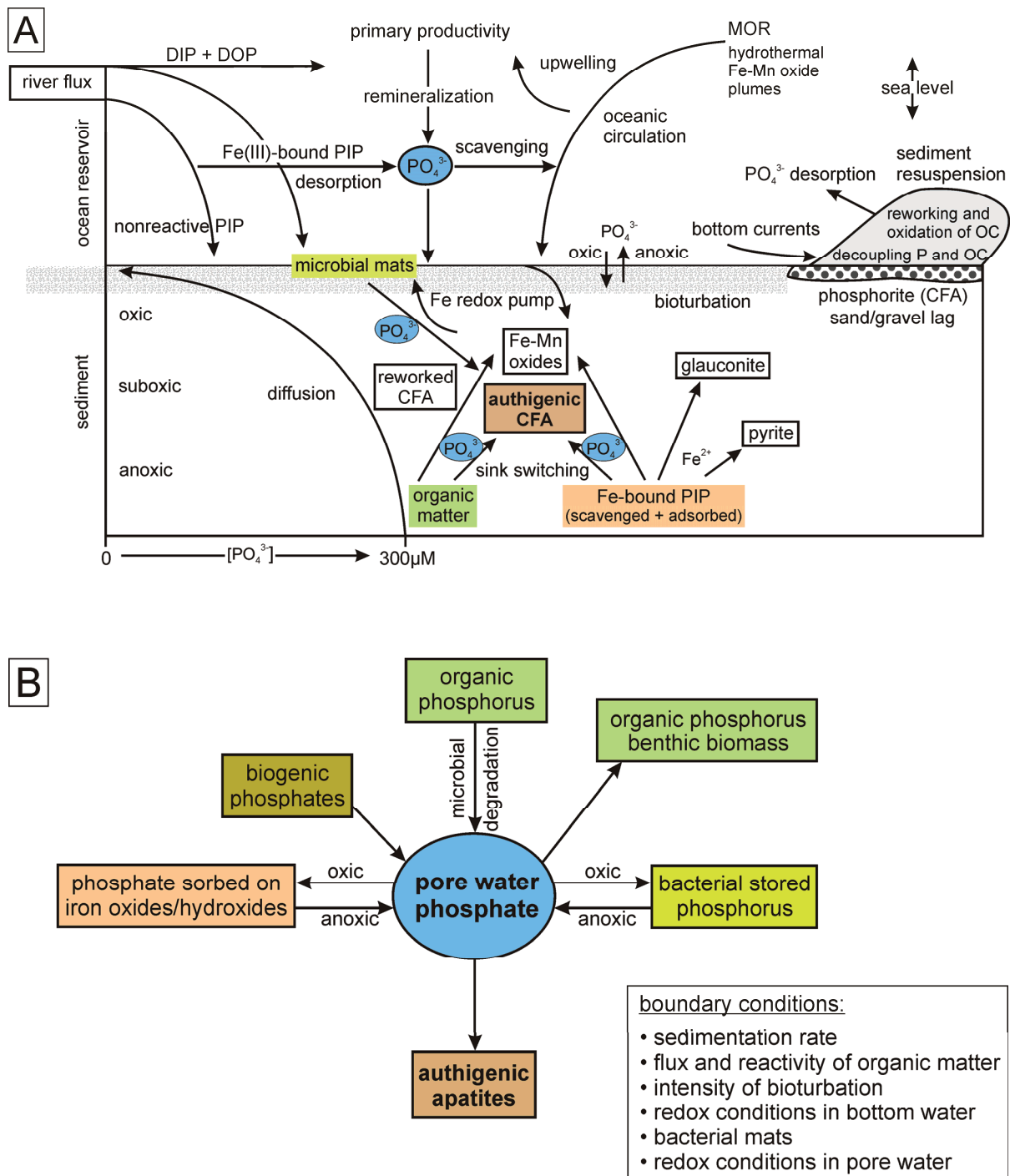


Figure 5 A) Scheme of the processes involved in phosphogenesis and phosphorus burial in marine sediments of coastal upwelling systems (modified after Compton *et al.*, 2000). PIP: particulate inorganic phosphorus, DIP: dissolved inorganic phosphorus, DOP: dissolved organic phosphorus, CFA: carbonate fluorapatite, OC: organic carbon, P: phosphorus. **B)** Simplified scheme of processes influencing the pore water phosphate concentration in marine sediments close to the sediment-water interface (modified after Krajewski *et al.*, 1994).

1.5 Coastal upwelling systems – aspects for phosphorite formation

Large phosphorite deposits have formed in the last six million years in the upwelling areas of the Peru-Chile and Namibian margins. The Peru-Chile margin is the site of a giant modern phosphorite deposit containing an estimated 140 to $746 \cdot 10^{12}$ g phosphorus (Glenn *et al.*, 1994). Phosphatic sediment recovered from the Peru margin suggests that this area has been a major phosphogenic province since the late Miocene (Garrison & Kastner, 1990). Large phosphorite deposits were formed on the shelf and upper slope areas during marine transgression and were then reworked during regression (Birch, 1979; Birch *et al.*, 1983; Glenn *et al.*, 1994).

On shelf areas, microbial degradation of organic matter occurs most intensely just below the sea floor in freshly deposited sediments (*e.g.* Aller, 1994; Canfield, 1994; Krajewski *et al.*, 1994). The remineralization of organic matter is maximized and thus the release of phosphate will be high. In most marine upwelling sediments, the degradation of organic matter via sulfate reduction (eq. 1) is the dominant anaerobic oxidation process (*e.g.* Jørgensen, 1982; Thamdrup & Canfield, 1996; Ferdelman *et al.*, 1999):



The stoichiometry of marine phytoplankton including nitrate and phosphate (C:N:P = 106:16:1) was suggested by Redfield (1958). The pathways of organic matter oxidation in marine sediments are summarized in Table 1 in a simplified manner.

Table 1 Simplified pathways of organic matter oxidation in marine sediments. Organic matter is symbolized by $[\text{CH}_2\text{O}]$ (from Jørgensen, 2005).

pathway	reaction
oxic respiration	$[\text{CH}_2\text{O}] + \text{O}_2 \rightarrow \text{CO}_2 + \text{H}_2\text{O}$
denitrification	$5[\text{CH}_2\text{O}] + 4\text{NO}_3^- \rightarrow 2\text{N}_2 + 4\text{HCO}_3^- + \text{CO}_2 + 3\text{H}_2\text{O}$
manganese(IV) reduction	$[\text{CH}_2\text{O}] + 3\text{CO}_2 + \text{H}_2\text{O} + 2\text{MnO}_2 \rightarrow 2\text{Mn}^{2+} + 4\text{HCO}_3^-$
iron(III) reduction	$[\text{CH}_2\text{O}] + 7\text{CO}_2 + 4\text{Fe}(\text{OH})_3 \rightarrow 4\text{Fe}^{2+} + 8\text{HCO}_3^- + 3\text{H}_2\text{O}$
sulfate reduction	$2[\text{CH}_2\text{O}] + \text{SO}_4^{2-} \rightarrow \text{H}_2\text{S} + 2\text{HCO}_3^-$
methanogenesis	$4\text{H}_2 + \text{HCO}_3^- + \text{H}^+ \rightarrow \text{CH}_4 + 3\text{H}_2\text{O}$ $\text{CH}_3\text{COO}^- + \text{H}^+ \rightarrow \text{CH}_4 + \text{CO}_2$

Ocean margin areas with strong upwelling and a high input of organic matter, which is sufficient for intense microbial activity that results in a subsequent establishment of suboxic to anoxic conditions close to the sediment-water interface, are places of present day phosphorite formation (Figure 2). Here, highest phosphate concentrations typically occur in the uppermost part of the sediment column, close to the sediment-water interface (*e.g.* Jahnke *et al.*, 1983; Froelich *et al.*, 1988; Schulz & Schulz, 2005). This leads to a supersaturation of the pore water with respect to CFA and its subsequent precipitation (Figure 6). Due to high phosphate concentrations near the sediment surface, diffusive fluxes of phosphate can be either directed upward into the water column or downward into the anoxic sediment zone (Figure 6).

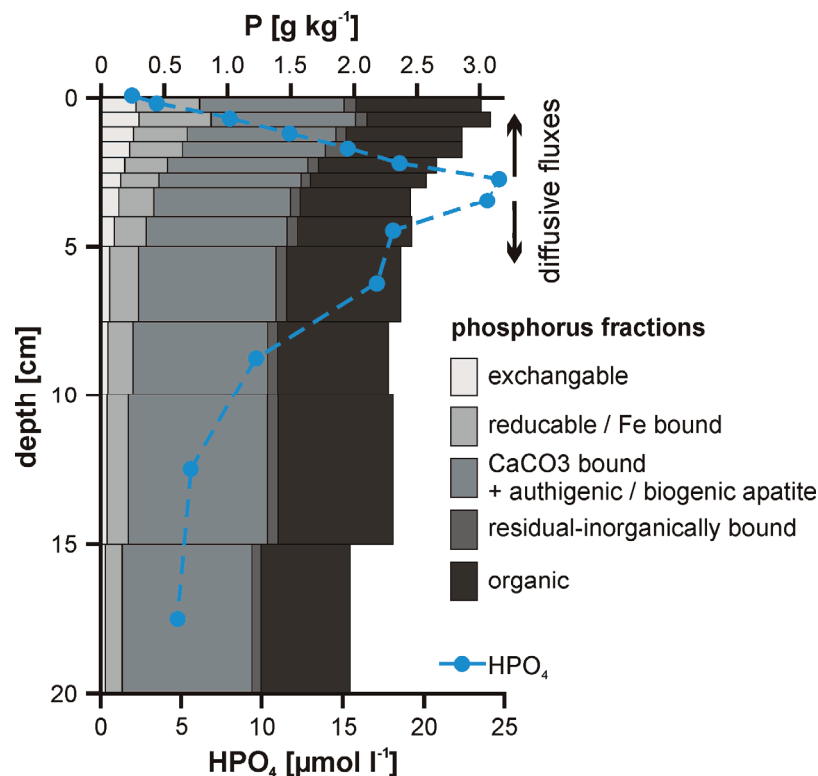


Figure 6 Typical pore water phosphate profile and reservoirs of phosphorus in surface sediments of coastal upwelling areas, exemplarily shown on sediments from the continental margin off Namibia (modified after Hensen *et al.*, 2005).

Remarkably, these areas of modern phosphorite formation (Froelich *et al.*, 1988; Glenn & Arthur, 1988) are also the specific habitats of dense and widespread populations of large, nitrate-storing sulfur bacteria (Figure 7; *e.g.* Gallardo, 1977). These bacteria comprise the filamentous *Beggiatoa* and *Thioploca* and the bead-shaped *Thiomargarita* species (Schulz & Jørgensen, 2001). Moreover, abundant microfossils resembling large filamentous sulfur

bacteria have been found embedded in phosphorite deposits of the Monterey Formation (Williams & Reimers, 1983) and spherical microfossils in the Neoproterozoic Doushantuo Formation were recently re-interpreted as phosphatized giant vacuolated sulfide-oxidizing bacteria (Bailey *et al.*, 2007).

Large sulfur bacteria tend to develop where the O₂- or NO₃-rich zone and the underlying H₂S-rich zone nearly overlap. They gain energy by oxidizing sulfide using oxygen (eq. 2) or nitrate (eq. 3) (*e.g.* Schulz & Jørgensen, 2001):

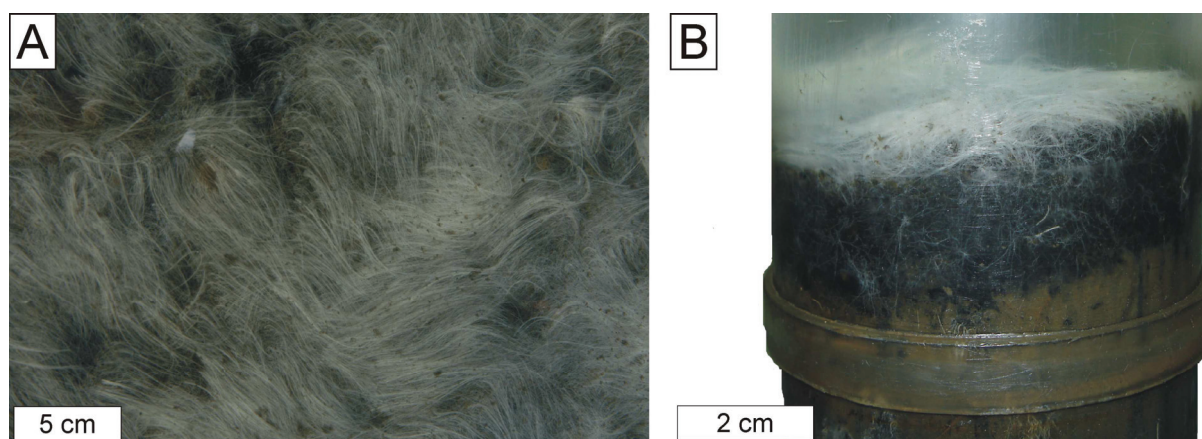
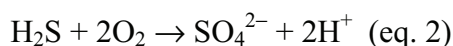


Figure 7 *Thioploca* from the shelf off central Chile. (A) *Thioploca* filaments stretching out from the sediment surface into the water column. (B) *Thioploca* form dense mats on top of a sediment core. Sheaths penetrate several centimeters deep into the sediment.

The close connection between phosphorites/phosphogenic sediments and microbial organisms has raised the question of the significance of this link and its geological implications. Nevertheless, the exact role of microbes in CFA precipitation remains unclear. It is evident, that to a large extent, microbes influence pore water chemistry and may thus indirectly promote CFA precipitation. So far, direct and active participation of microbes in phosphate enrichment has only been shown in studies by Gächter *et al.*, (1988), Konhauser *et al.*, (1994), and Schulz & Schulz (2005), who demonstrated the redox dependent intracellular storage and release of phosphate by bacteria.

Large sulfur bacteria have been found to be able to store polyphosphate under oxic conditions. When redox conditions episodically switch from oxic to anoxic, polyphosphate is used as an additional energy source, and phosphate will be released (Schulz & Schulz, 2005). It has been proposed, that polyphosphate storing bacteria could play a role in the phosphorus cycle of the ocean (Nathan *et al.*, 1993). In particular, polyphosphate storing bacteria have been suspected to be important in phosphorite formation (Williams & Reimers, 1983; Reimers *et al.*, 1990; Schulz & Schulz, 2005). However, the role of large sulfur bacteria in phosphogenesis is not well understood. To date, the study by Schulz & Schulz (2005) is the only one providing direct evidence for a linkage of large sulfide-oxidizing bacteria and phosphogenesis.

2. TOOLS TO DECIPHER MICROBIAL INVOLVEMENT IN PHOSPHORITE FORMATION

In order to decipher microbial involvement in phosphorite formation and to identify microbial signatures, I applied various biogeochemical methods together with petrographic analyses. Due to the application of various methods it is possible to obtain information from different perspectives that improves today's understanding about the biogeochemical, ecological, sedimentological, and oceanographic conditions important for phosphorite formation.

A powerful tool to identify an involvement of bacteria in authigenic rock formation is the analyses of **molecular biomarkers**. Molecular biomarkers are thought to be preserved excellently as molecular fossils in authigenic phases (here phosphorites), and thus display a fingerprint of the dominant microbial organisms in the system of phosphorite formation. The ideal biomarker should be specific for one organism or at least one group of organisms. Furthermore, the biomarker, or its altered compounds that can be unambiguously attributed to particular molecular precursor molecules, has to be sufficiently resistant to chemical and biological degradation, in order to be identified in the geological record (Brassel, 1993; Hedges & Prahl, 1993; Killops & Killops, 1993).

Stable sulfur isotope measurements of sulfur species associated with phosphorites provide insights in the sulfur cycle during phosphogenesis and reveal whether bacterial or abiotical processes are involved (*e.g.* Jørgensen, 1979; Canfield, 2001). This tool is especially important because the degradation of organic matter in the sediments via sulfate reduction is the dominant anaerobic respiration process in sediments of the studied upwelling regions (see section 1.5). Furthermore, large sulfide-oxidizing bacteria play a crucial role in these sediments and leave their signatures in sulfur isotopic composition of sulfate.

Geochemical analyses of trace elements and rare earth elements help to characterize the geochemical environment during phosphorite formation. Trace elements within phosphorites provide ambiguous redox signals and give information on the redox environment during phosphorite formation. Rare earth element distributions in phosphorites may be interpreted as sea water signatures (*e.g.* Piper, 1994) and thus provide information on bottom-water redox conditions.

The biogeochemical analyses were supported by **petrographic studies** on thin sections. The interpretation of sedimentary structures provides information on the sedimentary history of the studied phosphorites. It is important to know whether the studied phosphorites are authigenic or reworked and transported. A valid interpretation of the results obtained from

biogeochemical analyses is only possible on authigenic phosphorites, because only authigenic phases preserve primary signatures. The identification of mineral paragenesis provides additional insights into the redox environment during phosphogenesis and helps to define the temporal sequence of the formation of carbonate fluorapatite and the precipitation of other associated minerals, in particular sulfide minerals.

CHAPTER II:

CASE STUDIES – PHOSPHOGENESIS IN UPWELLING SYSTEMS AND THE IMPORTANCE OF MICROORGANISMS

PAPER 1:**Lipid Biomarker Patterns of Phosphogenic Sediments from Upwelling Regions****Running head: LIPID BIOMARKERS IN PHOSPHOGENIC SEDIMENTS**

Esther T. Arning and Daniel Birgel

DFG-Forschungszentrum Ozeanränder, Universität Bremen, D-28334 Bremen, Germany

Heide N. Schulz-Vogt

Max-Planck-Institut für Marine Mikrobiologie, D-28359 Bremen, Germany

Lars Holmkvist and Bo Barker Jørgensen

Max-Planck-Institut für Marine Mikrobiologie, D-28359 Bremen, Germany

Alyssa Larson

University of California, Santa Barbara, CA-93106, USA

Jörn Peckmann

DFG-Forschungszentrum Ozeanränder, Universität Bremen, D-28334 Bremen, Germany

Keywords: sulfate-reducing bacteria, sulfide-oxidizing bacteria, *Thiomargarita*, *Beggiatoa*, *Thioploca*, lipid biomarkers, phosphogenesis, sulfur cycle, Namibia, Peru, Chile

Geomicrobiology Journal, 2008, v. 25: 69-82. DOI: 10.1080/01490450801934854

ABSTRACT

Sediments of upwelling regions off Namibia, Peru, and Chile contain dense populations of large nitrate-storing sulfide-oxidizing bacteria, *Thiomargarita*, *Beggiatoa*, and *Thioploca*. Increased contents of monounsaturated C₁₆ and C₁₈ fatty acids have been found at all stations studied, especially when a high density of sulfide oxidizers in the sediments was observed. The distribution of lipid biomarkers attributed to sulfate reducers (10MeC_{16:0} fatty acid, *ai*-C_{15:0} fatty acid, and mono-*O*-alkyl glycerol ethers) compared to the distribution of sulfide oxidizers indicate a close association between these bacteria. As a consequence, the distributions of sulfate reducers in sediments of Namibia, Peru, and Chile are closely related to differences in the motility of the various sulfide oxidizers at the three study sites. Depth profiles of mono-*O*-alkyl glycerol ethers have been found to correlate best with the occurrence of large sulfide-oxidizing bacteria. This suggests a particularly close link between mono-*O*-alkyl glycerol ether-synthesizing sulfate reducers and sulfide oxidizers. The interaction between sulfide-oxidizing bacteria and sulfate-reducing bacteria reveals intense sulfur cycling and degradation of organic matter in different sediment depths.

INTRODUCTION

Coastal upwelling characterizes the eastern margins of the Atlantic and the Pacific Ocean. Due to the upwelling of nutrients, extended oxygen minimum zones develop as a consequence of high primary productivity in the surface waters. Where oxygen minimum zones impinge on the seafloor, benthic environments with suboxic to anoxic conditions are established over extended periods of time. The early diagenetic degradation of organic matter in these environments plays a significant role for nutrient cycling in the sediments and for dissolution or precipitation processes of sedimentary particles (Müller and Suess 1979; Berelson et al. 1987; Martin et al. 1991). In most marine upwelling sediments the degradation of organic matter via sulfate reduction is the dominant anaerobic respiration process (e.g., Jørgensen 1982; Thamdrup and Canfield 1996; Ferdelman et al. 1999). The liberation of phosphate into the pore water during microbial degradation of organic matter may lead to the precipitation of phosphate minerals. This phosphogenesis takes place near the sediment/water interface and is an important sink in the global marine phosphorous cycle (Ingall and Jahnke 1994; Föllmi 1996; van Cappellen and Ingall 1996; Baturin 2000). Recent phosphogenesis has been noted to occur mainly in the suboxic to anoxic marine sediments of ocean upwelling regions, e.g.

off Namibia, Chile, or Peru, in the Gulf of California, and in the Arabian Sea (Föllmi 1996; Schenau et al. 2000).

A common and striking feature of the major modern upwelling regions is the abundant occurrence of large colorless, nitrate-storing sulfide-oxidizing bacteria on the seafloor. These bacteria, such as *Thioploca*, *Beggiatoa*, and *Thiomargarita*, gain energy by oxidizing sulfide using nitrate or oxygen (Schulz and Jørgensen 2001). They play a crucial role in the benthic sulfur cycle by reoxidizing sulfide produced during bacterial sulfate reduction (Ferdelman et al. 1997; Jørgensen and Gallardo 1999; Otte et al. 1999). Furthermore they constitute an important link between the sulfur cycle and the nitrogen cycle in marine upwelling sediments (Fossing et al. 1995; Jørgensen and Gallardo 1999; Otte et al. 1999; Zopfi et al. 2001).

Different genera of large sulfide-oxidizing bacteria can be found in distinct upwelling regions. *Thiomargarita* have been discovered in Namibian shelf sediments, whereas *Beggiatoa* and *Thioploca* predominate along the Pacific coast of South America (Gallardo 1977; Fossing et al. 1995; Schulz et al. 1996; Schulz et al. 1999; Pantoja and Lee 2003). *Thioploca* also inhabit sediments of the Arabian Sea (Schmaljohann et al. 2001). Different ecological niches are colonized by these sulfide-oxidizing bacteria (Schulz and Jørgensen 2001). *Beggiatoa* grow and accumulate at the oxygen-sulfide interface (Jørgensen and Revsbech 1983; Nelson et al. 1986). Even though *Beggiatoa* need a high supply of both oxygen and sulfide, they can tolerate only low concentrations of each. Therefore, they inhabit only a millimeter-thick zone at the sediment-water interface where their respiration rate is strongly diffusion limited (Jørgensen and Revsbech 1983; Nelson et al. 1986). Nevertheless they consume up to 70% of the total oxygen flux and possibly the entire diffusing sulfide (Jørgensen and Revsbech 1983; Fenchel and Bernard 1995). The large marine *Thioploca*, on the other hand, are primarily anaerobes and use mainly nitrate as electron acceptor (Huettel et al. 1996; Otte et al. 1999), but they can also take up oxygen (Revsbech pers. comm.). *Thioploca* live as bundles in common sheaths, which penetrate several centimeters deep into the sediments, and commute up and down in the sediment. Therefore, they are able to continuously oxidize sulfide using the internally stored nitrate (Schulz and Jørgensen 2001). Despite high sulfate reduction rates in sediments densely populated by *Thioploca*, sulfide concentrations are often low (Ferdelman et al. 1997). In contrast to *Beggiatoa* and *Thioploca*, *Thiomargarita* are not motile (Schulz et al. 1999). They colonize semifluid diatom oozes with high sulfide concentrations. *Thiomargarita* are not harmed by high oxygen concentrations and may also use oxygen instead of nitrate as an electron acceptor (Schulz and Jørgensen 2001).

The aim of this work is to compare the biogeochemistry and ecology of phosphogenic sediments from three distinct major upwelling regions with intense sulfur cycling. By means of lipid biomarker analysis, supported by pore water analyses and cell counts, differences in the microbial ecology of the respective sites and their consequences for nutrient cycling in phosphogenic sediments will be discussed.

SAMPLE LOCATIONS

Shelf sediments from upwelling regions off Namibia, Peru, and Chile were studied (Figure 1). Water depths are 70 m (Namibia), 256 m (Peru), and 87 m (Chile). Samples off Namibia were taken during *RV Meteor* cruise M57/3 in March/April 2003 (Brüchert et al. 2005), samples off Peru during *RV Olaya* cruise MPI/IMARPE in April 2005, and samples off Chile during January 2006 with *RV Kay Kay* of the Marine Biological Station of Dichato (University of Concepción). All stations are within the oxygen minimum zone (OMZ) of the respective region (Reimers and Suess 1983; Emeis et al. 1991, 2000; Lückge and Reinhardt 2000; Hebbeln et al. 2001). Sediments of the Namibian and Peruvian shelves contain organic-rich nanofossil and diatom oozes (Calvert and Price 1983; Suess and von Huene 1988). Schubert et al. (2000) described the Chilean sediments from their station 18, corresponding to our station, as clayey silty to silty clayey mud.

All stations are characterized by intense upwelling, which results in high primary productivity. Over $200 \text{ g C m}^{-2} \text{ yr}^{-1}$ are produced off Namibia and even higher (over $350 \text{ g C m}^{-2} \text{ yr}^{-1}$) rates were observed off Peru and Chile (Müller and Suess 1979; Berger et al. 1987; Shannon et al. 1987; Berger 1989; Fossing et al. 1995). This increased productivity results in extreme oxygen depletion in the water column. On the Namibian shelf episodic sulfidic bottom waters arise (Brüchert et al. 2005). The same applies to coastal upwelling sediments off Peru (e.g., Fossing 1990; Raiswell and Canfield 1996; Suits and Arthur 2000). While off Namibia and Peru constant upwelling is observed (Calvert and Price 1983 and references therein; Shannon 1985; Suess et al. 1986), a strong seasonality has been documented off Chile. Intense upwelling occurs only during austral summers, whereas during winter upwelling is reduced (Ahumada et al. 1983).

The occurrence of sulfide oxidizers is characteristic for the studied sediments. They were observed in great abundances at all sites, but the genera differ from site to site. Sediments from the Namibian shelf were almost exclusively populated by *Thiomargarita* (Schulz and Schulz 2005). In the Peruvian samples *Beggiatoa* were present, whereas

Thioploca were not detected. *Thioploca*, on the other hand, predominated in sediments sampled off Chile where *Beggiatoa* were scarcely found.

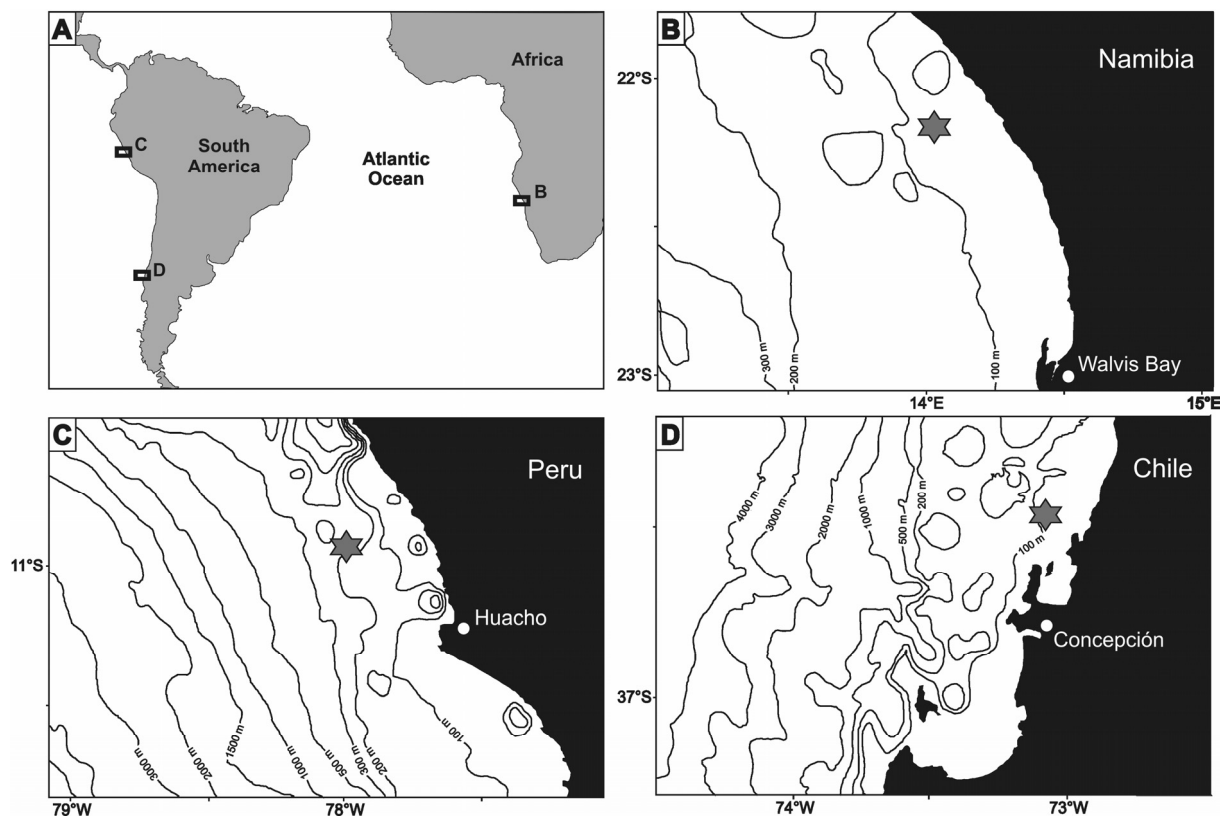


FIG. 1. Maps indicating the study sites. (A) Sampling areas detailed in frames B, C, and D. (B) Benguela upwelling region off the coast of Namibia. (C) Upwelling region off Peru (corresponding to ODP-site 1228). (D) Upwelling region off Chile, close to the Bay of Concepción.

METHODS

Contents of total organic carbon (TOC) were measured from dry, carbonate free and homogenized samples using a Leco CS 200. To remove the inorganic carbon, the samples were treated with 12.5 % HCl prior to measurements.

For lipid biomarker analyses, 1 to 4 g freeze dried sediment collected with a multi-corer was extracted three times with 60 ml dichlormethane:methanol (3:1) by microwave-extraction (CEM, MARS X) at 80°C and 600 W. Internal standards of different polarities (cholestane, behenic acid methylester, 1-nonadecanol, 2-Me-octadecanoic acid) were added to the sediments prior to extraction. The extracts were combined and washed with 0.05 M KCl. The organic phases were collected and dried with sodium sulfate. The resulting total lipid extracts (TLEs) were purified by separation in DCM soluble asphaltenes and in hexane soluble

maltenes. The maltenes were desulfurized with activated copper powder and subsequently separated by column chromatography (supelco LC-NH₂[®] glass cartridges; 500 g sorbed). Maltenes were separated into four fractions of increasing polarity (1. alkanes, 2. ketones/esters, 3. alcohols, and 4. free fatty acids). Fatty acid methyl esters (FAMES) were derivatized from free fatty acids by adding 1 ml of 12 % BF₃ in methanol to the dried fatty acid fraction. Reaction time was 1 h at 70°C. The alcohols were reacted to trimethylsilyl- (TMS-) derivatives with 100 µl BSTFA and 100 µl pyridine (1 h at 70°C). All fractions were examined with coupled gas chromatography-mass spectrometry (GC-MS) using a Thermo Electron Trace GC-MS equipped with a 30-m DB-5MS fused silica capillary column (0.32 mm i.d., 0.25 µm film thickness). The carrier gas was helium. We quantitatively analyzed fractions 3. and 4. Contents are given in µg g⁻¹ dry sediment.

Double bond positions in FAMES were determined exemplary at one sample from each location by preparation of dimethyl disulfide (DMDS) adducts according to the method of Nichols et al. (1986). An aliquot of the derivatized fatty acid fraction was treated with 100 µl DMDS and 20 µl 6 % iodine solution in diethyl ether (48 h at 50°C). Afterwards 500 µl of hexane was added and the iodine excess was reduced with 500 µl of 5 % sodium thiosulfate solution. The organic phase was removed and the aqueous phase extracted twice with hexane. The combined extracts were measured with GC-MS.

Biomass distribution of large sulfide-oxidizing bacteria in sediments off Peru and Chile was determined by counting filaments and measuring their diameter and length by microscopy. For this purpose, sediment in subcores was washed away in centimeter steps using a squeeze bottle (Schulz et al. 1996).

Pore water phosphate concentrations in sediments off Peru and Chile were measured spectrophotometrically with the molybdenum blue method after Murphy and Riley (1962) on filtered and acidified pore water samples. Acid volatile sulfide (AVS = FeS + H₂S) was measured after Fossing and Jørgensen (1989).

MOLECULAR BIOMARKER INVENTORY

Alcohol fractions

All sediments analyzed reveal a broad distribution of lipids. Representative chromatograms of alcohol fractions from two different depths of sediments off Namibia highlight the variability of lipids in sediments of upwelling regions (Figure 2).

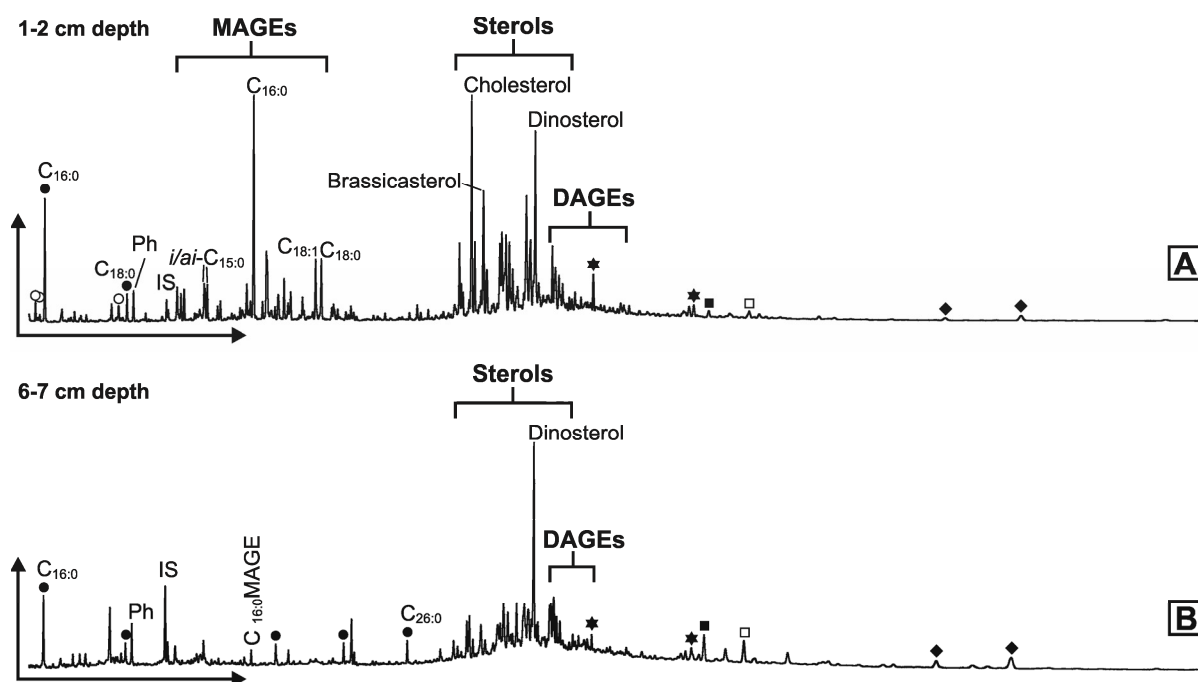


FIG. 2. Gas chromatograms (FID) of the alcohol fraction of Namibian sediments. (A) Biomarker distribution in surface sediments (1 to 2 cm depth). (B) Biomarker distribution in 6 to 7 cm depth. Black circles: *n*-alcohols, white circles: monounsaturated alcohols, stars: hopanols, black squares: archaeol, white squares: hydroxyarchaeol, diamonds: biphytanediols, MAGEs = mono-*O*-alkyl glycerol ethers, DAGEs = di-*O*-alkyl glycerol ethers, Ph = phytanol, IS = Internal Standard.

Sterols are prominent biomarkers in all extracted sediments. They are synthesized by various eukaryotic organisms and most likely derive mainly from phytoplankton. High contents of brassicasterol have been found in surface sediments of all stations (Namibia: up to $21 \mu\text{g g}^{-1}$, Peru: up to $65 \mu\text{g g}^{-1}$, Chile: up to $34 \mu\text{g g}^{-1}$). Deeper in the sediments, contents are lower, 1 to $2 \mu\text{g g}^{-1}$ in Namibian and Chilean stations and 2 to $3 \mu\text{g g}^{-1}$ off Peru. Brassicasterol is produced by diatoms, but can also be found in other microalgae such as haptophytes and cryptophytes, as well as in higher plants (Volkman et al. 1998 and references therein; Volkman 2003). Dinosterol, synthesized by dinoflagellates (e.g., Boon et al. 1979), is commonly used as indicator for algal input to sediments. Namibian sediments show highest contents of this compound in the surface layer (23 to $24 \mu\text{g g}^{-1}$), while in deeper layers contents are around 2 to $9 \mu\text{g g}^{-1}$, except for two peaks in 4 to 5 cm and 17 cm depth with $17 \mu\text{g g}^{-1}$ each (Figure 3). Off Peru, high contents of dinosterol were found in surface sediments ($105 \mu\text{g g}^{-1}$), however in deeper sediments contents are lower (17 to $35 \mu\text{g g}^{-1}$). In 9 to 10 cm depth, dinosterol contents increase up to $64 \mu\text{g g}^{-1}$ (Figure 4). Off Chile no significantly higher contents of dinosterol were found in sediments close to the surface ($6 \mu\text{g g}^{-1}$),

compared to deeper sediments (2 to 4 $\mu\text{g g}^{-1}$). Maximum contents (15 $\mu\text{g g}^{-1}$) have been found at 6 to 7 cm (Figure 5).

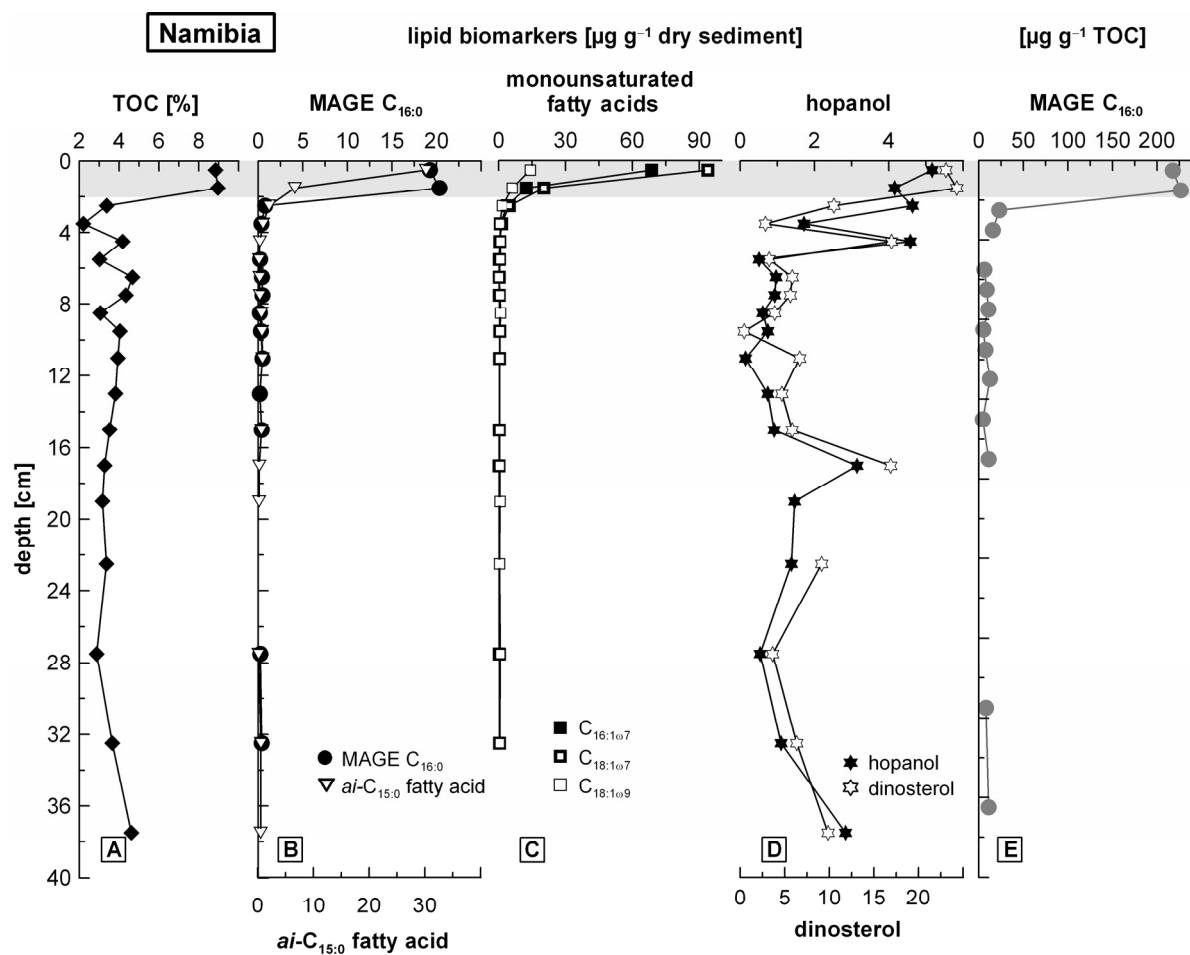


FIG. 3. Namibian core. (A) TOC-content of Namibian sediments. (B) and (C) Depth profiles of selected lipid biomarkers ($\mu\text{g g}^{-1}$ dry sediment). MAGE $\text{C}_{16:0}$ = mono-*O*-alkyl glycerol ether $\text{C}_{16:0}$. (D) Allochthonous marine input is indicated by dinosterol and hopanol ($\mu\text{g g}^{-1}$ dry sediment). (E) Content of MAGE $\text{C}_{16:0}$ ($\mu\text{g g}^{-1}$ TOC). The shaded area indicates the surface layer of these sediments with high microbial activity.

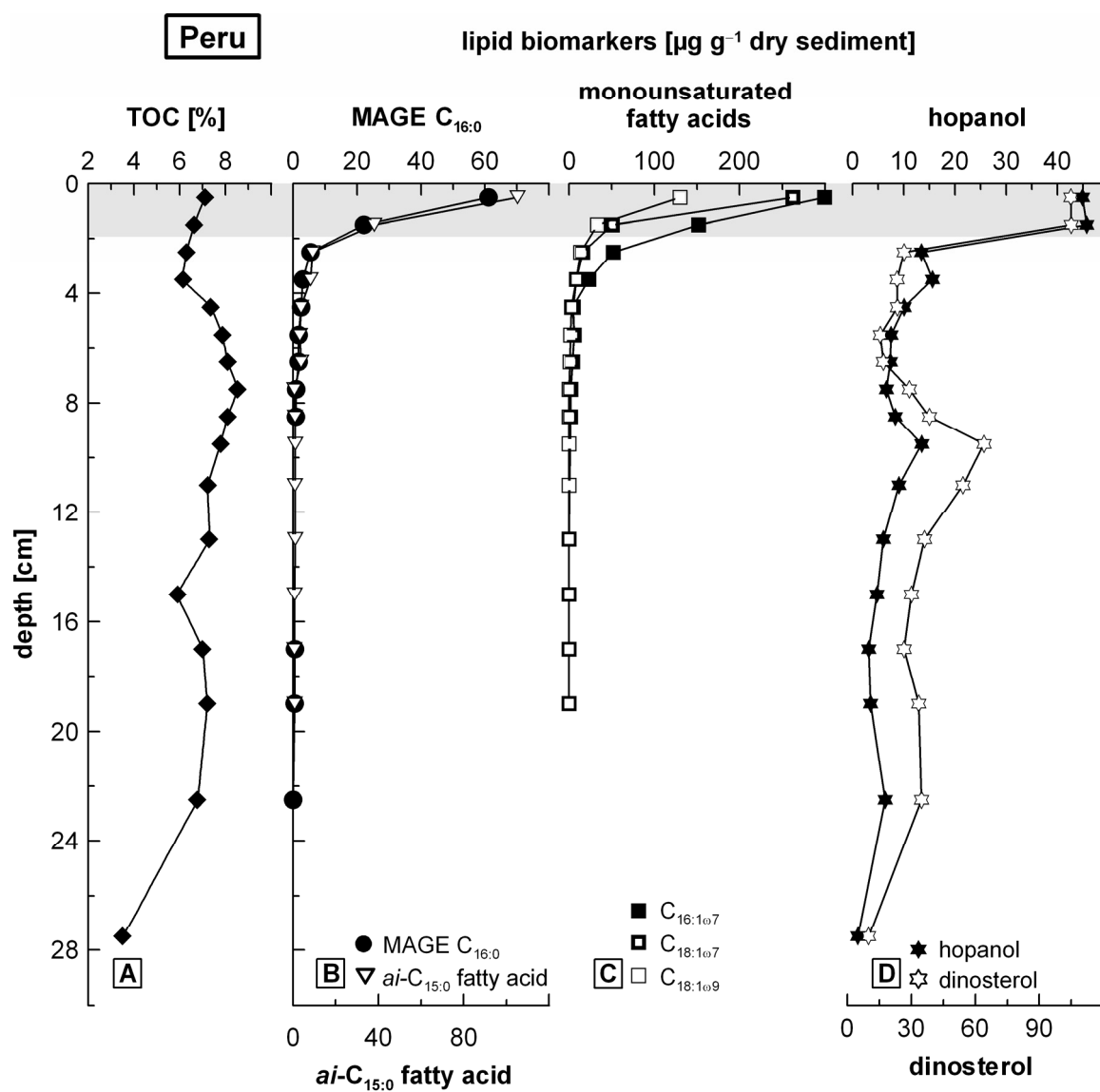


FIG. 4. Peruvian core. (A) TOC-content of Peruvian sediments. (B) and (C) Depth profiles of selected lipid biomarkers ($\mu\text{g g}^{-1}$ dry sediment). MAGE $C_{16:0}$ = mono-*O*-alkyl glycerol ether $C_{16:0}$. (D) Allochthonous marine input is indicated by dinosterol and hopanol ($\mu\text{g g}^{-1}$ dry sediment). The shaded area indicates the surface layer of these sediments with high microbial activity.

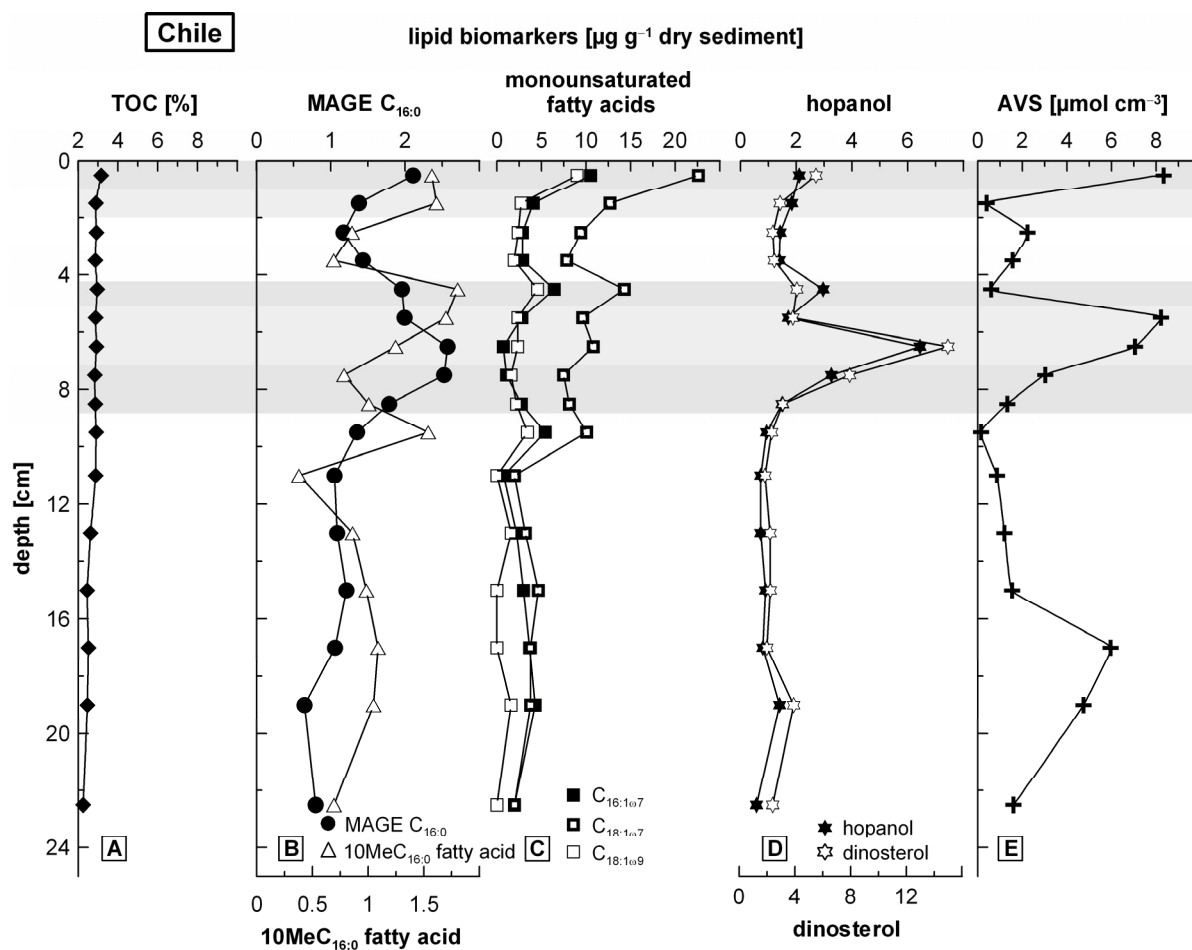


FIG. 5. Chilean core. (A) TOC-content of Chilean sediments. (B) and (C) Depth profiles of selected lipid biomarkers ($\mu\text{g g}^{-1}$ dry sediment). MAGE $C_{16:0}$ = mono-*O*-alkyl glycerol ether $C_{16:0}$. (D) Allochthonous marine input is indicated by dinosterol and hopanol ($\mu\text{g g}^{-1}$ dry sediment). (E) Distribution of acid volatile sulfides (AVS) in sediments off Chile ($\mu\text{mol cm}^{-3}$). The upper shaded area indicates the surface layer of these sediments with high microbial activity. The second shaded area highlights an additional microbial zone of high activity.

Di- and tricyclic biphytandiol, diagenetic products of glycerol dialkyl glycerol tetraethers (GDGTs), assigned to planktonic crenarchaea (e.g., Schouten et al. 1998) are only present in sediments off Namibia (1 to $2 \mu\text{g g}^{-1}$) and Peru (2 to $8 \mu\text{g g}^{-1}$). Archaeol (1 to $3 \mu\text{g g}^{-1}$) and hydroxyarchaeol (1 to $2 \mu\text{g g}^{-1}$), indicating the presence of methanogens (Boone et al. 1993; Koga et al. 1993; Sprott et al. 1993; Koga et al. 1998), were only identified in Namibian sediments. Some non-isoprenoidal *sn*-1,2-di-*O*-alkyl glycerol ethers (DAGEs) occur in sediments off Namibia and Peru, but are absent in sediments off Chile. DAGEs are most abundant in surface sediments of Namibian and Peruvian sediments, with contents ranging from 2 to $10 \mu\text{g g}^{-1}$ and 35 to $75 \mu\text{g g}^{-1}$, respectively. Hinrichs et al. (2000) and Pancost et al. (2001) suggested phylogenetically deeply-branching sulfate reducers as source organisms.

Hopanol represents the most abundant hopanoid in sediments of this study. Hopanoids have been thought to be synthesized only by aerobic bacteria, including cyanobacteria, methanotrophs, and heterotrophs (e.g., Ourisson et al. 1987; Rohmer et al. 1992; Summons et al. 1999). However, some anaerobic bacteria have recently been found to be potential sources of hopanoids as well (Sinninghe Damsté et al. 2004; Fischer et al. 2005; Härtner et al. 2005; Blumenberg et al. 2006). Profiles of hopanol correlate with profiles of dinosterol at all stations (Figures 3-5). Surface sediments off Namibia and Peru contain more hopanol ($5.2 \mu\text{g g}^{-1}$ and $45 \mu\text{g g}^{-1}$, respectively) than Chilean sediments. Increased contents of hopanol were also found in deeper sediments at all stations. The highest contents were found at 17 cm depth off Namibia ($3 \mu\text{g g}^{-1}$) and 10 cm depth off Peru ($13.5 \mu\text{g g}^{-1}$). The highest hopanol contents in the Chilean core were measured at 7 to 8 cm depth ($6.4 \mu\text{g g}^{-1}$).

Non-isoprenoidal *sn*-1-mono-*O*-alkyl glycerol ethers (MAGEs) are abundant in surface sediments, whereas at depth they are almost absent (Figure 2). Biosynthesis of non-isoprenoidal MAGEs is known to occur in phylogenetically deeply-branching thermophilic bacteria (Langworthy et al. 1983; Huber et al. 1992; see also Table 1). In a study by Rütters et al. (2001), MAGEs with C_{16} and C_{18} alkyl moieties were also found in mesophilic *Desulfosarcina*. Furthermore, MAGEs have been found in sediments at methane seeps in the Santa Barbara and Eel River basins, as well as Hydrate Ridge, where they have been assigned to bacterial syntrophic partners of methanotrophic archaea, possibly representing sulfate reducers (Hinrichs et al. 2000; Orphan et al. 2001; Elvert et al. 2005). Teske et al. (2002) observed MAGEs in hydrothermal sediments of the Guaymas Basin and suggested a new, phylogenetically deeply-branching bacterial phylotype as possible producer of MAGEs.

TABLE. 1

Possible biological sources of selected lipids extracted from the sediments. Listed are compounds from the alcohol and fatty acid fractions (MAGEs = mono-*O*-alkyl glycerol ethers).

Compound	Probable source	References
non-isoprenoidal MAGEs	<ul style="list-style-type: none"> – thermophilic bacteria – mesophilic <i>Desulfosarcina variabilis</i> – syntrophic partners of methanotrophic archaea – phylogenetically deeply-branching bacterial phylotype 	<ul style="list-style-type: none"> – Langworthy et al. 1983; Huber et al. 1992 – Rütters et al. 2001 – Hinrichs et al. 2000; Orphan et al. 2001 – Teske et al. 2002
10MeC _{16:0} fatty acid	<ul style="list-style-type: none"> – <i>Desulfobacter</i> (sulfate reducers) – <i>Desulfobacula</i> (sulfate reducers) – <i>Geobacter</i> 	<ul style="list-style-type: none"> – Taylor and Parkes 1983; Dowling et al. 1986 – Kuever et al. 2001 – Zhang et al. 2003
<i>i/ai</i> -C _{15:0} fatty acids	<ul style="list-style-type: none"> – sulfate reducers (<i>i.a.</i> <i>Desulfosarcina</i>, <i>Desulfococcus</i>) 	<ul style="list-style-type: none"> – Perry et al. 1979; Taylor and Parkes 1983; Dowling et al. 1986; Kaneda, 1991; Wakeham and Beier 1991; see also in Elvert et al. 2003
C _{16:1ω5} fatty acid	<ul style="list-style-type: none"> – several sulfate reducers (<i>Desulfosarcina</i>, <i>Desulfococcus</i>, <i>Desulfotalea</i>, <i>Desulfobulbus</i>, <i>Desulforhopalus</i>) 	<ul style="list-style-type: none"> – Taylor and Parkes 1983; Dowling et al. 1986; Knoblauch et al. 1999; Rütters et al. 2001; Sass et al. 2002; Elvert et al. 2003
C _{16:1ω7} fatty acid	<ul style="list-style-type: none"> – <i>Thioploca</i> / <i>Beggiatoa</i> – sulfate reducers – marine phytoplankton, Cyanobacteria 	<ul style="list-style-type: none"> – McCaffrey et al. 1989; Grant 1991 – Londry et al. 2004 – e.g. Volkmann et al. 1989; Viso and Marty 1993; Wakeham 1995
C _{18:1ω7} fatty acid	<ul style="list-style-type: none"> – <i>Thioploca</i> / <i>Beggiatoa</i> – marine phytoplankton and zooplankton, Cyanobacteria 	<ul style="list-style-type: none"> – McCaffrey et al. 1989; Grant 1991 – e.g. Wakeham, 1995; Albers et al. 1996; Graeve et al. 1997
C _{18:1ω9} fatty acid	<ul style="list-style-type: none"> – <i>Beggiatoa</i> – sulfate reducers – marine phytoplankton and zooplankton 	<ul style="list-style-type: none"> – Grant 1991 – Londry et al. 2004 – e.g. Wakeham 1995; Albers et al. 1996; Graeve et al. 1997

The distribution of the most abundant MAGE C_{16:0}, is shown for all three study sites (Figures 3-5). High contents of MAGEs are found in all surface sediments. In the Namibian sediments, MAGEs are prominent over the first two centimeters reaching contents of up to 20 µg g⁻¹ (Figure 3), whereas in the Peruvian station contents decrease within the first two centimeters from 61 to 22 µg g⁻¹. *sn*-1-MAGEs other than MAGE C_{16:0} present in the Namibian and Peruvian sediments include saturated C_{14:0}, C_{15:0}, C_{17:0}, and C_{18:0}, monounsaturated C_{16:1}, C_{17:1} and C_{18:1}, as well as *i/ai*-C_{15:0} and -C_{16:0}. Contents vary between 1 and 6 µg g⁻¹ in the first two centimeters off Namibia and between 8 and 36 µg g⁻¹ in the top centimeter off Peru. Contents of MAGEs do not correlate with the TOC-contents of sediments at any of the stations (Figures 3-5). This is particularly obvious in Peruvian and Chilean

sediments, where TOC-contents vary only slightly with depth (Figures 4 and 5). In the Namibian core, increased TOC-contents have been measured in the first 2 centimeters. For these samples, the independence of bacterial biomarker contents from TOC, which predominantly originates from the water column, is exemplarily shown by MAGE C_{16:0} contents calculated per g TOC. This has little effect on the overall pattern agreeing with an *in situ* source of these compounds and excludes an input from the water column (Figure 3E).

While the Namibian and Peruvian MAGE profiles are similar, sediments off Chile show a different pattern (Figure 5B). Here, the contents of MAGE C_{16:0} are one order of magnitude lower compared to the other locations. In addition to a maximum close to the surface (2 µg g⁻¹), a second maximum was found at 4 to 5 cm with contents up to 2.5 µg g⁻¹ (Figure 5). In the Chilean surface sediment the diversity of MAGEs is also lower compared to the other study sites. Besides MAGE with a C₁₆ alkyl moiety, only a MAGE with a C₁₄ side chain was abundant enough to be quantified (0.6 µg g⁻¹). In the deeper zone, however, a cluster of several MAGEs with C_{14:0}, C_{15:0}, C_{16:0}, and C_{17:0}, monounsaturated C_{16:1}, and C_{17:1} as well as *i/ai*-C_{15:0} alkyl moieties was detected with contents up to 1.9 µg g⁻¹ for C_{17:0} MAGE. Additionally, MAGEs with *sn*-2 moieties were found in the Namibian and Peruvian surface sediments, as well as in the deeper zone of Chilean sediments where MAGEs peak.

Fatty acid fractions

The fatty acid distribution is exemplarily shown from two chromatograms obtained from Namibian sediments (Figure 6). *n*-fatty acids with chain lengths of C₁₄ to C₃₀ were detected as well as short chain branched fatty acids with chain lengths of C₁₅ to C₁₇. Relative abundances of long chain saturated fatty acids (C_{20:0} to C_{30:0}) increased with sediment depth. This can be explained by the fact that long chain fatty acids are more resistant to degradation than shorter saturated or monounsaturated chains. Among the long chain fatty acids a strong predominance of even-numbered carbon chains is apparent. This indicates a source from higher land plants (Eglinton et al. 1968; Simoneit 1978; Naraoka and Ishiwatari 2000). A minor contribution of long chain fatty acids in these sediments from phytoplankton is likely (cf., Volkmann et al. 1998 and references therein).

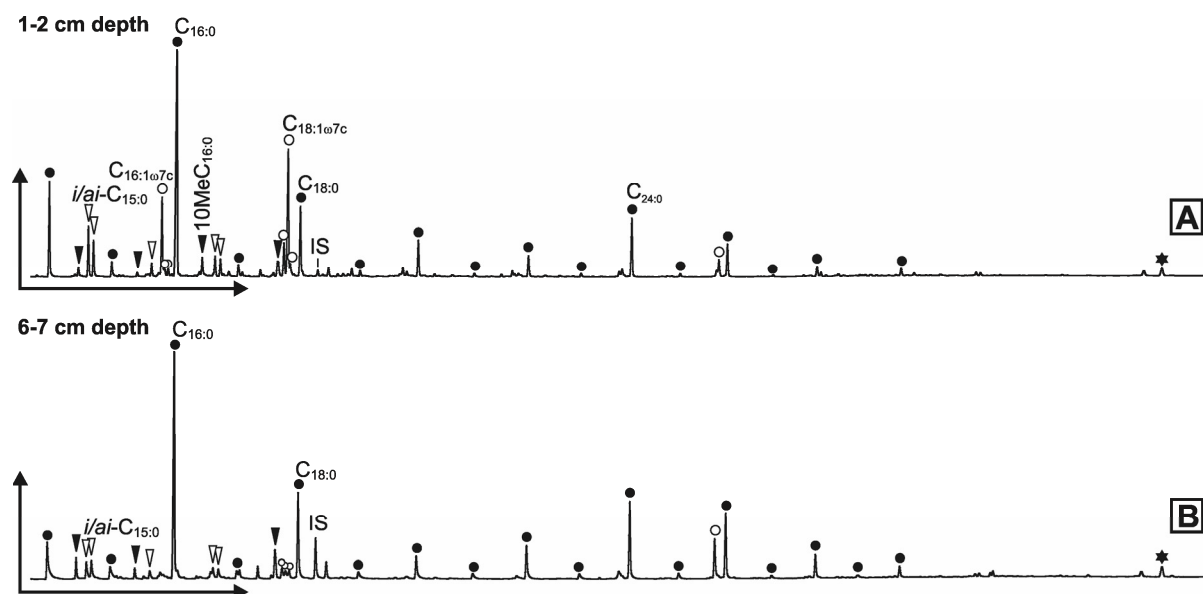


FIG. 6. Gas chromatograms (FID) of the fatty acid fraction of Namibian sediments. (A) Biomarker distribution in surface sediments (1 to 2 cm depth). (B) Biomarker distribution in 6 to 7 cm depth. Black circles: *n*-fatty acids, white circles: monounsaturated fatty acids, stars: C₃₂ hopanoic acid, white triangles: *iso* and *anteiso* fatty acids, black triangles: branched fatty acids, IS = Internal Standard.

Surface sediments are dominated by saturated C_{16:0} and C_{18:0} *n*-fatty acids and monounsaturated C_{16:1ω7} and C_{18:1ω7} fatty acids (contents are listed in Table 2). With increasing depth, C_{16:0} and C_{18:0} fatty acids decrease in their relative abundance, but are still predominant among the fatty acids. C_{16:1} and C_{18:1} fatty acids decrease rapidly with depth (Figure 6). In Peruvian sediments, for example, contents of C_{16:0} and C_{18:0} fatty acids decrease from > 800 μg g⁻¹ in the first centimeter to < 10 μg g⁻¹ below 4 cm depth (Table 2). In sediments off Chile, C_{16:0} and C_{18:0} fatty acids also decrease below the first centimeter, from 28.8 to 8.4 μg g⁻¹ and from 16.2 to 5.8 μg g⁻¹, respectively (Table 2). But contrary to Namibian and Peruvian stations, C_{16:0} fatty acid content increases again at 4 cm depth (11.1 μg g⁻¹).

TABLE. 2
Contents ($\mu\text{g g}^{-1}$ dry sediment) of $\text{C}_{16:0}$ and $\text{C}_{18:0}$ fatty acids and their monounsaturated homologues found in sediments off Namibia, Peru, and Chile.

Depth [cm]	Saturated fatty acids [$\mu\text{g g}^{-1}$ dry sediment]		Monounsaturated fatty acids [$\mu\text{g g}^{-1}$ dry sediment]			
	$\text{C}_{16:0}$	$\text{C}_{18:0}$	$\text{C}_{16:1\omega7}$	$\text{C}_{16:1\omega5}$	$\text{C}_{18:1\omega9}$	$\text{C}_{18:1\omega7}$
Namibia						
0-1	145.8	24.7	68.6	6.3	14.1	93.9
1-2	38.2	10.7	12.4	1.9	6.1	20.2
4-5	8.0	6.7	-	-	0.8	0.5
6-7	6.2	5.1	-	0.1	0.1	0.2
18-20	5.7	5.0	-	-	0.6	-
Peru						
0-1	863.4	428.9	299.3	59.9	130.2	262.3
1-2	183.8	52.3	151.8	30.4	33.3	50.7
4-5	7.7	16.9	4.4	0.2	2.7	5.2
6-7	8.2	3.6	4.5	0.9	1.1	4.1
18-20	4.9	2.4	-	-	-	-
Chile						
0-1	28.8	16.2	10.5	-	9.0	22.6
1-2	8.4	5.8	4.1	-	2.7	12.7
4-5	11.1	2.0	6.5	-	4.6	14.3
6-7	3.4	3.9	0.7	-	2.3	10.8
18-20	4.4	1.4	4.3	-	1.6	3.8

$\text{C}_{16:1\omega7}$ and $\text{C}_{18:1\omega7}$ fatty acids, high contents of which are found in Namibian surface sediments (68.6 and $93.9 \mu\text{g g}^{-1}$, respectively), nearly vanish below 4 cm sediment depth (Figure 3C). In Peruvian surface sediments $\text{C}_{16:1\omega7}$ fatty acid ($299.3 \mu\text{g g}^{-1}$) dominates over $\text{C}_{18:1\omega7}$ fatty acid ($262.3 \mu\text{g g}^{-1}$). Both compounds disappear below 9 cm depth (Figure 4C). In Chilean sediments $\text{C}_{16:1\omega7}$ and $\text{C}_{18:1\omega7}$ fatty acids decline below the surface layer from 10.5 to $4.1 \mu\text{g g}^{-1}$ and from 22.6 to $12.7 \mu\text{g g}^{-1}$, respectively. However, in contrast to Namibia and Peru, contents increase again in 4 cm (6.5 and $14.3 \mu\text{g g}^{-1}$, respectively), as well as in 9 cm sediment depth (5.4 and $10.1 \mu\text{g g}^{-1}$, respectively; Figure 5C).

$\text{C}_{16:0}$, $\text{C}_{18:0}$, as well as $\text{C}_{16:1\omega7}$, and $\text{C}_{18:1\omega7}$ fatty acids are known components of sulfide-oxidizing bacteria like *Beggiatoa* and *Thioploca* (McCaffrey et al. 1989; Grant 1991), but sulfate reducers are also known to synthesize fatty acids including $\text{C}_{18:1\omega9}$, $\text{C}_{16:1\omega5}$, and $\text{C}_{16:1\omega7}$ (e.g., Taylor and Parkes 1983; Dowling et al. 1986; Elvert et al. 2003; Londry et al. 2004). Furthermore, unsaturated fatty acids are common constituents in the lipid fraction of diverse phytoplankton species (e.g., diatoms) and other organisms (Volkmann et al. 1989; Viso and Marty 1993; Wakeham 1995). $10\text{MeC}_{16:0}$ and *ai*- $\text{C}_{15:0}$ fatty acids are compounds of sulfate

reducers with moderate to high source specificity. They are synthesized by various sulfate-reducing bacteria (e.g., Perry et al. 1979; Taylor and Parkes 1983; Dowling et al. 1986; see also Table 1). For the Namibian and Peruvian stations *ai*-C_{15:0} is the most abundant branched fatty acid (Figures 3B and 4B). In Namibian surface sediments *ai*-C_{15:0} fatty acid (30.2 $\mu\text{g g}^{-1}$) dominates over 10MeC_{16:0} fatty acid (17.4 $\mu\text{g g}^{-1}$). *ai*-C_{15:0} fatty acid decreases rapidly below the first centimeter (Figure 3B). 10MeC_{16:0} fatty acid behaves in the same way but is no longer detectable below 5 cm depth (data not shown). In Peruvian sediments, *ai*-C_{15:0} fatty acid shows a similar profile with a high content (105.2 $\mu\text{g g}^{-1}$) in the first centimeter and a steep decrease below (Figure 4B). 10MeC_{16:0} fatty acid is only present in trace amounts in deeper sediments off Peru (data not shown). Surface sediments off Chile revealed high contents of 10MeC_{16:0} fatty acid (1.6 $\mu\text{g g}^{-1}$; Figure 5B). Other than for Namibian and Peruvian stations, increased contents of 10MeC_{16:0} fatty acid occur at 5 to 6 cm depth (1.8 $\mu\text{g g}^{-1}$), as well as at 10 cm depth (1.5 $\mu\text{g g}^{-1}$). *ai*-C_{15:0} fatty acid is only abundant in deeper Chilean sediments (below 15 cm depth) with a maximum content of 2.4 $\mu\text{g g}^{-1}$ (data not shown).

DISCUSSION

Specificity of biomarker patterns of the large sulfide oxidizers

The occurrence of large sulfide-oxidizing bacteria in upwelling regions is striking. Interestingly, different genera of sulfide oxidizers are abundant in various upwelling regions. To test a potential association of sulfide-oxidizing bacteria with biogeochemical cycles, in particular with the phosphorous cycle, of different upwelling regimes, we compared the lipid biomarker signatures of sediments off Namibia, Peru, and Chile. Typical lipids found in microbial mats of *Beggiatoa* and *Thioploca* comprise C_{14:0}, C_{16:0}, and C_{18:0} fatty acids as well as abundant monounsaturated C_{16:1 ω 7}, C_{18:1 ω 7}, and C_{18:1 ω 9} fatty acids (McCaffrey et al. 1989; Grant 1991). These fatty acids are most abundant where large sulfide-oxidizing bacteria occur in sediments from the three upwelling regions.

At the Chilean station the highest abundance of *Thioploca* was found in the uppermost sediments (Figure 7C) where also the highest contents of C_{16:1 ω 7} and C_{18:1 ω 7} fatty acids have been found (Figure 5). It is likely that these compounds predominantly derive from *Thioploca*. Other potential producers, like sulfate-reducing bacteria, are less likely to be dominant source organisms as typical biomarkers of these bacteria are more prominent at greater depth where

$C_{16:1\omega7}$ and $C_{18:1\omega7}$ fatty acids contents are much lower. Only MAGE $C_{16:0}$ has its maximum abundance at 0 to 1 cm. $10MeC_{16:0}$ fatty acid, on the other hand, does not show an increased abundance in this depth. Although the $C_{16:1\omega7}$ and $C_{18:1\omega7}$ fatty acids are of very limited source specificity, the overall biomarker pattern suggests that they predominantly derive from sulfide oxidizers. Yet, additional inputs of these compounds from allochthonous sources (e.g., phytoplankton) are also likely (see Table 1). Deeper in the Chilean sediments, the profiles of monounsaturated $C_{16:1\omega7}$, $C_{18:1\omega7}$, and $C_{18:1\omega9}$ fatty acids correlate well with the $10MeC_{16:0}$ fatty acid typically produced by sulfate-reducing bacteria (Figure 5). Here, presumably *Desulfobacter/Desulfobacula* or *Geobacter* contribute significantly to the production of monounsaturated fatty acids. Apart from smaller contributions from *Thioploca* biomass, the overall decline of unsaturated fatty acids with depth may also partially be caused by degradation, reflecting a lower stability of unsaturated compared to saturated fatty acids (cf., Canuel and Martens 1996; Sun et al. 1997).

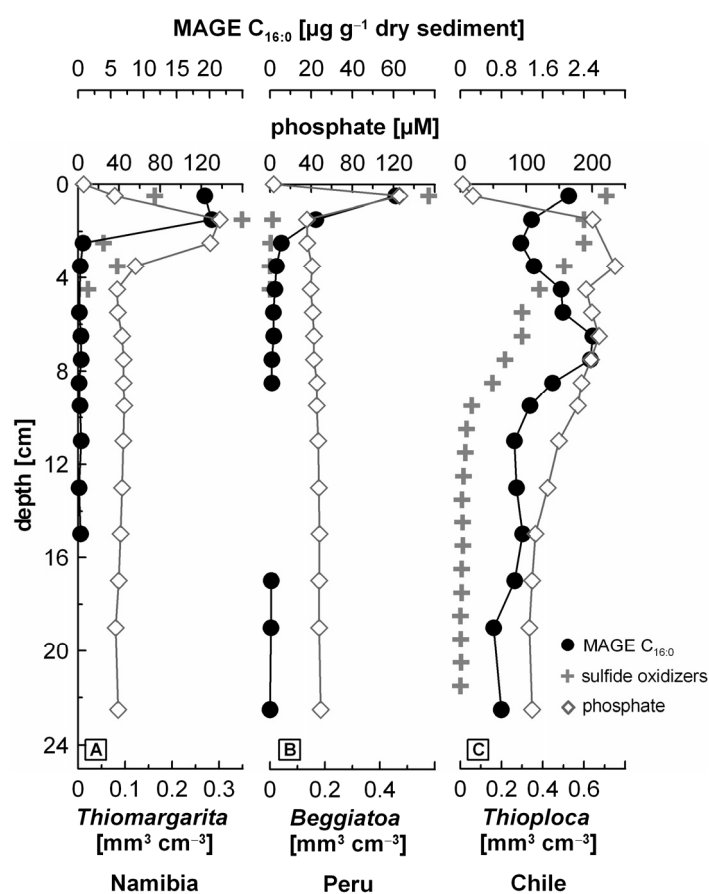


FIG. 7. Interrelation between the occurrence of large sulfide-oxidizing bacteria, mono-O-alkyl glycerol ether (MAGE), and pore water phosphate concentrations. (A) *Thiomargarita* populated sediments off Namibia. *Thiomargarita* abundance and phosphate concentrations are from Schulz and Schulz (2005). (B) *Beggiatoa* covered sediments off Peru. (C) *Thioploca* populated sediments off Chile.

In Peruvian and Namibian sediments a correlation between the occurrence of large sulfide-oxidizing bacteria and $C_{16:1}$ and $C_{18:1}$ fatty acids is obvious as well. Off Peru, *Beggiatoa* are most abundant in the first centimeter of the sediments (Figure 7B), the same applies for saturated and monounsaturated C_{16} and C_{18} fatty acids (Table 2; Figure 4). Because of significantly higher contents of these compounds compared to deeper sediments, it is most likely that a major portion of these fatty acids is derived from *Beggiatoa*. Nonetheless, *ai*- $C_{15:0}$ fatty acids and $C_{16:0}$ MAGE indicate the presence of sulfate reducers in this layer as well. The source of $C_{16:1}$ and $C_{18:1}$ fatty acids is consequently even more difficult to assess than for Chile. Highest biomass of *Thiomargarita* was found between 1 and 2 cm depth in the Namibian sediments (Figure 7A; Schulz and Schulz 2005), but highest contents of $C_{16:1}$ and $C_{18:1}$ fatty acids were found between 0 and 1 cm (Table 2). Orcutt et al. (2005) compared fatty acid signatures of sediments populated by *Beggiatoa* and *Thiomargarita*-like sulfide-oxidizing bacteria and suggested that a predominance of $C_{18:1\omega7}$ fatty acid over $C_{16:1\omega7}$ fatty acid reflects a biosignature of *Thiomargarita*. This agrees with our data. Where *Thiomargarita* are most abundant, $C_{18:1\omega7}$ fatty acid is predominating over $C_{16:1\omega7}$ fatty acid. Vice versa, the *Beggiatoa* populated Peruvian station shows a predominance of $C_{16:1\omega7}$ fatty acid over $C_{18:1\omega7}$ fatty acid. However, this might be an oversimplification of the relationship as the influence of allochthonous sources is difficult to evaluate. Moreover, the presence of *ai*- $C_{15:0}$ fatty acid and MAGE $C_{16:0}$, indicating sulfate reducers, in the same layers points to potential additional in situ sources of $C_{16:1}$ and $C_{18:1}$ fatty acids other than sulfide oxidizers.

All studied stations show variations in the depth profiles with respect to monounsaturated C_{16} and C_{18} fatty acids that correlate with the abundance of sulfide oxidizers. However, because of the low source specificity of lipids of sulfide oxidizers, it is problematic to evaluate the distribution of these bacteria based on lipid biomarkers alone.

Interaction between large sulfide oxidizers and sulfate reducers

Several studies using experimental rate measurements have found sulfate reduction to be the dominant process for anaerobic organic matter degradation in sediments of upwelling regions off Namibia, Peru, and Chile (Fossing 1990; Thamdrup and Canfield 1996; Brückert et al. 2003). Our depth profiles of biomarkers specific for sulfate reducers reveal a close relationship between these bacteria and the occurrence of large sulfide-oxidizing bacteria based on cell counts (cf., Schulz et al. 1996). Close association of sulfate-reducing bacteria and sulfide-oxidizing bacteria may indicate effective sulfur cycling, providing sulfide

oxidizers with their electron donor and preventing the accumulation of sulfide concentrations unfavorable for sulfate reducers (cf., Fukui et al. 1999). Knowledge on differences in motility and strategies of different large sulfide-oxidizing bacteria is crucial for the interpretation of our data. In sediments off Namibia and Peru, populated by *Thiomargarita* and *Beggiatoa*, sulfate reducers are abundant in surface sediments and rapidly decline in abundance with depth. The spherical *Thiomargarita* are immotile and the required contact with nitrate or oxygen presumably happens when the loose diatom ooze of the Namibian shelf episodically becomes suspended (Schulz et al. 1999). When the sediment settles down again, sulfide oxidation takes place (Schulz and Jørgensen 2001). *Beggiatoa* grow as free filaments in mats at the oxygen/sulfide transition zone of highly sulfidic sediments (Schulz and Jørgensen 2001). *Thioploca*, on the other hand, form bundles surrounded by a common sheath, which penetrate many centimeters deep into the sediments. Individual filaments are able to glide up and down and thereby commute between the sediment surface, where they take up nitrate, and several centimeters depth to oxidize sulfide (Jørgensen and Gallardo 1999; Schulz and Jørgensen 2001). Because of this high vertical motility of *Thioploca*, profiles of Chilean sediments (Figure 5) are more complex compared to those of Namibian and Peruvian sediments where sulfate reducers are mostly present in a narrow zone at the sediment-water interface (Figure 3 and 4). On the Chilean shelf, sulfate reducers are not so highly concentrated in the near-surface sediment but are also abundant at 5 to 7 cm and at 10 cm depth as indicated by the distribution of MAGE C_{16:0}.

Not only do distributions of sulfate reducers differ in the studied stations, different types of sulfate reducers also appear to be responsible for organic matter remineralization. While in Namibian and Peruvian sediments *Desulfosarcina* seem to predominate as indicated by the abundance of *ai*-C_{15:0} fatty acid (Table 1), off Chile these bacteria appear to be less common. Here, the higher content of 10MeC_{16:0} fatty acid is in accordance with *Desulfobacter* or *Desulfobacula* as the dominant sulfate reducers (Table 1). The distribution patterns of sulfate reducers are apparently influenced by the chemical environment created by the large sulfide-oxidizing bacteria. Profiles of *ai*-C_{15:0} fatty acid and MAGEs indicate that MAGE-synthesizing bacteria and *Desulfosarcina* are even closer coupled to the large sulfide-oxidizing bacteria than *Desulfobacter/Desulfobacula*. At the Namibian and Peruvian stations the abundance of MAGEs correlates well with the distribution of sulfide oxidizers. In the *Thioploca* populated Chilean sediments, the correlation between MAGEs and the density of *Thioploca* is less obvious. MAGEs peak close to the surface and also deeper in the sediment. This might be related to the variable distribution of cells as a function of the motility of

Thioploca. *Thioploca* are most abundant near the surface and penetrate several centimeters into the sediment. A good correlation exists between the near-surface enrichment of MAGEs and the enrichment of monounsaturated C_{16:1ω7} and C_{18:1ω7} fatty acids, arguing for a coexistence of large sulfide-oxidizing bacteria and MAGE-synthesizing sulfate reducers even in the case of the Chilean sediments. It is highly unlikely that the MAGEs have been produced by sulfide oxidizers, as these compounds have not been identified in sulfide-oxidizing bacteria. Several studies on methane seeps and hydrothermal sediments reported the occurrence of MAGEs. Interestingly, *Beggiatoa* or other large sulfide-oxidizing bacteria are always present at those sites (Hinrichs et al. 2000; Orphan et al. 2001; Teske et al. 2002; Elvert et al. 2005). Teske et al. (2002) analyzed three cores from hydrothermal sediments in the Guaymas Basin, reporting MAGEs only in core sections containing *Beggiatoa*. These observations agree with our hypothesis that MAGE-synthesizing sulfate reducers may be closely associated with sulfide oxidizers. Fukui et al. (1999) and Jørgensen and Gallardo (1999) observed a close association between *Desulfonema* and *Thioploca*. *Desulfonema* sometimes grow densely in an oriented manner on the surface of *Thioploca* sheaths. Based on our data and previous observations, it is obvious that MAGEs derive from other sulfate reducers than branched 10MeC_{16:0} fatty acid (see Figure 5). The same seems to apply to *ai*-C_{15:0} fatty acid, which does not correlate with MAGEs (e.g., Figure 3). An exception from this pattern is found in Peruvian cores (Figure 4) where profiles of MAGEs and *ai*-C_{15:0} fatty acid correlate well.

10MeC_{16:0} fatty acid is not only known to be produced by sulfate-reducing bacteria but also by iron-reducing *Geobacter* (Zhang et al. 2003). Furthermore, some sulfate-reducing bacteria are also able to reduce iron instead of sulfate (Coleman et al. 1993; Lovley et al. 1993). Only recently it was reported that iron reducers produce hopanoids (Fischer et al. 2005; Härtner et al. 2005). Because of various potential sources of hopanoids in the upwelling sediments studied, it is impossible to assign them with certainty to iron reducers. Since there is a good correlation between hopanol and dinosterol profiles (Figure 5D), hopanol probably reflects input from the water column rather than an in situ signature generated by iron reducers. Therefore, only 10MeC_{16:0} fatty acid may be used as a biomarker indicator for potential microbial iron reduction. As a consequence of iron reduction in marine sediments, iron monosulfides are formed. Remarkably, peaks in acid volatile sulfides (AVS) were observed in Chilean sediments (Figure 5). One of the maxima was found at the sediment surface, correlating with the 10MeC_{16:0} fatty acid peak. A second peak of AVS was located at 6 to 7 cm and correlated with the second 10MeC_{16:0} fatty acid maximum at 5 to 6 cm depth

(Figure 5). Iron oxides and hydroxides can be also reduced abiotically with sulfide, produced during sulfate reduction (e.g., Berner 1984). In Peruvian and Namibian sediments no similar indication for dissimilatory iron reducers was found, as 10MeC_{16:0} fatty acid only occurs in low abundance. At both sites the profiles of 10MeC_{16:0} fatty acid and *ai*-C_{15:0} fatty acid correlate well, suggesting that sulfate reducers produce both fatty acids. Assuming similar environmental conditions in all studied sediments, this could be taken as an argument for a predominance of abiotic iron reduction and production of 10MeC_{16:0} fatty acid by sulfate reducers in Chilean sediments. Similarly, Thamdrup and Canfield (1996) reported that microbial iron reduction is only a minor process at the Chilean station from which our sediments were taken. Based on our data, however, we cannot rule out that iron-reducing bacteria are an additional source of 10MeC_{16:0} fatty acid. Whether or not microbial iron reduction is accompanying sulfate reduction remains to be tested by other methods.

Do benthic bacterial communities stimulate phosphogenesis in upwelling regions?

Based on lipid biomarker data from three upwelling regions, the coexistence of large sulfide-oxidizing bacteria and sulfate reducers indicates that these organisms play a key role in sulfur cycling and in remineralization of organic matter. As a result of the mineralization, nutrients, especially phosphate, become enriched in pore water (Figure 7). Additionally, abiotic or microbial iron reduction may also contribute to phosphate enrichment in the pore water. Phosphate is preferentially adsorbed to iron oxides and hydroxides and is released to the pore water when these become reduced (e.g., Froelich et al. 1988).

Profiles of biomarkers of sulfate-reducing bacteria correlate well with phosphate concentration profiles in Namibian and Peruvian sediments (Figure 7). In Chilean sediments, where *Thioploca* and associated sulfate reducers cover a wide depth range of 20 cm, no sharp peak in phosphate concentration occurs (Figure 7C). In sediments off Namibia and Peru, where large sulfide-oxidizing bacteria and associated sulfate reducers are confined to specific depth intervals, sharp peaks in pore water phosphate concentrations develop. In the Peruvian station the phosphate peak is situated just below the sediment/water interface, coinciding with the distribution of *Beggiatoa* and sulfate-reducers (Figure 7B). In Namibian sediments, the phosphate peak was found a few centimeters deeper in the sediment, which is in accordance with the *Thiomargarita* distribution and the MAGE profile (Figure 7A). Our data thus suggest that accumulation of phosphate is somehow related to the distribution of sulfate-reducing bacteria. Phosphate enrichment could be a consequence of the cooccurrence of sulfide-

oxidizing and sulfate-reducing bacteria. However, it remains to be tested whether this bacterial interaction is essential to phosphogenesis.

Several authors have suggested a co-occurrence, and thus a potential relationship, between sulfide-oxidizing bacteria and phosphogenesis (Reimers et al. 1990; Nathan et al. 1993; Krajewski et al. 1994). Only recently, a mechanism has been documented by which *Thiomargarita namibiensis* induce the accumulation of phosphorus on the Namibian shelf leading to phosphorite precipitation (Schulz and Schulz 2005). To date, the study by Schulz and Schulz (2005) is the only direct evidence for a link between large sulfide-oxidizing bacteria and phosphogenesis. Our data are in accordance with such a relationship but do not prove it.

CONCLUSIONS

Lipid biomarker data from sediments of upwelling regions reveal that the distribution of sulfate-reducing bacteria mirrors that of various large sulfide-oxidizing bacteria, as indicated by cell counts. While the relationship between sulfate reducers and sulfide oxidizers is obvious off Namibia and Peru, the pattern observed in Chilean sediments is more complex, probably due to the motility of *Thioploca*. The close spatial association of sulfide oxidizers and sulfate reducers in sediments of upwelling regimes appears to be most beneficial for the sulfide oxidizers, which benefit from the proximity of production of their electron donor. Sulfate reducers, on the other hand, are possibly favored by the consumption of sulfide, keeping its concentration in favorable limits, and possibly by solutes excreted or leaking from the sulfide oxidizers.

Sulfate-reducing bacteria are critical for organic matter remineralization in upwelling sediments populated by large sulfide-oxidizing bacteria as indicated by the distribution of mono-*O*-alkyl glycerol ethers (MAGEs), 10MeC_{16:0} fatty acid, and *ai*-C_{15:0} fatty acid. A minor contribution of iron-reducing bacteria in remineralization cannot be ruled out with our data set. In terms of biomarkers, a spatial association of sulfate-reducing bacteria and sulfide-oxidizing bacteria is most evident from profiles of MAGEs and monounsaturated fatty acids (C_{16:1ω7}, C_{18:1ω7}, and C_{18:1ω9}). The latter are the dominant lipids of sulfide oxidizers, but are unfortunately of rather low source specificity.

Phosphate enrichment in the pore waters of the sediments due to high mineralization rates favor precipitation of phosphate minerals. Sulfate reducers and sulfide oxidizers co-

occur as a result of these high mineralization rates. Their interaction leads to intense sulfur cycling in the organic rich sediments. Whether these bacteria also play an important role in triggering phosphogenesis remains to be tested.

ACKNOWLEDGEMENTS

We thank Xavier Prieto Mollar (Bremen) for his support in the lab. Further thanks go to two anonymous reviewers, Karl Föllmi (Neuchâtel), and Marcus Elvert (Bremen) for helpful comments, Victor Ariel Gallardo (Concepción, Chile) as well as other cruise participants for their support during sampling off Chile, and Brit Kockisch (Bremen) for organic carbon analysis of sediments. Financial support was provided by the “Deutsche Forschungsgemeinschaft” through the DFG-Forschungszentrum Ozeanränder, Bremen (contribution no. RCOM0550).

Address correspondence to Esther T. Arning, DFG-Forschungszentrum Ozeanränder, Universität Bremen, Postfach 330 440, D-28334, Bremen, Germany. E-mail: earning@uni-bremen.de

REFERENCES

- Ahumada R, Rudolph GA, Martinez MM. 1983. Circulation and fertility of waters in Concepción Bay. *Estuar Coast Shelf S* 16:95-105.
- Albers CS, Kattner G, Hagen W. 1996. The compositions of wax esters, triacylglycerols and phospholipids in Arctic and Antarctic copepods: evidence of energetic adaptations. *Mar Chem* 55:347–358.
- Baturin GN. 2000. Formation and evolution of phosphorite grains and nodules on the Namibian shelf, from recent to Pleistocene. In: Glenn CR, Prévot L, Lucas J, editors. *Marine authigenesis: from global to microbial*. SEPM Special Publication No. 66, pp. 185-199.
- Berelson WM, Hammond DE, Johnson KS. 1987. Benthic fluxes and the cycling of biogenic silica and carbon in two southern California borderland basins. *Geochim Cosmochim Acta* 51:1345-1363.
- Berger WH, Fischer K, Lai C, Wu G. 1987. Ocean productivity and organic carbon flux. Part I. Overview and maps of primary production and export production. SIO Ref, Univ. Calif., San Diego, La Jolla:87-130.

- Berger WH. 1989. Global maps of ocean productivity. In: Berger WH, Smetacek VS, Wefer G, editors. *Productivity of the Ocean: Present and Past*. Wiley-Interscience, pp. 429-455.
- Berner RA. 1984. Sedimentary pyrite formation: An update. *Geochim Cosmochim Acta* 48:605-615.
- Blumenberg M, Krüger M, Nauhaus K, Talbot HM, Oppermann BI, Seifert R, Pape T, Michaelis W. 2006. Biosynthesis of hopanoids by sulfate-reducing bacteria (genus *Desulfovibrio*). *Environ Microbiol* 8:1220-1227.
- Boon JJ, Rijpstra WIC, de Lange F, de Leeuw JW, Yoshioka M, Shimizu Y. 1979. The Black sea sterol: a molecular fossil for dinoflagellate blooms. *Nature* 277:125-127.
- Boone DR, Whitman WB, Rouvière P. 1993. Microbiology: diversity and taxonomy of methanogens. In: Ferry JG, editor. *Methanogenesis: ecology, physiology, biochemistry, and genetics*. Chapman and Hall, pp. 35-80.
- Brüchert V, Jørgensen BB, Neumann K, Riechmann D, Schlösser M, Schulz H. 2003. Regulation of bacterial sulfate reduction and hydrogen sulfide fluxes in the central Namibian coastal upwelling zone. *Geochim Cosmochim Acta* 67:4505-4518.
- Brüchert V, Altenbach A, Bening G, Bockelmann F, Currie B, Donath J, Dübecke A, Endler R, Erdmann S, Ertan T, Fuchs B, Klockgether G, Krüger S, Kuypers M, Lass U, Lavik G, Lilienthal S, Leipe T, Nickel G, Noli-Pearce K, Ohde T, Schulz B, Schulz H, Siegel H, Struck U, Wulf J, Zitzmann S, Zonneveld K. 2005. Cruise Report Meteor M 57/3 (March 15 – April 13, 2003, Walvis Bay-Dakar), The Benguela upwelling system. pp. 53.
- Calvert SE, Price NB. 1983. Geochemistry of Namibian sediments. In: Thiede J, Suess E, editors. *Coastal upwelling, Part A: Responses of the sedimentary regime to present coastal upwelling*. Plenum Press, pp. 333-375.
- Canuel EA, Martens CS. 1996. Reactivity of recently deposited organic matter: Degradation of lipid compounds near the sediment-water interface. *Geochim Cosmochim Acta* 60:1793-1806.
- Coleman ML, Hedrick DB, Lovley DR, White DC, Pye K. 1993. Reduction of Fe(III) in sediments by sulfate-reducing bacteria. *Nature* 361:436-438.
- Dowling NJE, Widdel F, White DC. 1986. Phospholipid ester-linked fatty acid biomarkers of acetate-oxidizing sulfate-reducers and other sulfide-forming bacteria. *J Gen Microbiol* 132:1815-1825.

- Eglinton G, Hunnemann DH, Douraghi-Zadeh K. 1968. Gas-chromatographic-mass spectrometric studies of long chain hydroxy acids: II. The hydroxy acids and fatty acids of a 5000 year old lacustrine sediment. *Tetrahedron* 24:5929-5941.
- Elvert M, Boetius A, Knittel K, Jørgensen BB. 2003. Characterization of specific membrane fatty acids as chemotaxonomic markers for sulfate-reducing bacteria involved in anaerobic oxidation of methane. *Geomicrobiol J* 20:403-419.
- Elvert M, Hopmans EC, Treude T, Boetius A, Suess E. 2005. Spatial variations of methanotrophic consortia at cold methane seeps: implications from a high-resolution molecular and isotopic approach. *Geobiology* 3:195-209.
- Emeis KC, Whelan J K, Tarafa M. 1991. Sedimentary and geochemical expression of oxic and anoxic conditions on the Peru shelf. In: Tyson RV, Pearson TH, editors. *Modern and Ancient Continental Shelf Anoxia*. Geological Society of London, pp. 155-170.
- Emeis KC, Currie B, Noli K, Shidjuu A, Bening G, Berger J, Brüchert V, Endler R, Ferdelman T, Finke N, Graco M, Haferburg G, Heyn T, Kiessling A, Lage S, Leipe T, Mollenhauer G, Sonnabend K, Stregel S, Struck U, Treppke U, Vogt T, Zenskaya T. 2000. Cruise Report Meteor 48-2 (Walvis Bay-Walvis Bay, 5-23 August, 2000) IOW.
- Fenchel T, Bernard C. 1995. Mats of colourless sulphur bacteria. I. Major microbial processes. *Mar Ecol Prog Ser* 128:161-70.
- Ferdelman TG, Lee C, Pantoja S, Harder J, Bebout BM, Fossing H. 1997. Sulfate reduction and methanogenesis in a *Thioploca*-dominated sediment off the coast of Chile. *Geochim Cosmochim Acta* 61:3065-3079.
- Ferdelman TG, Fossing H, Neumann K. 1999. Sulfate reduction in surface sediments of the southeast Atlantic continental margin between 15°38'S and 27°57'S (Angola and Namibia). *Limnol Oceanogr* 44:650-661.
- Fischer WW, Summons RE, Pearson A. 2005. Targeted genomic detection of biosynthetic pathways: anaerobic production of hopanoid biomarkers by a common sedimentary microbe. *Geobiology* 3:33-40.
- Föllmi KB. 1996. The phosphorus cycle, phosphogenesis and marine phosphate-rich deposits. *Earth Sci Rev* 40:55-124.
- Fossing H, Jørgensen BB. 1989. Measurement of bacterial sulfate reduction in sediments: evaluation of a single-step chromium reduction method. *Biogeochemistry* 8:223-245.
- Fossing H. 1990. Sulfate reduction in shelf sediments in the upwelling region off Central Peru. *Cont Shelf Res* 10:355-167.

- Fossing H, Gallardo VA, Jørgensen BB, Huettel M, Nielsen LP, Schulz H, Canfield DE, Forster S, Glud RN, Gundersen JK, Kuever J, Ramsing NB, Teske A, Thamdrup B, Ulloa O. 1995. Concentration and transport of nitrate by the mat-forming sulfur bacterium *Thioploca*. *Nature* 374:713-715.
- Froelich PN, Arthur MA, Burnett WC, Deakin N, Hensley V, Jahnke R, Kaul L, Kim K-H, Roe K, Soutar A, Vathakanon C. 1988. Early diagenesis of organic matter in Peru continental margin sediments: Phosphorite precipitation. *Mar Geol* 80:309-343.
- Fukui M, Teske A, Aßmus B, Muyzer G, Widdel F. 1999. Physiology, phylogenetic relationships, and ecology of filamentous sulfate-reducing bacteria (genus *Desulfonema*). *Arch Microbiol* 172:193-203.
- Gallardo VA. 1977. Large benthic microbial communities in sulfide biota under Peru-Chile subsurface countercurrent. *Nature* 286:331-332.
- Graeve M, Kattner G, Piepenburg D. 1997. Lipids in arctic benthos: does the fatty acid and alcohol composition reflect feeding and trophic interactions? *Polar Biol* 18:53-61.
- Grant CW. 1991. Lateral and vertical distributions of filamentous bacterial mats (*Beggiatoa* spp.) in Santa Barbara Basin, California: a modern analog for organic rich facies of the Monterey Formation. PhD Thesis, College of Natural Science and Mathematics, California State University, Long Beach.
- Härtner T, Straub KL, Kannenberg E. 2005. Occurrence of hopanoid lipids in anaerobic *Geobacter* species. *FEMS Microbiol Lett* 243:59-64.
- Hebbeln D, cruise participants. 2001. PUCK: Report and preliminary results of R/V Sonne Cruise SO 156, Valparaiso (Chile) - Talcahuano (Chile), March 29 - May 14. Fachbereich Geowissenschaften, University of Bremen, pp. 195.
- Hinrichs K-U, Summons RE, Orphan V, Sylva SP, Hayes JM. 2000. Molecular and isotopic analysis of anaerobic methane-oxidizing communities in marine sediments. *Org Geochem* 31:1685-1701.
- Huber R, Wilharm T, Huber D, Trincone A, Burggraf S, Rachel R, Rockinger I, Fricke H, Stetter KO. 1992. *Aquifex pyrophilus* gen. nov., sp. nov., represents a novel group of marine hyperthermophilic hydrogen-oxidizing bacteria. *Syst Appl Microbiol* 15:340-351.
- Huettel M, Forster S, Klöser S, Fossing H. 1996. Vertical migration in the sediment-dwelling sulfur bacteria *Thioploca* spp. in overcoming diffusion limitations. *Appl Environ Microbiol* 62:1863-1872.

- Ingall E, Jahnke R. 1994. Evidence for enhanced phosphorous regeneration from marine sediments overlain by oxygen depleted waters. *Geochim Cosmochim Acta* 58:2571-2575.
- Jørgensen BB. 1982. Mineralization of organic matter in the sea bed – the role of sulphate reduction. *Nature* 296:643-645.
- Jørgensen BB, Revsbech NP. 1983. Colorless sulfur bacteria, *Beggiatoa* spp. and *Thiovulum* spp. in O₂ and H₂S microgradients. *Appl Environ Microbiol* 45:1261-1270.
- Jørgensen BB, Gallardo VA. 1999. *Thioploca* spp.: filamentous sulfur bacteria with nitrate vacuoles. *FEMS Microbiol Ecol* 28:301-313.
- Kaneda T. 1991. *Iso*- and *anteiso*-fatty acids in bacteria: biosynthesis, function, and taxonomic significance. *Microbiol Rev* 55:288-302.
- Knoblauch C, Sahm K, Jørgensen BB. 1999. Psychrophilic sulfate-reducing bacteria isolated from permanently cold arctic marine sediments: description of *Desulfofrigus oceanense* gen. nov., sp. nov., *Desulfofrigus fragile* sp. nov., *Desulfofaba gelida* gen. nov., sp. nov., *Desulfotalea psychrophila* gen. nov., sp. nov. and *Desulfotalea arctica* sp. nov. *Int J System Bacteriol* 49:1631-1643.
- Koga Y, Nishihara M, Morii H, Akagawa-Matsushita M. 1993. Ether lipids of methanogenic bacteria: structures, comparative aspects, and biosynthesis. *Microbiol Rev* 57:164-182.
- Koga Y, Morii H, Akagawa-Matsushita M, Ohga M. 1998. Correlation of polar lipid composition with 16S rRNA phylogeny in methanogens. Further analysis of lipid component parts. *Biosci Biotech Bioch* 62:230-236.
- Krajewski KP, van Cappellen P, Trichet J, Kuhn O, Lucas J, Martín-Algarra A, Prévôt L, Tewari VC, Gaspar I, Knight RI, Lamboy M. 1994. Biological processes and apatite formation in sedimentary environments. *Eclogae Geol Helv* 87:701-745.
- Kuever J, Könneke M, Galushko A, Drzyzga O. 2001. Reclassification of *Desulfobacterium phenolicum* as *Desulfobacula phenolica* comb. nov. and description of strain Sax^T as *Desulfotignum balticum* gen. nov. *Int J System Evolution Microbiol* 51:171-177.
- Langworthy TA, Holzer G, Zeikus JG, Tornabene TG. 1983. *Iso*- and *anteiso* branched glycerol diethers of thermophilic anaerob *Thermodesulfotobacterium commune*. *Syst Appl Microbiol* 4:1-17.
- Londry KL, Jahnke LL, Des Marais DJ. 2004. Stable carbon isotope ratios of lipid biomarkers of sulfate-reducing bacteria. *Appl Environ Microbiol* 70:745-751.
- Lovley DR, Roden EE, Phillips EJP, Woodward JC. 1993. Enzymatic iron and uranium reduction by sulfate-reducing bacteria. *Mar Geol* 113:41-53.

- Lückge A, Reinhardt L. 2000. CTD measurements in the water column off Peru. In: Kudrass HR, editor. Cruise Report SO147 Peru Upwelling: Valparaiso- Callao, 29.05.-03.07.2000. BGR Hannover, pp. 35-37.
- Martin WR, Bender M, Leinen M, Orchardo J. 1991. Benthic organic carbon degradation and biogenetic silica dissolution in the central equatorial Pacific. Deep-Sea Res Pt I 38:1481-1516.
- McCaffrey MA, Farrington JW, Repeta DJ. 1989. Geochemical implications of the lipid composition of *Thioploca* spp. from the Peru upwelling region - 15°S. Org Geochem 14:61-68.
- Müller PJ, Suess E. 1979. Productivity, sedimentation-rate, and sedimentary organic-matter in the oceans 1: Organic-carbon preservation. Deep-Sea Res 26:1347-1362.
- Murphy J, Riley JP. 1962. A modified single solution method for determination of phosphate in natural waters. Analyt Chim Acta 27:31-36.
- Naraoka H, Ishiwatari R. 2000. Molecular and isotopic abundances of long-chain *n*-fatty acids in open marine sediments of the western North Pacific. Chem Geol 165: 23–36.
- Nathan Y, Bremner JM, Lowenthal RE, Monteiro P. 1993. Role of bacteria in phosphorite genesis. Geomicrobiol J 11:69-76.
- Nelson DC, Jørgensen BB, Revsbech NP. 1986. Growth-pattern and yield of a chemoautotrophic *Beggiatoa* sp. in oxygen-sulfide microgradients. Appl Environ Microbiol 52:225-233.
- Nichols PD, Guckert JB, White DC. 1986. Determination of monounsaturated fatty acid double-bond position and geometry for microbial monocultures and complex consortia by capillary GC-MS of their dimethyl disulphide adducts. J Microbiol Meth 5:49-55.
- Orcutt B, Boetius A, Elvert M, Samarkin V, Joye SB. 2005. Molecular biogeochemistry of sulfate reduction, methanogenesis and the anaerobic oxidation of methane at Gulf of Mexico cold seeps. Geochim Cosmochim Acta 69:4267-4281.
- Orphan VJ, Hinrichs K-U, Ussler W, Paull CK, Taylor LT, Sylva SP, Hayes JM, DeLong EF. 2001. Comparative analysis of methane-oxidizing archaea and sulfate-reducing bacteria in anoxic marine sediments. Appl Environ Microbiol 67:1922-1934.
- Otte S, Kuenen JG, Nielsen LP, Paerl HW, Zopfi J, Schulz HN, Teske A, Strotmann B, Gallardo VA, Jørgensen BB. 1999. Nitrogen, carbon, and sulfur metabolism in natural *Thioploca* samples. Appl Environ Microbiol 65:3148-3157.
- Ourisson G, Rohmer M, Poralla K. 1987. Prokaryotic hopanoids and other polyterpenoid sterol surrogates. Annu Rev Microbiol 41:301-333.

- Pancost RD, Bouloubassi I, Aloisi G, Sinninghe Damsté JS, the Medinaut Shipboard Scientific Party. 2001. Three series of non-isoprenoidal dialkyl glycerol diethers in cold-seep carbonate crusts. *Org Geochem* 32:695–707.
- Pantoja S, Lee C. 2003. Amino acid remineralization and organic matter lability in Chilean coastal sediments. *Org Geochem* 34:1047-1056.
- Perry GJ, Volkman JK, Johns RB. 1979. Fatty acids of bacterial origin in contemporary marine sediments: *Geochim Cosmochim Acta* 43:1715-1725.
- Raiswell R, Canfield DE. 1996. Rates of reaction between silicate iron and dissolved sulfide in Peru Margin sediments. *Geochim Cosmochim Acta* 60:2777-2787.
- Reimers CE, Suess E. 1983. Spatial and temporal patterns of organic matter accumulation on the Peru continental margin. In: Suess E, Thiede J, editors. *Coastal Upwelling-Its Sediment Record, Part B: Sedimentary records of ancient coastal upwelling*. Plenum Press, pp. 311-345.
- Reimers CE, Kastner M, Garrison RE. 1990. The role of bacterial mats in phosphate mineralization with particular reference to the Monterey Formation. In: Burnett WC, Riggs SR, editors. *Phosphate Deposits of the World*, vol. 3. Cambridge Univ. Press, pp. 300-311.
- Rohmer M, Bissleret P, Neunlist S. 1992. The hopanoids, prokaryotic triterpenoids and precursors of ubiquitous molecular fossils. In Moldowan JM, Albrecht P, Philp RP, editors. *Biological Markers in Sediments and Petroleum*. Prentice-Hall, pp. 1-17.
- Rütters H, Sass H, Cypionka H, Rullkötter J. 2001. Monoalkylether phospholipids in the sulfate reducing bacteria *Desulfosarcina variabilis* and *Desulforhadus amnigenus*. *Arch Microbiol* 176:435-442.
- Sass A, Rütters H, Cypionka H, Sass H. 2002. *Desulfobulbus mediterraneus* sp. nov., a sulfate-reducing bacterium growing on mono- and disaccharides. *Arch Microbiol* 177:468-474.
- Schenau SJ, Slomp CP, De Lange GJ. 2000. Phosphogenesis and active Phosphorite formation in sediments from the Arabian Sea oxygen minimum zone. *Mar Geol* 169:1-20.
- Schmaljohann R, Drews M, Walter S, Linke P, von Rad U, Imhoff JF. 2001. Oxygen-minimum zone sediments in the northeastern Arabian Sea off Pakistan: a habitat for the bacterium *Thioploca*. *Mar Ecol-Prog Ser* 211:27-42.

- Schouten S, Hoefs MJL, Koopmans MP, Bosch H-J, Sinninghe Damsté JS. 1998. Structural characterization, occurrence and fate of archeal ether-bound acyclic and cyclic biphytanes and corresponding diols in sediments. *Org Geochem* 29:1305-1319.
- Schubert CJ, Ferdelman TG, Strotmann B. 2000. Organic matter composition and sulfate reduction rates in sediments off Chile. *Org Geochem* 31:351-361.
- Schulz HN, Jørgensen BB, Fossing HA, Ramsing NB. 1996. Community Structure of Filamentous, Sheath-Building Sulfur bacteria, *Thioploca* spp., off the Coast of Chile. *Appl Environ Microbiol* 62:1855-1862.
- Schulz HN, Brinkhoff T, Ferdelman TG, Hernández Mariné M, Teske A, Joergensen BB. 1999. Dense Populations of a Giant Sulfur Bacterium in Namibian Shelf Sediments. *Science* 284:493-495.
- Schulz HN, Jørgensen BB. 2001. Big Bacteria. *Annu Rev Microbiol* 55: 105-137.
- Schulz HN, Schulz HD. 2005. Large sulfur bacteria and the formation of phosphorite. *Science* 307:416-418.
- Shannon LV. 1985. The Benguela ecosystem, Part I: Evolution of the Benguela, physical features and processes. *Oceanogr Mar Biol* 23:105-182.
- Shannon LV, Agenbag JJ, Buys MEL. 1987. Large- and mesoscale features of the Angola-Benguela front. *S Afr J Mar Science* 65:11-34.
- Simoneit BRT. 1978. The organic chemistry of marine sediments. In: Riley JP, Chester R, editors. *Chemical Oceanography* vol. 7. Academic Press, pp. 233-311.
- Sinninghe-Damsté JS, Rijpstra WIC, Schouten S, Fuerst JA, Jetten MSM, Strous M. 2004. The occurrence of hopanoids in planctomycetes: implications for the sedimentary biomarker record. *Org Geochem* 35:561-566.
- Sprott GD, Dicaire CJ, Choquet CG, Patel GB, Ekiel I. 1993. Hydroxydiether lipid structures in *Methanosarcina* spp. and *Methanococcus voltae*. *Appl Environ Microbiol* 59:912-914.
- Suess E, Kulm LD, Killingley JS. 1986. Coastal upwelling and a history of organic-rich mudstone deposition off Peru. In: Brooks J, Fleet AJ, editors. *Marine Petroleum Source Rocks*. Geological Society, pp. 181-197.
- Suess E, von Huene R. 1988. Ocean Drilling Program Leg 112, Peru continental margin; Part 2, Sedimentary history and diagenesis in a coastal upwelling environment. *Geology* 16:939-943.
- Suits NS, Arthur MA. 2000. Sulfur diagenesis and partitioning in Holocene Peru shelf and upper slope sediments. *Chem Geol* 163:219-234.

- Summons RE, Jahnke LL, Hope JM, Logan GA. 1999. 2-Methylhopanoids as biomarkers for cyanobacterial oxygenic photosynthesis. *Nature* 400:554-557.
- Sun M-Y, Wakeham SG, Lee C. 1997. Rates and mechanisms of fatty acid degradation in oxic and anoxic coastal marine sediments of Long Island Sound, New York, USA. *Geochim Cosmochim Acta* 61:341-355.
- Taylor J, Parkes RJ. 1983. The cellular fatty acids of the sulfate-reducing bacteria *Desulfobacter* sp., *Desulfobulbus* sp. and *Desulfovibrio desulfuricans*. *J Gen Microbiol* 129:3303-3309.
- Teske A, Hinrichs K-U, Edgcomb V, de Vera Gomez A, Kysela D, Sylva SP, Sogin ML, Jannasch HW. 2002. Microbial Diversity of Hydrothermal Sediments in the Guaymas Basin: Evidence for Anaerobic Methanotrophic Communities. *Appl Environ Microbiol* 68:1994-2007.
- Thamdrup B, Canfield DE. 1996. Pathways of carbon oxidation in continental margin sediments off central Chile. *Limnol Oceanog* 41:1629-1650.
- van Cappellen P, Ingall ED. 1996. Redox stabilization of the atmosphere and oceans by phosphorus-limited marine productivity. *Science* 271:493-496.
- Viso, A-C, Marty J-C. 1993. Fatty acids from 28 marine microalgae. *Phytochemistry* 34:1521-1533.
- Volkman JK, Jeffrey SW, Nichols PD, Rogers GI, Garland CD. 1989. Fatty acid and lipid composition of 10 species of microalgae used in mariculture. *J Exp Mar Biol Ecol* 128:219-240.
- Volkman JK, Barrett SM, Blackburn SI, Mansour MP, Sikes EL, Gelin F. 1998. Microalgal biomarkers: a review of recent research developments. *Org Geochem* 29: 1163-1179.
- Volkman JK. 2003. Sterols in microorganisms. *Appl Microbiol Biot* 60:495-506.
- Wakeham SG, Beier JA. 1991. Fatty-acid and sterol biomarkers as indicators of particulate organic matter source and alteration processes in the Black Sea. *Deep-Sea Res* 38:943-968.
- Wakeham SG. 1995. Lipid biomarkers for heterotrophic alteration of suspended particulate organic matter in oxygenated and anoxic water columns of the ocean. *Deep-Sea Res Pt I* 42:1749-1771.
- Zhang CL, Li Y, Ye Q, Fong J, Peacock AD, Blunt E, Fang J, Lovley DR, White DC. 2003. Carbon isotope signatures of fatty acids in *Geobacter metallireducens* and *Shewanella algae*. *Chem Geol* 195:17-28.

Zopfi J, Kjaer T, Nielsen LP, Jørgensen BB. 2001. Ecology of *Thioploca* spp.: Nitrate and sulfur storage in relation to chemical microgradients and influence of *Thioploca* spp. on the sedimentary nitrogen cycle. Appl Environ Microbiol 67:5530-5537.

PAPER 2:**Genesis of phosphorite crusts off Peru**

E.T. Arning¹, A. Lückge², C. Breuer³, N. Gussone³, D. Birgel¹, J. Peckmann^{1,*}

¹ MARUM, Universität Bremen, D-28334 Bremen, Germany

² Bundesanstalt für Geowissenschaften und Rohstoffe (BGR), D-30655 Hannover, Germany

³ Institut für Mineralogie, Universität Münster, D-48149 Münster, Germany

* Corresponding author. Tel.: +49 421 218 65740.

E-mail address: peckmann@uni-bremen.de (J. Peckmann).

Keywords: phosphogenesis; phosphorites; phosphooids; suboxic conditions; anoxic conditions; sulfate reduction; Peru

submitted to: Marine Geology, June 2008.

ABSTRACT

Authigenic phosphorite crusts from the shelf off Peru (9°40'S to 13°30'S) consist of a phosphooid facies and later phosphatic laminite. The crusts are made of carbonate fluorapatite, which probably formed via an amorphous precursor close to the sediment water interface as indicated by low F/P₂O₅ ratios, Ca isotopes, as well as rare earth element patterns agreeing with sea water dominated fluids. Small negative Ce anomalies and U enrichment in the laminite suggest suboxic conditions close to the sediment-water interface during its formation. Increased contents of chalcophilic elements and abundant sulfide in the phosphooid facies as well as in the laminite denote sulfate reduction and, consequently, point to episodic development of anoxic conditions during phosphogenesis. The Peruvian phosphorites formed episodically over an extended period of time lasting from Middle Miocene to Pleistocene. Miocene phosphooids show a succession of phosphatic layers with varying contents of organic matter and sulfide-rich phosphatic layers. Phosphooids supposable formed on the inner shelf as a result of episodic suspension and shifting redox conditions. Episodic anoxia in the pore water induced pyritization in the outermost carbonate fluorapatite layer. Phosphooids were later transported to the outer shelf, where subsequent laminite formation was favored under lower energy conditions. A similar succession of phosphatic layers with varying contents of organic matter and sulfide-rich layers in the laminite suggests a formation mechanism analogous to phosphooids.

INTRODUCTION

The burial of phosphorus and the subsequent formation of phosphorites (phosphogenesis) in marine sediments represent an important sink in the global phosphorus cycle. Numerous basin-scale phosphorite deposits were formed in the geological past (e.g., Trappe, 1998), as for example the Miocene Monterey Formation in California (Föllmi et al., 2005; Föllmi and Garrison, 2007). Phosphogenesis has also been observed in recent suboxic to anoxic marine sediments of ocean upwelling regions: off Namibia, Chile, Peru, in the Gulf of California, and in the Arabian Sea (Föllmi, 1996; Schenau et al., 2000). On the shelves off Namibia and Peru ongoing phosphogenesis has been reported from the late Miocene until today (Garrison and Kastner, 1990; Watkins et al., 1995; Föllmi, 1996 and references therein). The organic carbon-rich, diatomaceous sediments off Peru have often been proposed to be a modern analog for ancient upwelling sequences in the geological record. Most previous studies on phosphorites of the Peru/Chile margin dealt with crusts and nodules not older than Late

Pleistocene to Holocene (e.g., Baturin et al., 1972; Veeh, 1973; Burnett and Veeh, 1977; Burnett, 1977; Burnett et al., 1982; Garrison and Kastner, 1990; Glenn et al., 1994; Burnett et al., 2000).

The initial step in the formation of phosphorites is the supersaturation of pore water with respect to carbonate-fluorapatite (CFA, $[\text{Ca}, \text{Na}, \text{Mg}]_{10}[\text{PO}_4]_{6-x}[\text{CO}_3]_x\text{F}_y[\text{F}, \text{OH}]_2$) and its imminent precipitation. In organic matter-rich sediments from various modern upwelling regions, increased phosphate concentrations in pore waters close to the sediment-water interface have been reported (Jahnke et al., 1983; Froelich et al., 1988; Schulz and Schulz, 2005; Arning et al., 2008). Supersaturation with respect to CFA and subsequent phosphogenesis is thought to take place at an early diagenetic stage close to the sediment-water interface in the suboxic zone (Glenn et al., 1988; Froelich et al., 1988; van Cappellen and Berner, 1988; Ingall and Jahnke, 1994; Glenn et al., 1994; Föllmi, 1996; van Cappellen and Ingall, 1996; Schuffert et al., 1998; Baturin, 2000; Schulz and Schulz, 2005). Similarly, Peruvian phosphorites were proposed to have formed during early diagenesis, either at the sea floor at water depths, where the sea floor impinges the oxygen minimum zone, or in oxygen-depleted pore waters (Burnett and Veeh, 1977; Burnett, 1977).

In phosphogenic sediments, suboxic conditions establish just below the sediment-water interface, where organic matter is degraded. It is well-known that microbial degradation of organic matter influences the pore water chemistry of sediments including an increase in phosphate concentrations (e.g., Krajewski et al., 1994; Jarvis et al., 1994; Reimers et al., 1996). For this reason it is commonly assumed that microbes play a crucial role in phosphogenesis (cf., Krajewski et al., 1994). Besides organic matter degradation, dissolution of fish and whale bones, as well as phosphate release from iron oxides/hydroxides by redox pumping also can contribute to high pore water phosphate concentrations (Froelich et al., 1988; van Cappellen and Berner, 1988; Schuffert et al., 1998). Subsequently, the pristine phosphorites will either be buried or experience sediment reworking. Processes like winnowing, re-deposition and re-crystallization are able to cumulate phosphate minerals, which finally may result in the formation of substantial phosphorite accumulations (e.g., Föllmi, 1996).

In this study, petrographic, mineralogical, elemental and isotopic studies on authigenic, laminated phosphorite crusts from off Peru have been conducted. The aim of this work is to integrate the results from these different approaches in order to improve our understanding of the formation of phosphorite crusts and to provide a feasible scenario for their genesis.

REGIONAL SETTING

The hydrography in the coastal region off Peru is characterized by the equator-ward flowing Peru Chile Current from the surface down to approximately 200 m water depth and the pole-ward flowing Peru Undercurrent underneath, in water depths varying between 100 to 400 m (Hill et al., 1998; Strub et al., 1998). Persistently blowing southerly winds drive perennial upwelling off Peru. Recent major upwelling cells are located at 7° to 8°S, 11° to 12°S, and 14° to 16°S (Suess et al., 1986). An extended oxygen minimum zone is established at 50 to 650 m water depth over the shelf and slope due to the decomposition of sinking organic matter (Reimers et al., 1990; Emeis et al., 1991; Lückge and Reinhardt, 2000).

The width of the Peru shelf is in general less than 50 km except for the northern part of the investigated area, the Chimbote platform, where the shelf width extends for up to 100 km (Fig. 1). The bathymetry of the shelf region affects current velocities and consequently sediment accumulation. The Peru Undercurrent accelerates while crossing the broad and shallow Chimbote platform, leading to erosion and consequently to the development of hardgrounds on this topographic height. Sediment accumulation is restricted to regions, which are protected from the erosive bottom currents. One important area is the mud-lens off Callao (at 12°S), where undisturbed sediments have been deposited (Reinhardt et al., 2002).

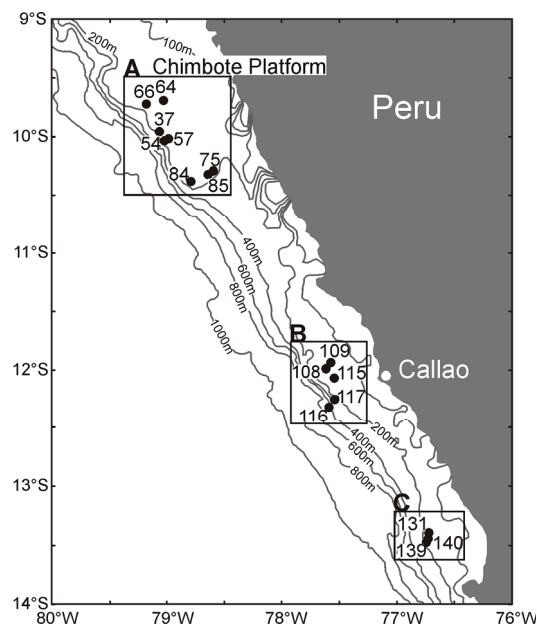


Fig. 1. Map indicating sampling sites of phosphorite crusts from the upwelling region off Peru.

MATERIAL AND METHODS

Material

Phosphatic crusts were sampled during SONNE cruise SO-147 with a TV-Grab and a box corer (Kudrass, 2000). According to the nomenclature of Garrison and Kastner (1990) these crusts correspond to D-phosphorites, which consist of well-lithified, often dark and dense nodules, gravels, and hardgrounds of carbonate-fluorapatite. The investigated samples were collected from the shelf off Peru from 9°40'S to 13°30'S in three different areas A to C (see boxes in Fig. 1). All sampling sites are located within the oxygen minimum zone (Lückge and Reinhardt, 2000). This study focuses for the most part on authigenic phosphatic crusts from area A.

Methods

Petrography and element geochemistry

Standard petrographic and fluorescence microscopy were performed on thin sections with a Zeiss Axioskop 40 A Pol equipped with a Axio-Cam MRc digital camera (University of Bremen). Element contents to characterize individual mineral phases were determined with a JXA 8900 R electron microprobe (University of Kiel). The electron microprobe is equipped with five WD spectrometers and an EDX system.

For bulk major and trace element analyses “mini-cores” (9 mm in diameter, approx. 1 g) were taken from rock slices with a hollow drill. Analyses were performed with x-ray fluorescence (XRF) using Philips PW 2400 and PW 1480 wavelength dispersive spectrometers (BGR, Hannover). Major and trace elements were quantitatively analyzed after fusion of the samples with lithiummetaborate at 1200 °C for 20 minutes (sample/LiBO₂ = 1/5). Quality of the results was controlled with certified reference materials (e.g., BCR, Community Bureau of Reference, Brussels). The precision for major elements was generally better than ± 0.5% and better than 5% for trace elements.

High resolution major and trace elements as well as rare earth elements (REE) in samples from sites A54 and A84 were analyzed on polished thin sections using an ELEMENT 2 laser-ablation inductively coupled plasma mass spectrometer (LA-ICP-MS) equipped with a UP193 laser (University of Bremen). For calibration, synthetic glass standard NIST 612 was used. Data processing was carried out with GeoPro(TM) software.

Isotope geochemistry

A profile of subsamples was drilled with a micro-drilltool from a sample of site A54. Sample powders were transferred into pre-cleaned 1.5 ml PP reaction tubes and leached for 1 h in 1 ml 0.05 N HCl to remove potentially present Ca-carbonates. The carbonate-free samples were transferred to 7 ml teflon vials and digested in 2 ml 6N HNO₃ on a hotplate at 100°C for 20 h. The sample solution was evaporated and re-dissolved in 2.5 N HCl. This solution was again dried down and recovered in 2.5 N HCl. Aliquots of the solution were used for the measurement of the Sr and Ca isotope ratios.

Strontium was purified for thermal ionization mass spectrometer (TIMS) analysis with an HCl column chemistry using 4 ml quartz columns filled with AG 50WX8 resin. The Sr-cut was evaporated and loaded on outgassed W-single-filaments with a TaF₅-activator. Strontium isotope ratios were analyzed in static mode and normalized to NBS 987 (National Bureau of Standards), whose ⁸⁷Sr/⁸⁶Sr ratio is 0.710248. A mean value of 0.710220 ± 0.000005 ($2\sigma_{\text{mean}}$, n=3) for repeated measurements of NBS 987 was obtained over the course of the study; the reproducibility (2σ) is 0.000009. All isotope ratios were normalized to a ⁸⁶Sr/⁸⁸Sr ratio of 0.1194. Measurements of recent sea water (Mulitza et al., 2007) revealed a value of 0.70914 (± 0.00001 , n=2).

For Ca isotope measurements, aliquots (~ 400 ng Ca) of the samples were mixed with a ⁴²Ca-⁴³Ca-doublespike (cf., Holmden, 2005; Gopalan et al., 2006) to correct for isotope fractionation during data acquisition in the mass spectrometer. The spike sample mixture was evaporated, recovered in 2.5 N HCl and loaded on outgassed Re-single filaments (zone refined) in sandwich technique (TaF₅-solution – sample – TaF₅-solution).

Calcium isotope ratios were determined by thermal ionization mass spectrometry. Measurements were performed in static mode, simultaneously measuring masses ⁴⁰Ca, ⁴²Ca, ⁴³Ca, and ⁴⁴Ca. Instrumental mass fractionation was corrected by an iterative approach using the routine of Heuser et al. (2002) based on the approach of Compston and Oversby (1969). The Ca isotope variations are expressed as $\delta^{44/40}\text{Ca}$ values relative to the NIST SRM 915a standard ($\delta^{44/40}\text{Ca} [\text{‰}] = ((^{44}\text{Ca}/^{40}\text{Ca})_{\text{sample}} / (^{44}\text{Ca}/^{40}\text{Ca})_{\text{SRM 915a}} - 1) * 1000$) and as $\delta^{\text{mu}}\text{Ca}$ ($\delta^{\text{mu}}\text{Ca} [\text{ppm}/\text{amu}] = 268.3 \cdot \delta^{44/40}\text{Ca}$ (Gussone et al., 2005). The NIST SRM 1486 standard (phosphate, bone) was regularly measured and revealed a $\delta^{44/40}\text{Ca}$ and $\delta^{\text{mu}}\text{Ca}$ value of -0.90‰ ($2\sigma_{\text{m}} \pm 0.025 \text{‰}$, n=8) and $-242 (\pm 7) \text{ ppm}/\text{amu}$, respectively, and a 2 S.D. of $\pm 0.07\text{‰}$ ($19 \text{ ppm}/\text{amu}$). Strontium and calcium isotope ratios were determined on a Thermo-Finnigan Triton T1

thermal ionization mass spectrometer (Zentrallabor für Geochronologie der Universität Münster).

RESULTS

Petrography

Different D-phosphorite (cf., Garrison and Kastner, 1990) crusts and nodules have been found in the three investigated areas A to C (Fig. 1). Phosphorite crusts from the Chimbote Platform (Area A, Fig. 2A, B) are mainly composed of two phases: (1) a phosphooid facies (Fig. 2A, B) consisting of phosphooids, phosphatic coated siliceous grains, fish bone fragments, and phosphatic peloids and (2) phosphatic laminite (Fig. 2A, B). The dark and dense phosphorite crusts predominantly represent hardgrounds that formed on a conglomeratic layer (Fig. 2B) and some crusts are heavily bored. In one sample from site A54, phosphatic laminite is covered by lithified phosphatic and siliceous sediments containing foraminiferal tests, shell fragments, allochthonous rock fragments and sedimentary clasts (Fig. 2A). In absence of sedimentary clasts, smooth surfaces of phosphorite crusts are developed that show a metallic glance. Phosphorites also encrust whale bones and well preserved shark teeth. Whale bones are commonly coated with a thin phosphatic layer. They are heavily bored by microborers from their surface inwards; the tubular borings are 3 to 4 μm in diameter. The tubes are partly filled with sulfide minerals.

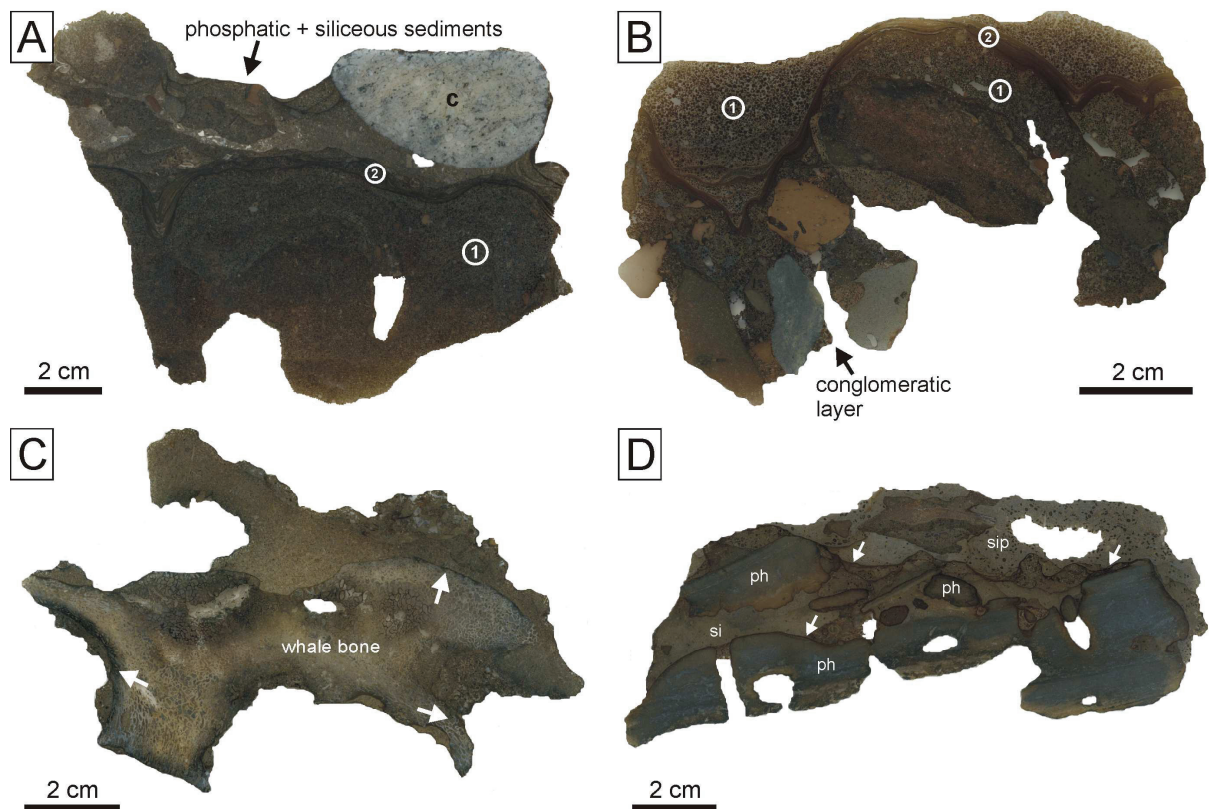


Fig. 2. Scanned thin sections of Peruvian phosphorite crusts. (A) and (B) Phosphorite crusts from area A (cf., Fig. 1) are mainly composed of the phosphooid facies (1) and phosphatic laminites (no. 2); c: volcanic clast. (C) Whale bone from area B encrusted by phosphatic phases. Arrows point to the altered outer parts of the whale bone, which are heavily bored by microborers. The tubes of the microborers are partly filled with pyrite (dark rim). (D) Phosphorite crust from area C, consisting of allochthonous phosphatic fragments (ph), and siliceous sediments (si). Siliciclastic siltstone (sip), containing structureless phosphatic peloids and phosphate-coated fish bones overlies these crusts. Arrows point to thin microlaminated phosphatic coatings.

Phosphorites from areas B and C significantly differ from the Chimbote platform (Area A) phosphorites in containing less authigenic phosphatic phases by volume (Table 1). In area B, phosphorites encrust whale bones and cement gray sand/silt. The whale bones in area B are similarly altered like the ones in area A, heavily bored by microborers, and borings are partly refilled by sulfide minerals (Fig. 2C). Phosphorite crusts from area C consist of phosphatic allochthonous fragments and siliceous sediments, which are encrusted by thin microlaminated phosphatic coatings. These crusts are overlain by grey siliciclastic siltstone, containing structureless phosphatic peloids and phosphate-coated fish bones (Fig. 2D). Other crusts consist of grey siliciclastic silt, are cavernous, and exhibit thin microlaminated phosphatic coatings. Phosphatic nodules from area C resemble nodules described by Burnett (1977).

Table 1 Comparison of general petrographic characteristics of the three investigated areas A, B, and C.

	Area A	Area B	Area C
phosphooids and other coated grains	very abundant	sparse, only in some samples present	not present
phosphoritic laminae	thick layers of laminated phosphoritic crusts, thin hardground forming crusts within phosphooid facies	thin laminae between clasts and different phosphate generations	thin laminae between clasts
glauconite	sporadic as nucleus of phosphooids, between phosphooids in some samples	present in all samples, in some samples abundant, partly associated with authigenic sulfides and a later phosphatic phase	abundant, partly associated with authigenic sulfides and a later phosphatic phase
pyrite and other sulfides	abundant in laminae and in depressions of laminae between phosphooids	abundant	abundant
detrital quartz borings	sparse present, walls lined with thick phosphorite laminae	abundant present, only thin phosphatic laminae line walls	very abundant present, but sparse, walls lined with thin, irregular phosphatic laminae
clasts	sparse, small (mm)	abundant, different lithified sediments (cm)	abundant different lithified sediments (cm)

Phosphatic crusts and nodules obtained from areas B and C are predominantly of allochthonous origin. In contrast, phosphorite crusts from area A are chiefly authigenic. Therefore petrographical as well as biogeochemical analyses will focus on the authigenic phosphorite crusts of area A.

Phosphooid facies

Phosphooids are the major compound identified in this lithologic unit. Most of the ooids are ovoid and 100 to 500 μm in diameter. They are typified by a distinct concentric zonation consisting of alternating light brown and dark brown phosphatic layers. Light brown layers as well as coatings of light phosphatic cement around the ooids exhibit a strong autofluorescence, while dark brown layers are hardly fluorescent (Fig. 3A, B). The concentric layers are irregular to different degrees. Layer thickness varies between 10 to 20 μm . Some layers thicken and thin out or are even discontinuous. The phosphatic layers consist of CFA. In the dark layers varying amounts of pyrite are present (Fig. 4).

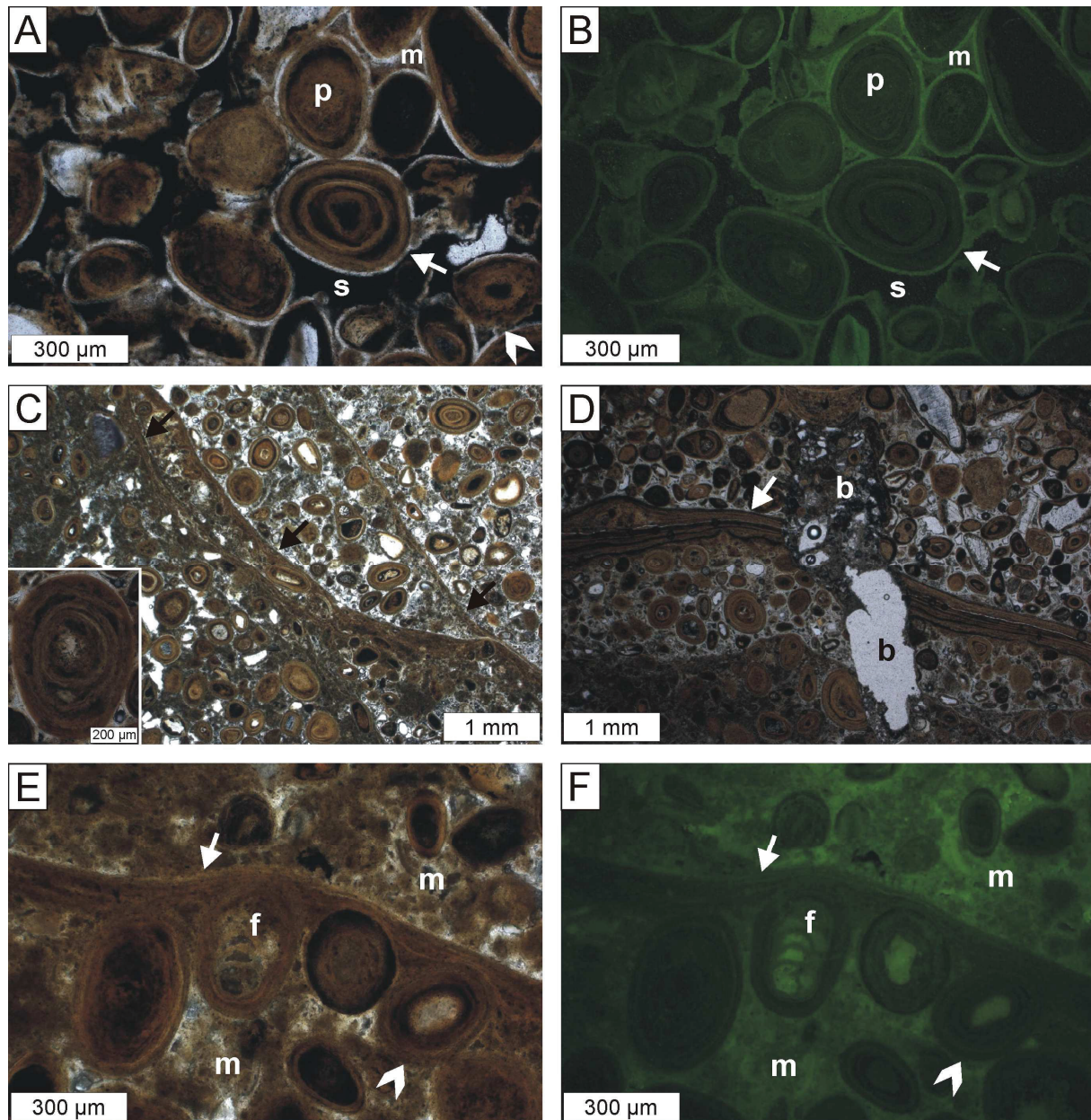


Fig. 3. Photomicrographs of the phosphooid facies. (A) Concentric phosphooids (arrow), consisting of alternating light brown and dark phosphatic layers, and coated phosphatic peloids (p) in a phosphatic matrix (m). In places, interstitial sulfides (s) are present. (B) Same detail as (A); fluorescence image. Light brown layers and phosphatic matrix (m) show strong autofluorescence. (C) Individual layers of phosphooids are separated by thin phosphatic laminae (arrows). Phosphooids have different nuclei including partly altered and sometimes heavily bored fish bone fragments, siliciclastic grains, and structureless phosphatic peloids. Inset: phosphooid with irregular phosphatic layers around a heavily bored fish bone fragment. (D) Phosphatic laminae accumulated to a thicker package of alternating light brown and dark phosphatic layers (arrow). Boring (b) penetrating the phosphooid facies and phosphatic laminae (arrow). (E) Microlaminated phosphatic laminae (arrow) exhibit an irregular lower boundary, a planar, smooth top, and partly encase phosphooids. Arrowhead points to a phosphooid without nucleus; f: foraminifers, m: light friable phosphatic matrix. (F) Same detail as (E); fluorescence image. Phosphatic laminae (arrow) with variable autofluorescence and fluorescent matrix (m).

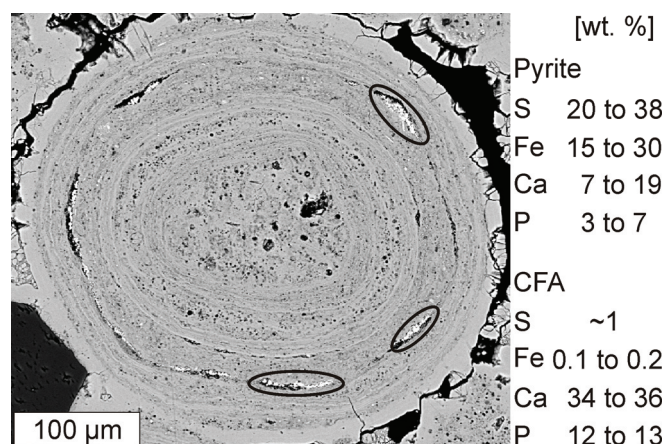


Fig. 4. Microprobe back scatter image of phosphoooid. Phosphoooid consisting of layers of carbonate fluor apatite (CFA; grey). Pyrite frambooids (bright spots, marked by black circles) are enriched in some CFA layers. Contents of S, Fe, Ca, and P are given for pyrite frambooids and CFA (wt. %).

Phosphoooids show different types of nuclei. Fish bones (sometimes heavily bored by unknown microorganisms), siliceous grains, and structureless phosphatic peloids are the most common nuclei (Fig. 3C). Only rarely glauconite grains or foraminifers serve as nuclei. Phosphoooids containing two nuclei and ooids without a nucleus (Fig. 3E, F) are scarce. Each nucleus is surrounded by multiple phosphatic layers. Minor components of the phosphoooid facies are structureless, sometimes coated, phosphatic peloids, detrital quartz grains, and fish bones, which are often bored and altered. Few foraminiferal tests, partly phosphatized, were found (Fig. 3E, F). The matrix of the phosphoooid facies consists of a light friable phosphatic phase exhibiting an intense autofluorescence (Fig. 3 E, F). Electron microprobe analyses indicate that this phase contains sulfate. Some of the interstitial space is filled by sulfide minerals (Fig. 3A, B).

Thin microlaminated phosphatic laminae sealed and thus separated different layers of phosphoooids resulting in a successive sequence (Fig. 3C). The irregular base of the laminae apparently follows the ancient microtopography of the sediment surface. Their smooth and planar top forms the base for the next layer of ooids. Laminae always partly encase ooids and are continuous on the scale of observation. Hardground forming phosphatic laminae show a weaker autofluorescence than the phosphate matrix (Fig. 3C-F).

Borings and burrows are common in the phosphoooid facies. Borings cut through phosphoooids and laminae (Fig. 3D) and are partly refilled with a later generation of sediment. The internal secondary surfaces are encrusted by later generations of phosphate. Most burrows are filled with a light laminated phosphatic phase (Fig. 5), which contains sulfide minerals and putative aggregations of organic matter. The phosphoooid facies contains

accessory interstitial glauconite (Fig. 6A). In one sample from area B abundant glauconite is present in a phosphatic foraminiferal sandstone facies, overlying thin phosphatic crusts (Fig. 6B, C). The glauconite is associated with authigenic sulfides and a phosphatic phase, which was formed during a later stage (cf., Burnett, 1980; Glenn and Arthur, 1988).

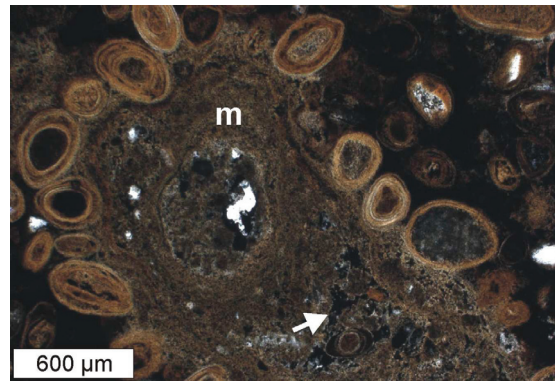


Fig. 5. Photomicrograph of a burrow in the phosphooid facies, refilled with a laminated phosphatic phase (m). Arrow points to sulfide minerals and associated aggregations of organic matter (dark).

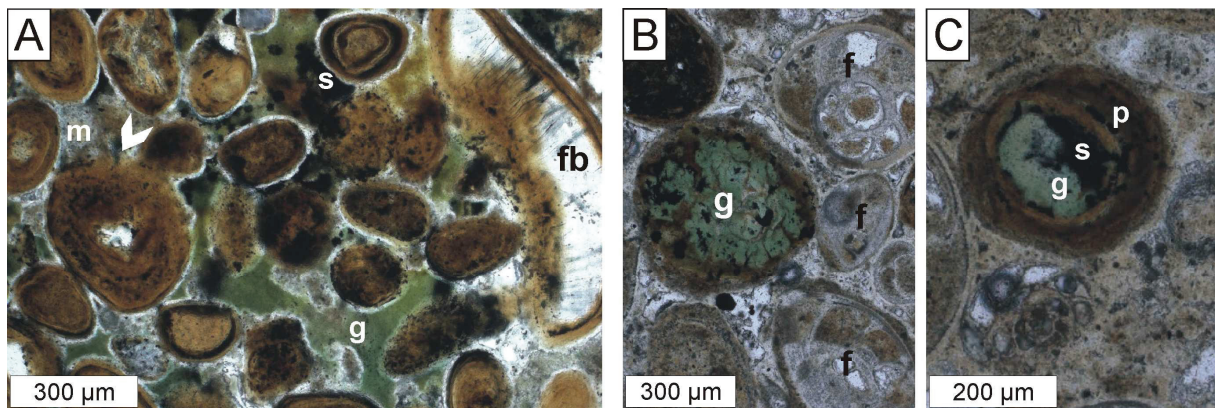


Fig. 6. Photomicrographs of glauconite phases. (A) Interstitial glauconite (g) in the phosphooid facies, partly associated with interstitial sulfide (s). Arrowhead points to the corroded outer rim of a phosphooid; m: phosphatic matrix, fb: altered fish bone fragment. (B) and (C) Glauconite (g) in phosphatic foraminiferal sandstone facies from area B associated with sulfides (s) and a surrounding phosphate phase (p); f: foraminifers.

Phosphatic laminite

Phosphatic laminite, much thicker than the individual internal laminae within the phosphooid facies, covers the phosphooid facies. Occasionally some packages of detrital sediment are intercalated in the laminite (Fig. 7A). Its matrix shows faint lamination with associated sulfide aggregates (10 to 20 µm in diameter) and strong autofluorescence (Fig. 7B, C). After cessation of sediment accumulation, laminite aggregation started again (Fig. 7A).

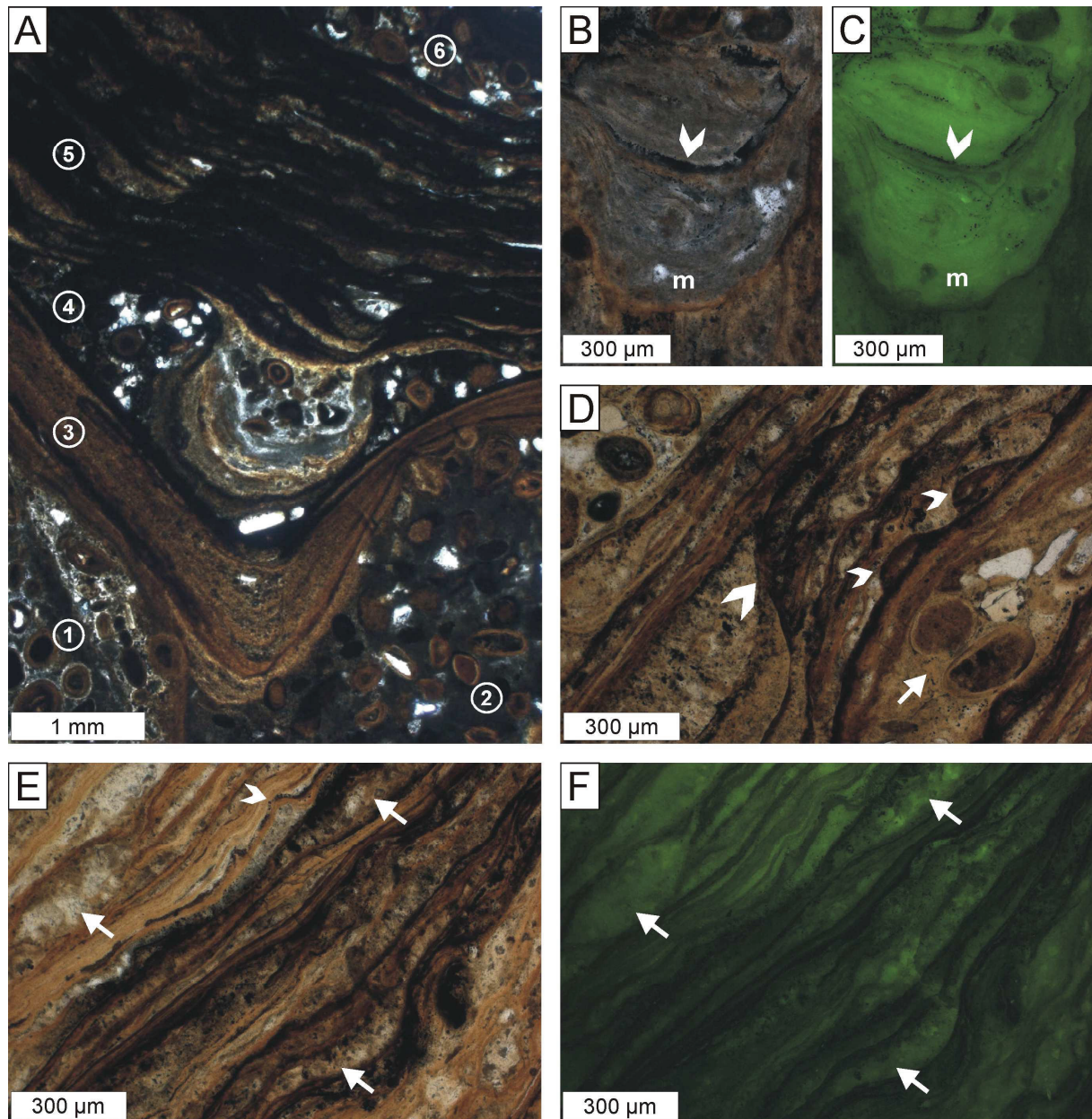


Fig. 7. Photomicrographs of phosphatic laminite. (A) The phosphooid facies (1 and 2) is sealed by phosphatic laminae (3). The phosphatic laminite (5) postdates the deposition of depression-filling phosphooids (4). In places the phosphatic laminite is covered by phosphooid facies (6). (B) Finely laminated light grey phosphatic matrix (m) of the depression-filling phosphooid facies. Arrowhead points to sulfides, arranged parallel to lamination. (C) Same detail as (B); fluorescence image. The phosphatic matrix (m) shows strong autofluorescence. (D) Laminae with smaller, second-order domes (small arrowheads) developed on larger domes (large arrowheads). Arrow points to phosphatic peloids, fish bone fragments, and detrital quartz grains bound by phosphatic layers. (E) Second-order doming and enrichment of sulfides parallel to lamination (arrowhead). Arrows point to light grey layers and lenses with enrichment. Note diffuse lower boundaries of sulfide layers. (F) Same detail as (E); fluorescence image. Light grey layers and lenses show strongest autofluorescence (arrows).

The oldest laminae (phase 3 in Fig. 7A) sealed the underlying phosphooid facies (Fig. 7A, phases 1 and 2). These laminae are characterized by more or less regular microlamination, an irregular base, and a smooth, planar top, similar to the laminae in the

phosphooid facies. Laminites tend to be thicker in depressions, mostly due to a thickening of light phosphatic laminae (Fig. 7A).

The top part of the phosphatic laminite (phase 5 in Fig. 7A) also consists of irregular light brown and dark brown layers of CFA, but is overall somewhat darker than the basal laminite. In the upper part some phosphatic lenses, which are irregularly intercalated with the layers, can be found (Fig. 7D, E). The lenses show a strong autofluorescence, whereas fluorescence of light brown layers is weaker and dark brown layers show no apparent fluorescence (Fig. 7E, F). The laminite exhibits unconformities (Fig. 7D) and some laminae show doming with smaller, second-order domes developed on larger domes (Fig. 7D). Sedimentary components, like detrital quartz grains, phosphatic peloids or fish bone fragments have been trapped and bound by some layers (Fig. 7D). Sulfide minerals are abundant in some horizons of the laminite. Remarkably, sulfides are enriched at the top of the strongly fluorescent layers and in some of the intercalated lenses. Apart from this enrichment in some layers and lenses, sulfides are only sparsely distributed in the laminite (Fig. 7D-F).

Element distribution patterns

Major, minor, and trace elements of phosphooid facies and phosphatic laminite

The P_2O_5 content ranges from 29 to 30% in the phosphooid facies. Phosphatic laminite exhibits between 27 and 28% P_2O_5 . CaO/P_2O_5 (1.57 to 1.60) is closer to CFA (1.580) than to pure fluorapatite (1.317), while F/P_2O_5 (0.086 to 0.094) is between the values of CFA (0.107) and pure fluorapatite (0.089). SO_3 (~ 5%) and Fe_2O_3 (1.3 to 1.6%) are enriched in the laminite compared to the phosphooid facies (SO_3 : ~ 3%, Fe_2O_3 : 0.5 to 0.7%) (Fig. 8, Table 2).

Chalcophilic trace elements like Zn, Cr, and Ni correlate with SO_3 and Fe_2O_3 contents and are enriched in the laminite compared to the phosphooid facies. U is also enriched in the laminite (Fig. 8). An exception displays the distribution pattern of Mo, which content increases upwards in the phosphooid facies, but again decreases in the laminite. Within and above the phosphatic laminae Mo is depleted (Fig. 8). Phosphatic laminite is also enriched in chalcophilic elements relative to the average phosphorite defined and reported in Altschuler (1980), while the phosphooid facies show lower contents than the average phosphorite. Phosphatic laminite and the phosphooid facies are both enriched in U and Sr compared to average phosphorite.

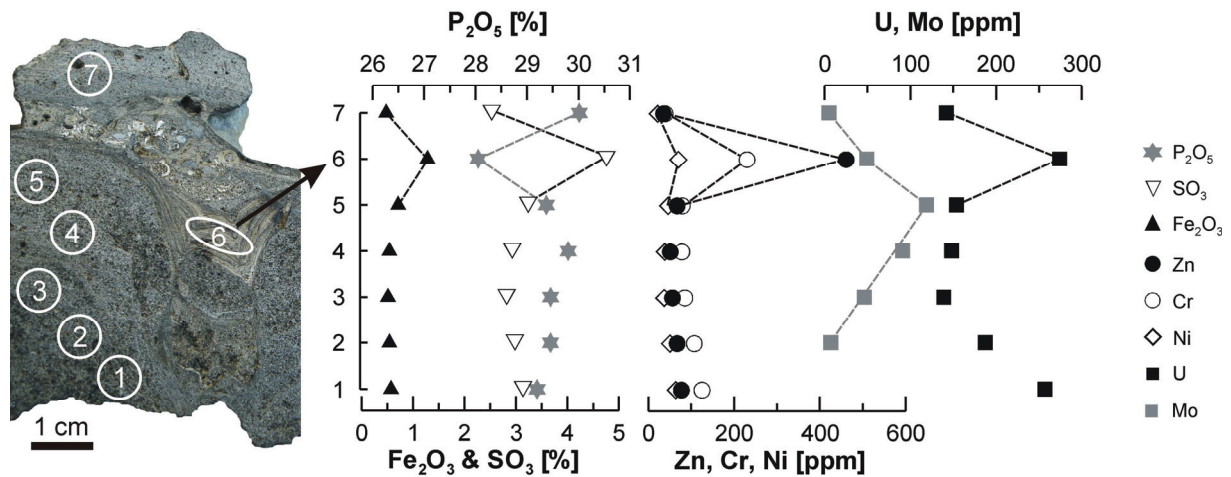


Fig. 8. Major [%], minor [%], and trace element [ppm] profiles through phosphorite crust A54-1 (cf., Tables 2, 3); (1) to (5): phosphooid facies, (6): phosphatic laminite, (7): lithified phosphatic sediment.

Table 2 Major and minor element contents (wt%) in two samples from area A, measured by XRF. OF: phosphooid facies, L: phosphatic laminite, S: lithified phosphatic sediment above phosphatic laminite.

	A54-1							A54-2					
	OF	OF	OF	OF	OF	L	S	OF	OF	OF	L	S	S
P_2O_5	29.2	29.5	29.5	29.8	29.4	28.1	30.0	29.7	29.6	29.3	27.6	23.8	24.3
CaO	46.6	46.6	46.4	46.9	46.4	44.9	48.0	47.2	47.0	46.4	44.6	45.1	45.0
F	2.7	2.7	2.7	2.6	2.6	2.6	2.7	2.6	2.7	2.5	2.4	2.3	2.3
SO_3	3.1	3.0	2.8	2.9	3.2	4.8	2.5	2.9	2.8	3.1	5.1	2.6	4.7
Fe_2O_3	0.6	0.5	0.5	0.5	0.7	1.3	0.5	0.5	0.5	0.6	1.6	0.7	2.1
Al_2O_3	0.6	0.6	0.7	0.6	0.7	0.4	0.7	0.5	0.6	0.7	0.7	1.5	0.9
K_2O	0.1	0.1	0.1	0.1	0.1	0.2	0.1	0.1	0.1	0.1	0.3	0.1	0.1
MgO	0.9	0.9	1.0	1.0	1.0	0.9	0.9	0.9	1.0	1.0	0.9	1.0	0.9
MnO	0.002	0.001	0.002	0.001	0.001	bd	0.002	bd	0.002	0.002	0.003	0.004	0.004
Na_2O	0.8	0.8	0.8	0.8	0.8	0.9	0.8	0.8	0.8	0.8	1.2	0.8	0.7
SiO_2	2.2	2.6	2.8	2.3	2.7	2.0	2.4	2.1	2.5	2.8	3.4	6.4	4.2
CaO/ P_2O_5	1.595	1.583	1.576	1.574	1.578	1.602	1.600	1.589	1.584	1.584	1.619	1.895	1.847
F/ P_2O_5	0.091	0.090	0.092	0.087	0.089	0.092	0.091	0.089	0.092	0.087	0.086	0.096	0.094
LOI ¹	13.6	12.9	13.0	12.6	12.6	14.3	11.7	12.9	12.6	12.9	12.5	16.1	14.8

bd: below detection limit

¹: lost in ignition

Detailed trace element measurements in phosphatic laminite reveal changes in trace element distribution between the individual laminae (Fig. 9). Black, irregular layers are strongly enriched in chalcophilic elements. While Zn is most abundant in the black layers 4 (1808 ppm), 8 (3611 ppm) and 9 (4311 ppm), Cu is most abundant in the black layer 14 (1500 ppm). In the smooth layers (1, 2) Cr contents are relatively high (208 and 227 ppm). In the

lighter non-enriched irregular layers (3 to 7, 10 to 13, 15) Zn is most abundant (547 to 798 ppm), in general. Fe is relatively enriched in black layers 8 (32286 ppm), 9 (22373 ppm), 11 (41299 ppm), and 14 (37416 ppm) of the phosphatic laminite. A general trend of weak autofluorescence corresponding to high contents of chalcophilic elements is apparent (Fig. 9). Sediment that fills depressions within the laminite (e.g., 16 in Fig. 9) shows rather low contents of chalcophilic trace elements. Zn contents vary from 65 to 418 ppm. Only the matrix between the phosphooids shows even lower Zn contents (27 to 30 ppm). Similarly, low Fe contents typify the sediment filling depressions (2852 to 18674 ppm) and only the phosphooid facies shows even lower Fe contents between 2710 and 7449 ppm.

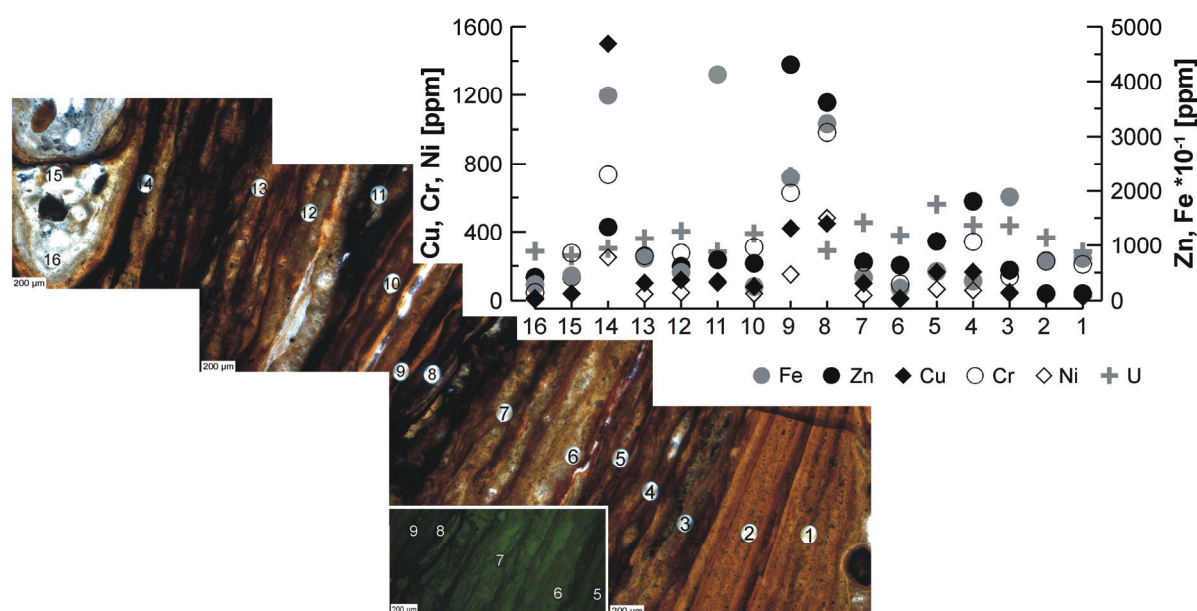


Fig. 9. High resolution trace element profiles [ppm] through a phosphatic laminite from station A54. Numbers indicate measuring spots. Inset: fluorescence image of measuring spots 5 to 9.

Rare earth elements

Rare earth elements (REE) are normalized against post-Archean shales from Australia (PAAS) reported in Taylor and McLennan (1985). Phosphatic laminae as well as the matrix between phosphooids show a flat shale-like sea water signal (Fig. 10) with weak negative Ce anomalies ranging from -0.15 to -0.39 and slight enrichments of heavy REE (cf., Elderfield and Greaves, 1982). Cerium anomalies were calculated according to Wright et al. (1987) by $Ce_{anom} = \log[3Ce_n/(2La_n + Nd_n)]$ where n signifies shale normalized contents.

The black laminae are most enriched in REE. High contents of chalcophilic elements correspond to high contents of REE. Compared to the average phosphorite defined in Altschuler (1980), only layers 9 (677 ppm) and 14 (740 ppm) show higher than average

contents. In other layers total REE contents vary between 26 and 274 ppm. Layer 6, which shows a strong autofluorescence, is significantly depleted in total REE (8 ppm) similar to the matrix. Sediments filling depressions within the laminite and the phosphooid facies exhibit total REE contents not higher than 3 ppm.

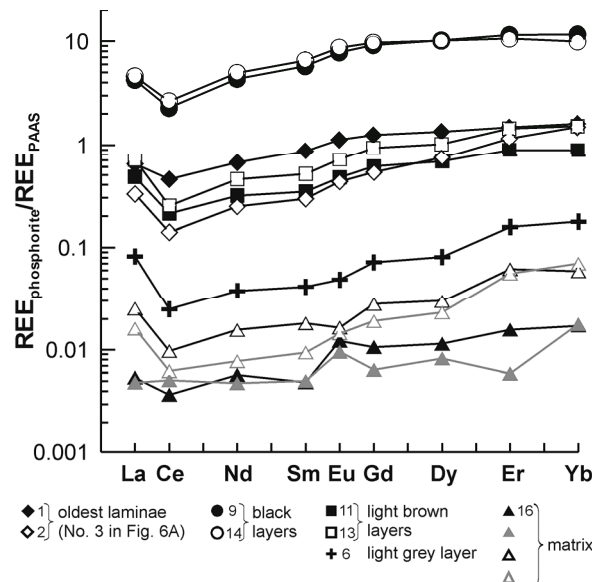


Fig. 10. Rare earth element (REE) patterns of the phosphatic laminite and phosphatic matrix of phosphorite crust from station A54. REE contents are normalized against post-Archean shales from Australia (PAAS). Numbers indicate measuring spots corresponding to spots shown in Fig. 9.

Strontium and calcium isotopes

Strontium isotope ratios ($^{87}\text{Sr}/^{86}\text{Sr}$) of the phosphorite crust show values from 0.70871 to 0.70918 (Table 3), which are in the range of Neogene sea water values. This observation indicates that the Sr of the phosphorite crusts is seawater-derived. Following this assumption, the Sr isotope composition can be used as geochronometer. Using the $^{87}\text{Sr}/^{86}\text{Sr}$ seawater evolution curves of Hodell et al. (1991), ages were calculated from the $^{87}\text{Sr}/^{86}\text{Sr}$ ratios of the respective samples (Fig. 11A). For the phosphooid facies $^{87}\text{Sr}/^{86}\text{Sr}$ indicate an age of 16.1 Ma (Middle Miocene), while the phosphatic laminite is obviously younger; the oldest laminae show a Sr age of 5.0 Ma (Pliocene). The younger laminae formed during a time of a small gradient in the Sr isotope curve of seawater. In that period the uncertainty/scatter of the $^{87}\text{Sr}/^{86}\text{Sr}$ is partially larger than the Sr isotope changes within time, resulting in some apparent age reversals. To better resolve the laminated part of the crust for comparison with Ca isotopes, Sr ages were modeled by calculating a linear regression, which reveals Pleistocene ages between 1.1 and 0.9 Ma (Table 3; Fig. 11A).

Ca isotope values range between 1.29 to 1.56‰ for $\delta^{44/40}\text{Ca}$ and 347 to 419 ppm/amu for $\delta^{\text{mu}}\text{Ca}$ (Table 3; Fig. 11B). The Ca isotope ratios of the phosphorite crusts follow the general trends of the sea water evolution curves of Heuser et al., (2005) and Sime et al. (2007) calculated from *Globigerinoides trilobus* and mixed species of planktonic foraminifera, respectively. Calcium isotope ratios of the phosphorite crusts are depleted in heavy Ca isotopes compared to those of the sea water curve.

Table 3 Sr, Ca isotopes, and measured Sr age (Ma) as well as model age (Ma) of phosphorite crust from area A (sample A54).

profile depth [mm] ¹	⁸⁷ Sr/ ⁸⁶ Sr ²	age ³ [Ma]	model age ⁴ [Ma]	$\delta^{44/40}\text{Ca}$ ⁵ [‰]	$\delta^{\text{mu}}\text{Ca}$ ⁵ [ppm/amu]
−15	0.70871	16.1	16.1	1.29	347
−10	0.70900	5.0	5.0	1.44	387
−9	0.70905	3.5	3.5	1.34	360
−7	0.70914	0.5	1.1	1.44	387
−6	0.70912	1.2	1.1	1.49	400
−3	0.70913	0.9	1.0	1.36	365
−2	0.70916	0.4	0.9	1.39	374
−1	0.70907	2.2	0.9	1.34	360
0	0.70911	1.3	0.9	1.47	395
+10	0.70918	0.1	0.5	1.56	419

¹: compare Figure 11A

²: NBS normalized

³: calculated from Sr isotopes

⁴: calculated with $Y = -0.03884x + 0.86724$ (Fig. 11A)

⁵: Ca isotopes given relative to the NIST SRM 915a, typical 2 S.D. are 0.07‰ or 19 ppm/amu

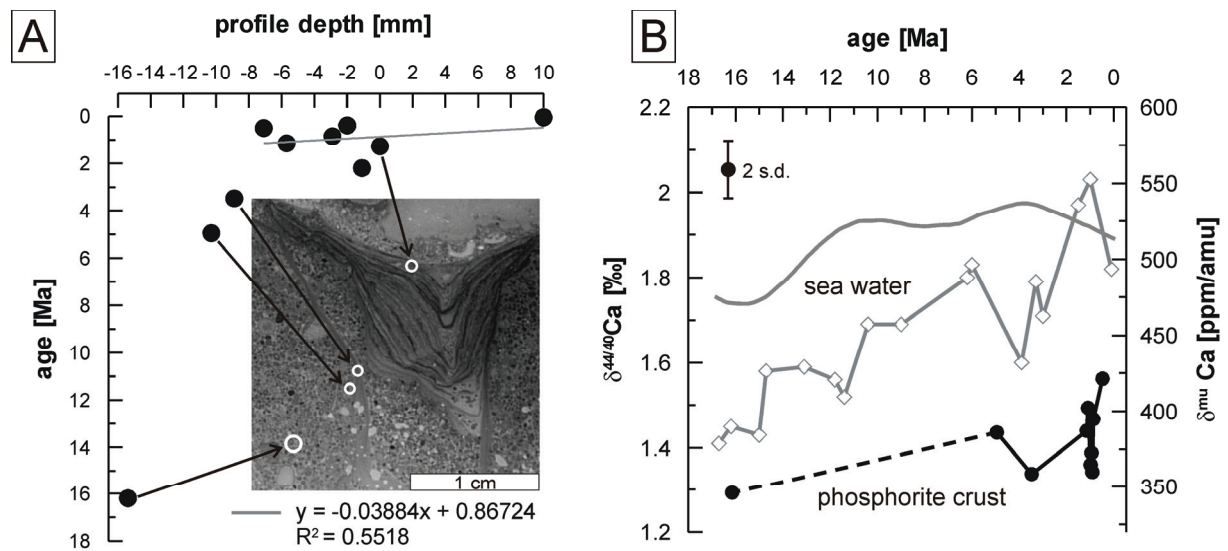


Fig. 11. (A) Strontium-ages (Ma) of a phosphorite crust from station A54. Grey line: linear regression through the phosphatic laminite. (B) Calcium isotope ratios of the same phosphorite crust from station A54 (black circles), given as $\delta^{44/40}\text{Ca}$ [‰] and as $\delta^{\text{mu}}\text{Ca}$ [ppm/amu] in comparison to global sea water evolution curves calculated from the planktonic foraminifera *Globigerinoides trilobus* (diamonds) by Heuser et al. (2005) and mixed species (grey line) by Sime et al. (2007). Age of the phosphorite crusts is calculated from strontium isotopes (cf., Fig. 11A, Table 4).

DISCUSSION

Phosphogenesis close to the sediment-water interface in the suboxic zone

Implications on the environmental setting of phosphorite formation

In the suboxic zone of sediments in upwelling areas, high rates of supersaturation of pore water with respect to CFA have been found in close proximity to the sediment-water interface, which subsequently led to rapid precipitation of CFA in this zone via an amorphous metastable precursor (e.g., amorphous calcium phosphate). A transformation of the metastable precursor into stable apatite involves the uptake of fluoride from sea water (e.g., Malone and Towe, 1970; Froelich et al., 1988; van Cappellen and Berner, 1991; Krajewski et al., 1994). $\text{CaO}/\text{P}_2\text{O}_5$ and $\text{F}/\text{P}_2\text{O}_5$ ratios of phosphorites studied here confirm a rapid formation of CFA from highly supersaturated pore waters via an amorphous precursor (see also Table 2). The observed $\text{CaO}/\text{P}_2\text{O}_5$ ratios are in accordance with ratios reported for CFA (cf., Roberts et al., 1990), while $\text{F}/\text{P}_2\text{O}_5$ ratios are significantly lower than ratios typically found for CFA (Table 2; cf., Roberts et al., 1990). This implies a lack of F in the CFA lattice compared to stoichiometrical CFA.

A formation of the Peruvian phosphorite crusts close to the sediment-water interface is also indicated by strontium and calcium isotopes (Fig. 11B), following the Sr and Ca isotope evolution curves of sea water and suggesting precipitation from a seawater dominated fluid.

Calcium isotope ratios of the phosphorite crusts are depleted in ^{40}Ca compared to the seawater, but the observed isotope fractionation between seawater and phosphate is smaller than previously reported by Schmitt et al. (2003). This difference might be related to different formation mechanisms of various phosphorite types. Schmitt et al. (2003) described peloidal phosphate grains from phosphate-rich sediments, while the present study investigates phosphorite crusts. Crusts that formed in the sediments are most likely precipitated from more closed pore water reservoirs, in which the light Ca isotopes can be increasingly depleted during precipitation by some Rayleigh-like fractionation. This effect was previously described for aragonite crusts forming at methane seeps (Teichert et al., 2005). Furthermore, the precipitation rate is an important factor, which is known to influence Ca isotope fractionation during inorganic mineral formation, as shown for inorganically-precipitated CaCO_3 (Lemarchand et al., 2004). It is therefore possible, that rapid and episodic precipitation of CFA via an amorphous precursor caused a less pronounced fractionation of Ca isotopes in the studied laminated phosphorite crusts compared to that in peloidal phosphate grains. In any case, differences in the fractionation between laminated phosphorite crusts and previous reported phosphates indicate that the fractionation of Ca isotopes between sea water and phosphates is not constant. Hence, using phosphorites for the reconstruction of Ca isotope sea water records by combining Ca isotope records of phosphates with different genesis might create artifacts in the resulting Ca isotope sea water curve.

Similarly, the REE patterns of phosphorite laminite crusts resemble REE patterns of modern sea water (Fig. 10), suggesting again precipitation from a sea water-dominated fluid. This observation also argues for phosphorite formation close to the sediment-water interface. Moreover, REE patterns of the phosphatic laminite closely resemble REE patterns of apatite pellets from phosphate-rich sediments of the Peru shelf described by Piper et al. (1988). These authors proposed a formation of the apatite pellets within the sediment and suggested that decomposed biogenic material represents the source of REE.

Redox conditions during phosphorite formation

The formation of the Miocene/Pliocene-aged phosphooid facies as well as the formation of the Pleistocene phosphatic laminite making up the Peru crusts most likely took place in the suboxic zone within the sediments (see chapter 5.1.1.). Autofluorescent organic matter inclusions in the laminae (Fig. 3F) agree with their formation within organic-rich sediments. The abundance of the redox sensitive elements Mo and U provide important information

about the redox conditions, which prevailed during formation of phosphorites, especially for the Pleistocene phosphatic laminite. U is known to be incorporated in the CFA lattice (Altschuler et al., 1958; Kolodny and Kaplan, 1970; Burnett and Veeh, 1977; Jarvis et al., 1994), which would consequently lead to an enrichment of U in phosphorites formed under suboxic conditions. In fact, it is widely accepted that suboxic sediments display sinks for U (Morford and Emerson, 1999). Mo on the other hand, only gets enriched in sediments under sulfidic conditions, with free H₂S present (Crusius et al., 1996; Morford and Emerson, 1999). In contrast to Fe, Zn, Cr, and Ni, which are enriched in the phosphatic laminite, much lower Mo contents are found compared to the phosphooid matrix, while U is showing maximum contents in the laminite (Fig. 8). Based on these element patterns, the laminite most likely formed under suboxic conditions without free H₂S. Moreover, only small negative Ce anomalies between -0.15 and -0.39 in the laminate indicate suboxic bottom water conditions. According to Wright et al. (1987), Ce anomalies of -0.1 indicate anoxic conditions, while Ce anomalies of -0.5 indicate oxic conditions. The presence of glauconite also point to suboxic conditions (Fig. 6; Odin and Matter, 1981; Bornhold and Giresse, 1985; Glenn and Arthur, 1988). An episodic shift to oxic bottom water conditions is indicated by abundant borings and burrows within the phosphooid facies (Figs. 3D, 5). With respect to the phosphooid facies, it is problematic to constrain the redox conditions from variations in U and Mo contents. Repeated reworking and transport of the phosphooids has to be taken into account, and therefore primary trace metals patterns are probably not preserved. In summary, geochemical evidence strongly suggests the presence of suboxic conditions rather than anoxic conditions close to the sediment-water interface during phosphorite formation.

Anoxic/sulfidic conditions most likely established in organic-rich layers directly underneath CFA laminae. After CFA laminae sealed subjacent organic-rich sediments, sulfate reduction became the dominant process and created anoxic/sulfidic environments. As a consequence, sulfides formed in the organic-rich matrix (Figs. 3A, B, 7B, C, 9). The early establishment of anoxic conditions and the limited supply of electron acceptors favored due to the sealing effect of laminae enhanced organic matter preservation in the phosphorite crusts. Similar mechanisms of organic matter preservation during phosphogenesis have been described by John et al. (2002) and Föllmi et al. (2005) for condensed beds in the Miocene Monterey Formation.

Accepting that phosphorite formation occurred in the suboxic zone very close to the sediment-water interface (Fig. 12B, D, E), a low net sedimentation rate is required that allows the crusts to remain in a zone favorable for phosphogenesis in contrast to fast burial (e.g.,

Filippelli, 1997). The low SiO_2 , Al_2O_3 , MgO , and K_2O contents of the Peruvian phosphorite crusts agree with little supply of terrigenous materials. Deeper in sediments, phosphogenesis is generally thought to be limited by high alkalinity that establishes due to cumulative degradation of organic matter, which favors carbonate precipitation instead of phosphogenesis (Glenn and Arthur, 1988). Likewise, the crusts from off Peru studied here reflect incomplete and relatively fast degradation of sedimentary organic matter and/or erosion (Fig. 12).

Longterm episodic formation of phosphorite crusts

Age and growth history

The mechanisms of phosphorite formation and their growth rates have received little attention so far. Burnett et al. (2000) suggested that Holocene phosphatic protocrusts form in shallow water depths in close proximity to the sediment-water interface in conjunction with a downward diffusion of phosphate from an interstitial pore water phosphate maximum. An upward growth with a rate of 7 to 9 mm ky^{-1} was proposed. Burnett et al. (1982) reported similar growth rates (<1 to 10 mm ky^{-1}) from modern phosphorite nodules off Peru, but suggested a downward growing of the nodules. Downward growth was also inferred for Pleistocene and Holocene phosphatic hardgrounds from off Peru (Garrison and Kastner, 1990; Glenn et al., 1994). In contrast to former studies of Late Pleistocene to Holocene phosphatic crusts (e.g. Baturin et al., 1972; Veeh, 1973; Burnett and Veeh, 1977; Burnett, 1977; Burnett et al., 1982; Garrison and Kastner, 1990; Glenn et al., 1994; Burnett et al., 2000), the laminated phosphorite crusts studied here formed over an extended period of time ranging from Middle Miocene to Pleistocene (Table 3, Fig. 11A). Remarkably, phosphogenesis was apparently interrupted after the formation of the Miocene phosphooid facies until phosphatic laminite formed in the Pleistocene, resulting in a significant hiatus. This hiatus can be explained either by intense erosion of formerly present phosphorite phases or the actual lack of phosphorite formation in this period of time. The latter scenario is favored by the observation that the phosphooid facies itself experienced episodic cycles of ooid formation including sedimentation of detrital particles, phosphorite aggregation, secondary mineralization (e.g., sulfides) and erosion.

Phosphooid formation

The formation of phosphooids was the initial phase in the genesis of the Miocene phosphooid facies. Phosphooids were most likely not formed in place, but presumably on the inner shelf closer the Peruvian coast. Positive Eu anomalies in the REE patterns of the phosphooid facies (Fig. 10) indicate an allochthonous magmatic rock signature and thus agree with a near shore formation. The overall low REE contents in the phosphatic matrix (Fig. 10) are also possibly related to reworking and relocation of the phosphooid facies crusts. Irregular boundaries and pronounced unconformities between single phosphooid layers indicate reworking and winnowing due to episodic undercurrent flows, storms, and/or shallow water currents associated with sea level low stands (Figs. 3A, C, 12). Remarkably, sea level low stands due to global cooling were common in the Middle Miocene (Vincent and Berger, 1985; Flower and Kennett, 1993).

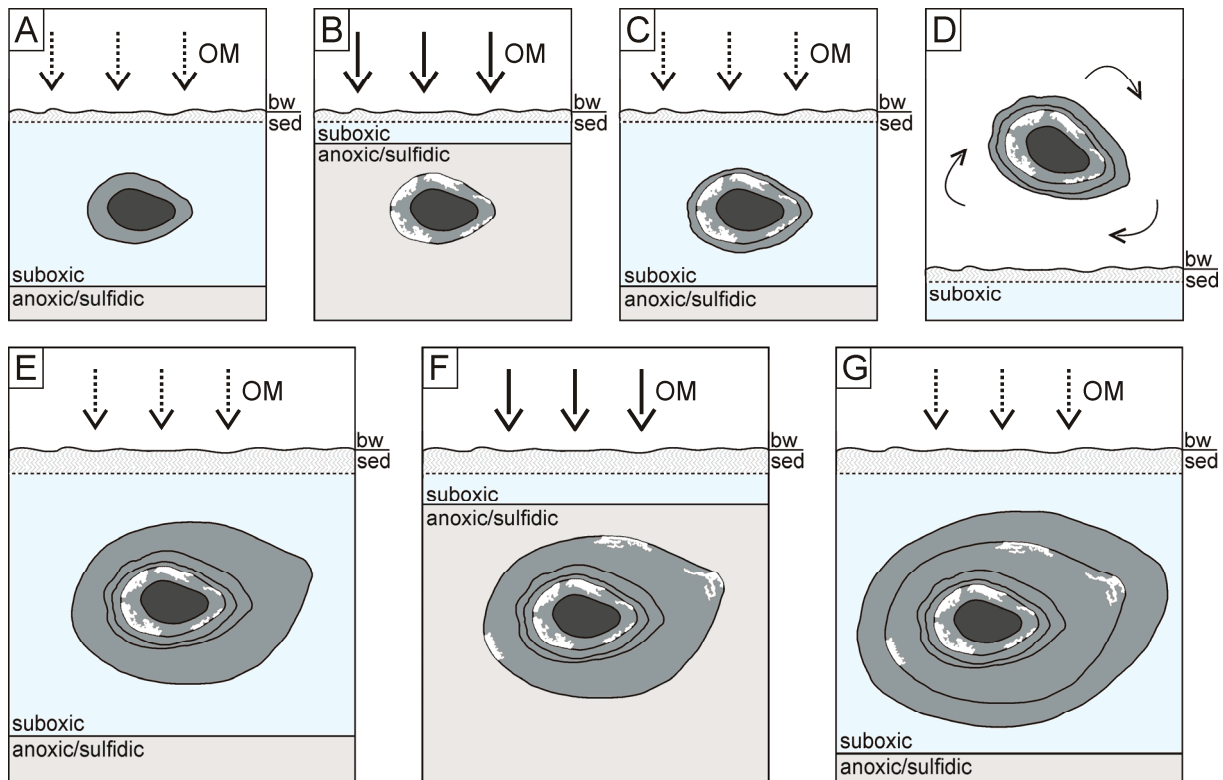


Fig. 12. Scenario of phosphooid genesis. (A) Carbonate flour apatite (CFA) layers formed in the suboxic zone close to the bottom water (bw)/sediment (sed) interface. Organic matter (OM) accumulated from the water column and was degraded. (B) During times of enhanced organic matter supply, the anoxic/sulfidic zone moved upwards. Hydrogen sulfide induced pyrite formation in the outer CFA layer. (C) Decreasing organic matter supply, and thus, a downward moving anoxic/sulfidic zone led to the formation of the next CFA layer. (D) Phosphooids were eroded, transported, and the outer CFA layer was partially abraded and corroded. (E) After the return to a lower energy regime and ooid re-deposition, CFA precipitation around phosphooids was reinitiated under the same conditions as in (A). (F) A new episode of increasing organic matter supply caused repeated pyrite formation. (G) Formation of the outermost CFA layer under conditions as in (A).

Phosphorite crusts are thought to form authigenically just below the sediment-water interface (Garrison and Kastner, 1990; Soudry, 2000; see also chapter 5.1.). Based on literature data and our own results, we propose the following scenario for phosphooid genesis (Fig. 12): Varying redox conditions and rapidly changing energy regimes were crucial to enable phosphooid formation in organic-rich phosphatic sediments off Peru. During times of quiet-water conditions, concentric layers of CFA formed around various kinds of nuclei within the suboxic sediment close to the sediment-water interface (Fig. 12A, C, E, G). Phosphooids without nuclei confirm a formation within the sediment, as it is difficult to envisage how such ooids could have formed in the water column (Fig. 3E, F). During episodes of high energy conditions, erosion, winnowing, and reworking of the phosphooids occurred (Fig. 12D). During extended times of quiet-water conditions and increased sedimentation rates of organic-rich material, anoxic-sulfidic conditions established near the sediment-water interface, in the zone of phosphooid formation. Episodic organic matter input to the sediments is mirrored by strong fluorescent layers in the phosphooids, indicating higher contents of organic material (Fig. 3B, F). Changes in pore water redox conditions induced pyritization in the outermost CFA layer of individual phosphooid layers (Fig. 12B, F). A sharp outer boundary but a more diffuse inner boundary, as well as an irregular thickness of the pyrite layer agree with pyritization in the outermost CFA layer rather than a formation of pyrite around the CFA (Figs. 3A, 4, 12). Glenn and Arthur (1988) postulated the synchronous precipitation of pyrite and CFA during an initial stage, while pyrite precipitation continued after ceasing of the CFA precipitation.

The proposed scenario of phosphooid formation (Fig. 12) is very similar to that of Pufahl and Grimm (2003). However, Pufahl and Grimm (2003) suggested formation of a pyrite layer around the phosphate grains and not pyritization in existing CFA layers during a very early diagenetic stage. Coated phosphate grains described by Pufahl and Grimm (2003) showed either pyrite laminae or indications for erosion and deposition cycles. Phosphooids of this study, on the other hand, clearly reveal that both erosion and pyritization affected the same ooids. Thus, the formation of phosphooids in the laminated Peruvian phosphorite crusts most likely resulted from the interplay between episodic shifting redox conditions within the sediments and episodic suspension and erosion cycles.

Formation of phosphorite crusts

In the Miocene, phosphooid gravity flows were deposited at the position of crust formation (Fig. 13A). Transport and reworking is corroborated by eroded outer rims of the phosphooids (Fig. 6A). After deposition of the phosphooids, thin hardground forming laminae of CFA sealed phosphooid layers (Figs. 3C, E, F, 13B). During longer time periods of non-deposition of phosphooids, thin hardgrounds accumulated to thicker packages, resulting in an upward growth of the crusts (Fig. 3D). Strong bottom currents most likely eroded the soft organic-rich sediment above phosphatic hardgrounds, leading to the planar surface of the laminae before the next phosphooid flow was deposited (Fig. 13C).

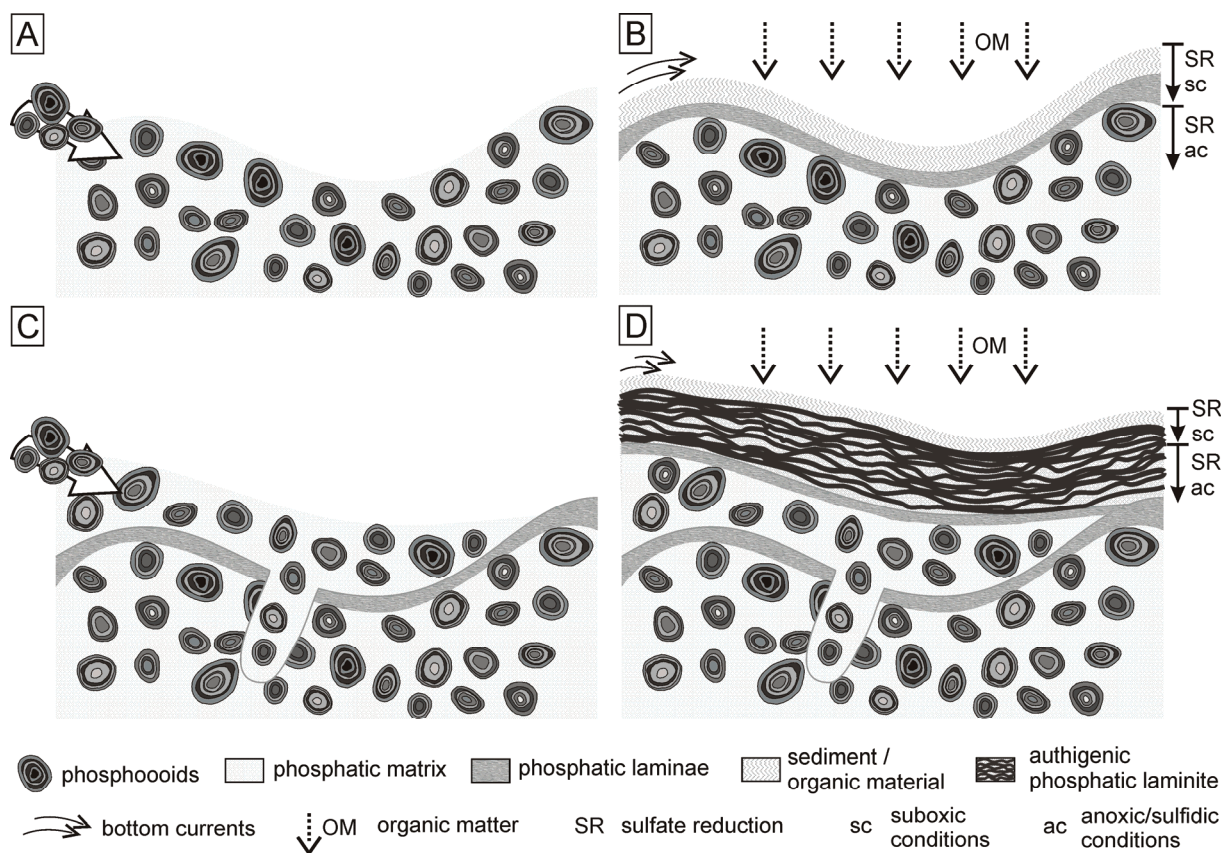


Fig. 13. Scenario of phosphorite crust formation off Peru. (A) Phosphooids were transported to the place of crust formation. (B) During quieter times, organic matter from the water column deposited. Microbial degradation of the organic material led to suboxic conditions close to the sediment-water interface and the liberation of phosphate to the pore water. Hardground forming phosphatic laminae developed and sealed subjacent phosphooid layers. Due to enhanced sulfate reduction in the sealed phosphooid layers, anoxic/sulfidic conditions established. Bottom currents eroded the soft organic matter above the phosphatic laminae from time to time. (C) During the next erosional event a subsequent phosphooid flow deposited on top of the phosphatic laminae. During times of more oxygenated bottom waters, organisms bored through the phosphatic hardgrounds. (D) The phosphatic laminite formed in the Pleistocene after a long time period without crust growth. Organic matter from the water column continuously deposited and microbial degradation led to establishment of suboxic conditions and phosphate enrichment close to the sediment-water interface. Phosphatic layers sealed organic rich layers and anoxic/sulfidic conditions developed within the laminite leading to local precipitation of sulfide minerals.

In the terminal stage of phosphorite crust formation, authigenic phosphatic laminite developed during the Pleistocene (Figs. 7, 13D). It formed on top of phosphatic hardgrounds after an extended period without phosphogenesis. The Pleistocene phosphatic laminite presumably did not grow continuously. A constant growth would reflect a growth rate of only 0.026 mm ky^{-1} , which is exceptionally low compared with growth rates of Holocene protocrusts (up to 10 mm ky^{-1}) proposed by Burnett et al. (1982). Therefore, an episodic but faster growth of the Peruvian laminite is much more likely. The pronounced layering also points to episodic growth. The phosphatic laminite consists of organic-rich, strongly fluorescent layers alternating with sulfide-rich layers (Fig. 7E, F). The laminite is significantly more enriched in sulfur, iron, zinc and other chalcophilic elements than the phosphooid facies (Fig. 8). Elemental measurements of single layers show that trace metals such as Zn, Cr, Cu, and Ni as well as Fe are strongly enriched in distinct black sulfidic layers (Fig. 9). Furthermore, layer-wise strong autofluorescence suggests an episodically increased deposition of organic matter. An enrichment of U, on the other hand, can be explained by increased degradation of organic matter (Veeh et al., 1974). Sulfides are enriched in fluorescent, organic-rich layers underneath pure phosphatic layers and show a sharp boundary at the top, but a diffuse lower boundary (Fig. 7D-F). These petrographic features suggest formation of sulfide minerals, especially pyrite, in layers with increased contents of organic matter during early diagenesis. As suggested for the phosphooid layers, an early recurrent establishment of anoxic/sulfidic conditions was probably favored by a sealing effect of subsequent phosphatic layers.

A similar succession of organic-rich layers, phosphatic layers, and sulfide-rich layers both in the laminite (Fig. 7E, F) and in the phosphooid facies (Figs. 3, 4) suggests analogous formation scenarios. The formation of laminite was presumably favored under lower energy conditions on the outer shelf, while phosphooids formed in an energetic, current-dominated sedimentary environment on the inner shelf. Bacterial mats of sulfide-oxidizing bacteria, which are particularly abundant on the Peruvian shelf (Gallardo, 1977; Fossing et al., 1995; Wieringa and Riechmann, 2002), and associated sulfate-reducing bacteria may possibly promote formation of laminites rather than phosphooids (cf., Schulz and Schulz, 2005; Arning et al., 2008). A potential relationship between sulfide-oxidizing bacteria and phosphogenesis has been previously suggested by Reimers et al. (1990), Nathan et al. (1993) and Krajewski et al. (1994). However, in order to decipher the role of prokaryotes in the genesis of phosphatic laminites, more analyses are needed including lipid biomarker studies or isotope studies.

CONCLUSIONS

Phosphorite crusts in the upwelling region off Peru formed episodically in a long time period lasting from Middle Miocene to Pleistocene. In the Middle Miocene, phosphooids formed, while authigenic laminite precipitated during the Pleistocene. Petrographical features, element patterns including trace elements and rare earth elements, as well as Sr and Ca isotope compositions provide insight into the mode of phosphogenesis and prevailing environmental conditions.

- (1) Phosphogenesis took place in suboxic sediments in the vicinity to the sediment-water interface. Slight negative Ce anomalies, U enrichment, as well as the presence of glauconite display suboxic conditions. Borings indicate that at least some oxygen must have been episodically present in the bottom water. Overall low oxygen contents agree with the predominance of suboxic conditions close to the sediment-water interface. Increased contents of chalcophilic elements, as well as abundant sulfide in phosphooid layers and laminite point to sulfate reduction and episodic anoxia in the course of phosphogenesis.
- (2) Abundant pyrite and other sulfides formed secondarily following the degradation of organic material, but still very early after organic-rich layers were sealed by subsequent phosphatic laminae. Phosphooids and laminite show similar successions of carbonate-fluorapatite layers, organic-rich carbonate-fluorapatite layers, and sulfide-rich phosphatic layers. This suggests similar formation mechanisms of both facies.
- (3) Phosphooids most likely resulted from the interplay between episodically shifting redox conditions within the sediments and episodic suspension and erosion cycles. During times of enhanced organic matter supply, changes in pore water redox conditions induced pyritization in the outermost CFA layer of individual phosphooids rather than a formation of pyrite around the CFA.
- (4) While laminite formation was favored on the outer shelf under low energy conditions, erosional surfaces and positive Eu anomalies in the phosphooid facies indicate formation on the inner shelf. Here, episodic high-energy conditions led to suspension and re-sedimentation of the phosphooids on the outer shelf, where the phosphooid facies was

encrusted by phosphatic laminite after a prolonged time without phosphorite accumulation.

ACKNOWLEDGEMENTS

We thank Sebastian Flotow for preparation of thin sections, and Benjamin Eickmann and Heike Anders (all Bremen) for their support with the LA-ICP-MS measurements. Further thanks go to Barbara Mader (Kiel) and Wolfgang Bach (Bremen) for help with the microprobe measurements. We are grateful to Alexander Heuser (Bonn) for providing the source code of the fractionation-correction routine and SRM 1486 standard material and Heide-Marie Baier (Münster) for supporting Sr and Ca isotope analyses.

Financial support was provided by the “Deutsche Forschungsgemeinschaft” through the DFG-Excellence Cluster MARUM, Bremen (contribution no. MARUMXXXX). The financial support by BMBF grant 03G0147A is gratefully acknowledged (Sonne cruise SO147).

REFERENCES

- Altschuler, Z.S., 1980. The geochemistry of trace metals in marine phosphorites: Part 1. Characteristic abundances and enrichment. In: Y.K. Bendor (Editor), *Marine Phosphorites*. SEPM special publication, no. 29. SEPM, Oklahoma, USA, pp. 19-30.
- Altschuler, Z.S., Clarke, R.S., Young, E.J., 1958. Geochemistry of uranium in apatite and phosphorite. *U.S. Geol. Surv. Prof. Pap.* 314-D.
- Arning, E.T., Birgel, D., Schulz-Vogt, H.N., Holmkvist, L., Jørgensen, B.B., Larson, A., Peckmann, J., 2008. Lipid biomarker patterns of phosphogenic sediments from upwelling regions. *Geomicrobiol. J.*, 25: 69-82.
- Baturin, G.N., 2000. Formation and evolution of phosphorite grains and nodules on the Namibian shelf, from recent to Pleistocene. In: C.R. Glenn, L. Prévot, J. Lucas (Editors), *Marine authigenesis: from global to microbial*. SEPM Special Publication No. 66. pp. 185-199.
- Baturin, G.N., Merkulov, K.I., Chalov, P.I., 1972. Radiometric evidence for recent formation of phosphatic nodules in marine shelf sediments. *Mar. Geol.*, 13: 37-43.
- Bornhold, B.D., Giresse, P., 1985. Glauconitic sediments on the continental-shelf off Vancouver Island, British-Columbia, Canada. *J. Sediment. Petrol.*, 55: 653-664.

- Burnett, W.C., 1980. Apatite-glaucinite associations off Peru and Chile - Paleooceanographic Implications. *J. Geol. Soc. London*, 137: 757-764.
- Burnett, W.C., 1977. Geochemistry and origin of phosphorite deposits from off Peru and Chile. *Geol. Soc. Am. Bull.*, 88: 813-823.
- Burnett, W.C., Beers, M.J., Roe, K.K., 1982. Growth-rates of phosphate nodules from the continental-margin off Peru. *Science*, 215: 1616-1618.
- Burnett, W.C., Glenn, C.R., Yeh, C.C., Schultz, M., Chanton, J., Kashgarian, M., 2000. U-series, ^{14}C , and stable isotope studies of recent phosphatic "protocrusts" from the Peru margin. In: C.R. Glenn, L. Prevôt-Lucas, J. Lucas (Editors), *Marine Authigenesis: from global to microbial*. SEPM Special Publications, pp. 163-183.
- Burnett, W.C. and Veeh, H.H., 1977. Uranium-series disequilibrium studies in phosphorite nodules from West Coast of South-America. *Geochim. Cosmochim. Acta*, 41: 755-764.
- Compston, W. and Oversby, V.M., 1969. Lead isotopic analysis using a double spike. *J. Geophys. Res.*, 74: 4338-4348.
- Crusius, J., Calvert, S., Pedersen, T., Sage, D., 1996. Rhenium and molybdenum enrichments in sediments as indicators of oxic, suboxic and sulfidic conditions of deposition. *Earth Planet. Sc. Lett.*, 145: 65-78.
- Elderfield, H. and Greaves, M.J., 1982. The rare-earth elements in sea-water. *Nature*, 296: 214-219.
- Emeis, K.-C., Whelan, J.K., Tarafa, M., 1991. Sedimentary and geochemical expressions of oxic and anoxic conditions on the Peru shelf. In: R.V. Tyson and T.H. Pearson (Editors), *Modern and Ancient Continental Shelf Anoxia*. Geological Society Special Publications 58, pp. 155-170.
- Filippelli, G.M., 1997. Controls on phosphorus concentration and accumulation in oceanic sediments. *Mar. Geol.*, 139: 231-240.
- Flower, B.P. and Kennett, J.P., 1993. Middle Miocene ocean climate transition: high-resolution oxygen and carbon isotopic records from Deep Sea Drilling Project Site 588A, Southwest Pacific. *Paleoceanography*, 8: 811-843.
- Föllmi, K.B., 1996. The phosphorus cycle, phosphogenesis and marine phosphate-rich deposits. *Earth-Sci. Rev.*, 40: 55-124.
- Föllmi, K.B., Badertscher, C., de Kaenel, E., Stille, P., John, C.M., Adatte, T., Steinmann, P., 2005. Phosphogenesis and organic-carbon preservation in the Miocene Monterey formation at Naples beach, California - The Monterey Hypothesis revisited. *Geol. Soc. Am. Bull.*, 117: 589-619.

- Föllmi, K.B. and Garrison, R.E., 2007. Phosphatic sediments, ordinary or extraordinary deposits? The example of the Miocene Monterey Formation (California). In: D.W. Müller, J.A. McKenzie, H. Weissert (Editors), *Controversies in modern geology: Evolution of geological theories in sedimentology, Earth History and Tectonics*. Academic Press, pp. 55-84.
- Fossing, H., Gallardo, V.A., Jørgensen, B.B., Huttel, M., Nielsen, L.P., Schulz, H., Canfield, D.E., Forster, S., Glud, R.N., Gundersen, J.K., Kuver, J., Ramsing, N.B., Teske, A., Thamdrup, B., Ulloa, O., 1995. Concentration and transport of nitrate by the mat-forming sulfur bacterium *Thioploca*. *Nature*, 374: 713-715.
- Froelich, P.N., Arthur, M.A., Burnett, W.C., Deakin, M., Hensley, V., Jahnke, R., Kaul, L., Kim, K.H., Roe, K., Soutar, A., Vathakanon, C., 1988. Early diagenesis of organic-matter in Peru continental-margin sediments - phosphorite precipitation. *Mar. Geol.*, 80: 309-343.
- Gallardo, V.A., 1977. Large benthic microbial communities in sulfide biota under Peru-Chile subsurface countercurrent. *Nature*, 268: 331-332.
- Garrison, R.E. and Kastner, M., 1990. Phosphatic sediments and rocks recovered from the Peru margin during ODP LEG 112. In: *Proceedings of the Ocean Drilling Program, Scientific Results*. pp. 111-134.
- Glenn, C.R. and Arthur, M.A., 1988. Petrology and major element geochemistry of Peru margin phosphorites and associated diagenetic minerals - authigenesis in modern organic-rich sediments. *Mar. Geol.*, 80: 231-267.
- Glenn, C.R., Arthur, M.A., Resig, J.M., Burnett, W.C., Dean, W.E., Jahnke, R.A., 1994. Are modern and ancient phosphorites really so different? In: A. Iijima, A.M. Abed, R.E. Garrison (Editors), *Siliceous, phosphatic and glauconitic Ssdiments of the Tertiary and Mesozoic*. VSP Sci. Publ., Zeist, pp. 159-188.
- Glenn, C.R., Arthur, M.A., Yeh, H.W., Burnett, W.C., 1988. Carbon isotopic composition and lattice-bound carbonate of Peru Chile margin phosphorites. *Mar. Geol.*, 80: 287-307.
- Gopalan, K., Macdougall, D., Macisaac, C., 2006. Evaluation of a Ca-42-Ca-43 double-spike for high precision Ca isotope analysis. *Int. J. Mass Spectrom.*, 248: 9-16.
- Gussone, N., Böhm, F., Eisenhauer, A., Dietzel, M., Heuser, A., Teichert, B.M.A., Reitner, J., Wörheide, G., Dullo, W.C., 2005. Calcium isotope fractionation in calcite and aragonite. *Geochim. Cosmochim. Acta*, 69: 4485-4494.

- Heuser, A., Eisenhauer, A., Böhm, F., Wallmann, K., Gussone, N., Pearson, P.N., Nagler, T.F., Dullo, W.C., 2005. Calcium isotope ($\delta^{44}\text{Ca}$) variations of Neogene planktonic foraminifera. *Paleoceanography*, 20: PA2013.
- Heuser, A., Eisenhauer, A., Gussone, N., Bock, B., Hansen, B.T., Nagler, T.F., 2002. Measurement of calcium isotopes ($\delta^{44}\text{Ca}$) using a multicollector TIMS technique. *Int. J. Mass Spectrom.*, 220: 385-397.
- Hill, E.A., Hickey, E.M., Shillington, F.A., Strub, P.T., Brink, K.H., Barton, E.D., Thomas, A.C., 1998. Eastern Ocean Boundaries. In: A.R. Robinson and K.H. Brink (Editors), *The Sea*, Vol. 11. Wiley, New York, pp. 29-67.
- Hodell, D.A., Mueller, P.A., Garrido, J.R., 1991. Variations in the strontium isotopic composition of seawater during the Neogene. *Geology*, 19: 24-27.
- Holmden, C., 2005. Measurement of $\delta^{44}\text{Ca}$ using a ^{43}Ca - ^{42}Ca double-spike TIMS Technique. Summary of Investigations 2005. *Saskatchewan Geol. Surv.*, 1: 1-7.
- Ingall, E. and Jahnke, R., 1994. Evidence for enhanced phosphorus regeneration from marine sediments overlain by oxygen depleted waters. *Geochim. Cosmochim. Acta*, 58: 2571-2575.
- Jahnke, R.A., Emerson, S.R., Roe, K.K., Burnett, W.C., 1983. The present-day formation of apatite in Mexican continental-margin sediments. *Geochim. Cosmochim. Acta*, 47: 259-266.
- Jarvis, I., Burnett, W.C., Nathan, Y., Almbaydin, F.S.M., Attia, A.K.M., Castro, L.N., Flicoteaux, R., Hilmy, M.E., Husain, V., Qutawnah, A.A., Serjani, A., Zanin, Y.N., 1994. Phosphorite geochemistry: state-of-the-art and environmental concerns. *Eclogae Geol. Helv.*, 87: 643-700.
- John, C.M., Follmi, K.B., de Kaenel, E., Adatte, T., Steinmann, P., Badertscher, C., 2002. Carbonaceous and phosphate-rich sediments of the Miocene Monterey Formation at El Capitan State Beach, California, USA. *J. Sediment. Res.*, 72: 252-267.
- Kolodny, Y. and Kaplan, I.R., 1970. Uranium isotopes in sea-floor phosphorites. *Geochim. Cosmochim. Acta*, 34: 3-24.
- Krajewski, K.P., van Cappellen, P., Trichet, J., Kuhn, O., Lucas, J., Martín-Algarra, A., Prevot, L., Tewari, V.C., Gaspar, L., Knight, R.I., Lamboy, M., 1994. Biological processes and apatite formation in sedimentary environments. *Eclogae Geol. Helv.*, 87: 701-745.
- Kudrass, H.R., 2000. Cruise Report SO-147 Peru-Upwelling: Valparaiso-Callao, 29.05.-03.07.2000. BGR Hannover, Germany.

- Lemarchand, D., Wasserburg, G.T., Papanastassiou, D.A., 2004. Rate-controlled calcium isotope fractionation in synthetic calcite. *Geochim. Cosmochim. Acta*, 68: 4665-4678.
- Lückge, A. and Reinhardt, L., 2000. CTD measurements in the water column off Peru. In: H.R. Kudrass (Editor), *Cruise Report SO147 Peru-Upwelling: Valparaiso-Callao, 29.05.-03.07.2000*. BGR Hannover, pp. 35-37.
- Malone, P.H.G. and Towe, K.M., 1970. Microbial carbonate and phosphate precipitates from seawater cultures. *Mar. Geol.*, 9: 301-309.
- Morford, J.L. and Emerson, S., 1999. The geochemistry of redox sensitive trace metals in sediments. *Geochim. Cosmochim. Acta*, 63: 1735-1750.
- Mulitza, S., Bouimetarhan, I., Brüning, M., Freesemann, A., Gussone, N., Filipsson, H., Heil, G., Hessler, S., Jaeschke, A., Johnstone, H., Klann, M., Klein, F., Küster, K., März, C., McGregor, H., Minning, M., Müller, H., Ochsenhirt, W.-T., Paul, A., Schewe, F., Schulz, M., Steinlöchner, J., Stuut, J.-B., Tjallingii, R., v.Dobeneck, T., Wiesmaier, S., Zabel, M., Zonneveld, K., 2007. Report and preliminary results of Meteor-cruise M65/1, Dakar-Dakar, 11.06.-1.07.2005, *Berichte Fachbereich Geowissenschaften*, No. 252. Universität Bremen.
- Nathan, Y., Bremner, J.M., Lowenthal, R.E., Monteiro, P., 1993. Role of bacteria in phosphorite genesis. *Geomicrobiol. J.*, 11: 69-76.
- Odin, G.S. and Matter, A., 1981. Origin of glauconites. *Sedimentology*, 28: 611-641.
- Piper, D.Z., Baedeker, P.A., Crock, J.G., Burnett, W.C., Loebner, B.J., 1988. Rare-earth elements in the phosphatic-enriched sediment of the Peru shelf. *Mar. Geol.*, 80: 269-285.
- Pufahl, P.K. and Grimm, K.A., 2003. Coated phosphate grains: Proxy for physical, chemical, and ecological changes in seawater. *Geology*, 31: 801-804.
- Reimers, C.E., Kastner, M., Garrison, R.E., 1990. The role of bacterial mats in phosphate mineralization with particular reference to the Monterey Formation. In: W.C Burnett and S.R. Riggs (Editors), *Phosphate deposits of the world: Neogene to modern phosphorites*. Cambridge University Press, pp. 300-311.
- Reimers, C.E., Rittenberg, K.C., Canfield, D.E., Christiansen, M.B., Martin, J.B., 1996. Porewater pH and authigenic phases formed in the uppermost sediments of the Santa Barbara Basin. *Geochim. Cosmochim. Acta*, 60: 4037-4057.
- Reinhardt, L., Kudrass, H.R., Lückge, A., Wiedicke, M., Wunderlich, J., Wendt, G., 2002. High-resolution sediment echosounding off Peru: Late Quaternary depositional

- sequences and sedimentary structures of a current-dominated shelf. *Mar. Geophys. Res.*, 23: 335-351.
- Roberts, W.L., Campbell, T.J., Rapp, G.R., 1990. *Encyclopedia of minerals*. Van Nostrand Reinhold, New York.
- Schenau, S.J., Slomp, C.P., de Lange, G.J., 2000. Phosphogenesis and active phosphorite formation in sediments from the Arabian Sea oxygen minimum zone. *Mar. Geol.*, 169: 1-20.
- Schmitt, A.D., Stille, P., Vennemann, T., 2003. Variations of the $^{44}\text{Ca}/^{40}\text{Ca}$ ratio in seawater during the past 24 million years: Evidence from $\delta^{44}\text{Ca}$ and $\delta^{18}\text{O}$ values of Miocene phosphates. *Geochim. Cosmochim. Acta*, 67: 2607-2614.
- Schuffert, J.D., Kastner, M., Jahnke, R.A., 1998. Carbon and phosphorus burial associated with modern phosphorite formation. *Mar. Geol.*, 146: 21-31.
- Schulz, H.N. and Schulz, H.D., 2005. Large sulfur bacteria and the formation of phosphorite. *Science*, 307: 416-418.
- Sime, N.G., de La Rocha, C.L., Tipper, E.T., Tripathi, A., Galy, A., Bickle, M.J., 2007. Interpreting the Ca isotope record of marine biogenic carbonates. *Geochim. Cosmochim. Acta*, 71: 3979-3989.
- Soudry, D., 2000. Microbial phosphate sediment. In: R.E. Riding and S.M. Awramik (Editors), *Microbial Sediments*. Springer-Verlag, pp. 127-136.
- Strub, P.T., Mesias, J.M., Montecino, V., Ruttland, J., Salinas, S., 1998. Coastal ocean circulation of Western South America. In: A.R. Robinson and K.H. Brink (Editors), *The global coastal ocean: Regional studies and syntheses*. Wiley, New York, pp. 273-314.
- Suess, E., Kulm, L.D., Killingley, J.S., 1986. Coastal upwelling and a history of organic-rich mudstone deposition off Peru. In: J. Brooks and A.J. Fleet (Editors), *Marine Petroleum Source Rocks*. The Geological Society, pp. 181-197.
- Taylor, S.R. and McLennan, S.M., 1985. *The continental crust: its composition and evolution*. Blackwell, Oxford.
- Teichert, B.M.A., Gussone, N., Eisenhauer, A., Bohrmann, G., 2005. Clathrites: Archives of near-seafloor pore-fluid evolution ($\delta^{44/40}\text{Ca}$, $\delta^{13}\text{C}$, $\delta^{18}\text{O}$) in gas hydrate environments. *Geology*, 3: 213-216.
- Trappe, J., 1998. *Phanerozoic phosphorite depositional systems - a dynamic model for a sedimentary resource system*. Springer Berlin, Heidelberg.

- van Cappellen, P. and Berner, R.A., 1988. A mathematical-model for the early diagenesis of phosphorus and fluorine in marine sediments - apatite precipitation. *Am. J. Sci.*, 288: 289-333.
- van Cappellen, P. and Ingall, E.D., 1996. Redox stabilization of the atmosphere and oceans by phosphorus-limited marine productivity. *Science*, 271: 493-496.
- van Cappellen, P. and Berner, R.A., 1991. Fluorapatite crystal-growth from modified seawater solutions. *Geochim. Cosmochim. Acta*, 55: 1219-1234.
- Veeh, H.H., 1973. Contemporary phosphorites on continental margin of Peru. *Science*, 181: 844-845.
- Veeh, H.H., Calvert, S.E., Price, N.B., 1974. Accumulation of uranium in sediments and phosphorites on the south-west African shelf. *Mar. Chem.*, 2: 189-202.
- Vincent, E. and Berger, W.H., 1985. Carbon dioxide and polar cooling in the Miocene: The Monterey hypothesis. In: E.T. Sundquist and W.S. Broecker (Editors), *The carbon cycle and atmospheric CO₂, natural variations Archean to Present*. American Geophysical Union, Geophysical Monographs, pp. 455-468.
- Watkins, R.T., Nathan, Y., Bremner, J.M., 1995. Rare earth elements in phosphorite and associated sediment from the Namibian and South African continental shelves. *Mar. Geol.*, 129: 111-128.
- Wieringa, E.B.A. and Riechmann, D., 2002. Abundance of nitrate-storing sulfur bacteria (*Thioploca* spp., *Beggiatoa* spp.) along the coast of Peru and microsensor profiling. In: H.R. Kudrass (Editor), *Peru upwelling, SONNE-cruise SO147, Final report*. BGR Hannover, Germany.
- Wright, J., Schrader, H., Holser, W.T., 1987. Paleoredox variations in ancient oceans recorded by rare-earth elements in fossil apatite. *Geochim. Cosmochim. Acta*, 51: 631-644.

PAPER 3:**Bacterial formation of phosphatic laminites off Peru**

E.T. Arning¹, D. Birgel¹, B. Brunner² and J. Peckmann¹

¹ MARUM, Universität Bremen, D-28334 Bremen, Germany

² Max-Planck-Institut für Marine Mikrobiologie, D-28359 Bremen, Germany

Corresponding author: J. Peckmann, Tel.: 0049 421 218 65740; fax: 0049 421 218 65715; e-mail: peckmann@uni-bremen.de

RRH: Bacterial phosphogenesis

Keywords: phosphorites, sulfate-reducing bacteria, sulfide-oxidizing bacteria, sulfur isotopes, lipid biomarkers, Peru

submitted to: Geobiology, August 2008

ABSTRACT

Authigenic phosphatic laminites enclosed in phosphorite crusts from the shelf off Peru (10°01'S and 10°28'S) consist of carbonate fluorapatite layers, which contain abundant sulfide minerals including pyrite (FeS₂) and sphalerite (ZnS), as well as iron oxides/hydroxides. Low $\delta^{34}\text{S}_{\text{pyrite}}$ values (average -28.8‰) agree with bacterial sulfate reduction and subsequent pyrite formation. Stable sulfur isotopic compositions of sulfate bound in carbonate fluorapatite are lower than that of sulfate from ambient sea water, suggesting bacterial reoxidation of sulfide by sulfide-oxidizing bacteria. The release of phosphorous and subsequent phosphogenesis is apparently caused by the activity of sulfate-reducing bacteria and associated sulfide-oxidizing bacteria. Following an extraction – phosphorite dissolution – extraction procedure, molecular fossils (lipid biomarkers) of sulfate-reducing bacteria (mono-*O*-alkyl glycerol ethers, di-*O*-alkyl glycerol ethers, as well as the short chain branched fatty acids *i*/*ai*-C_{15:0}, *i*/*ai*-C_{17:0}, and 10MeC_{16:0}) are found to be among the most abundant compounds. The fact that these molecular fossils of sulfate-reducing bacteria are distinctly enriched only after dissolution of the phosphorite reveals that the lipids are tightly bound to the mineral lattice of carbonate fluorapatite. This association confirms the importance of sulfate-reducing bacteria in carbonate fluorapatite precipitation. Model calculations highlight that organic matter degradation by sulfate-reducing bacteria has the potential to liberate sufficient phosphorous for phosphogenesis.

INTRODUCTION

Recent phosphogenesis (i.e. phosphorite authigenesis) has been noted to occur mainly in suboxic to anoxic marine sediments of ocean upwelling regions off Namibia, Chile, Peru, in the Gulf of California, and the Arabian Sea (Föllmi, 1996; Schenau *et al.*, 2000). On the shelves off Namibia and Peru ongoing phosphogenesis from the Late Miocene until today has been reported (Garrison & Kastner, 1990; Watkins *et al.*, 1995; Föllmi, 1996 and references therein). But so far, neither the source of phosphate of massive phosphorite deposits, nor the importance and function of microorganisms in phosphogenesis is known with certainty.

It is widely accepted that microbes increase phosphate concentrations in pore waters by degradation of organic matter, which has been taken as an argument for the involvement of bacteria in phosphogenesis (e.g. Krajewski *et al.*, 1994). In most sediments of upwelling areas, degradation of organic matter via bacterial sulfate reduction is the predominant

anaerobic respiration process (e.g. Jørgensen, 1982; Thamdrup & Canfield, 1996; Ferdelman *et al.*, 1999). In these sediments, supersaturation with respect to carbonate fluorapatite (CFA) is commonly reached. Resultant phosphogenesis is thought to be an early diagenetic process occurring close to the sediment-water interface in the suboxic zone (Froelich *et al.*, 1988; Glenn & Arthur, 1988; Glenn *et al.*, 1988; van Cappellen & Berner, 1988; Glenn *et al.*, 1994; Ingall & Jahnke, 1994; Föllmi, 1996; van Cappellen & Ingall, 1996; Schuffert *et al.*, 1998; Baturin, 2000; Schulz & Schulz, 2005). High levels of supersaturation with respect to CFA lead to its rapid precipitation via an amorphous metastable precursor, e.g. gel-like amorphous calcium phosphate. In a second step, the transformation of the precursor into stable apatite involves the uptake of fluoride from sea water (e.g. Malone & Towe, 1970; Froelich *et al.*, 1988; van Cappellen & Berner, 1991; Krajewski *et al.*, 1994; Föllmi, 1996).

A common and striking feature of many modern upwelling regions is the abundant occurrence of large colorless, nitrate-storing sulfide-oxidizing bacteria living on and in the surficial sediments. These bacteria, such as *Thioploca*, *Beggiatoa*, and *Thiomargarita*, gain energy by oxidizing sulfide using nitrate or oxygen (Schulz & Jørgensen, 2001). They are major players in the benthic sulfur cycle in reoxidizing sulfide produced by bacterial sulfate-reduction (Ferdelman *et al.*, 1997; Otte *et al.*, 1999; Jørgensen & Gallardo, 1999). Several authors have suggested a potential relationship between polyphosphate-storing bacteria and phosphogenesis (Reimers *et al.*, 1990; Nathan *et al.*, 1993; Krajewski *et al.*, 1994). Williams & Reimers (1983) found large filamentous fossils resembling sulfide-oxidizing bacteria in phosphorites of the Miocene Monterey Formation. Interestingly, spherical microfossils in the Neoproterozoic Doushantuo Formation were recently re-interpreted as phosphatized giant vacuolated sulfide-oxidizing bacteria (Bailey *et al.*, 2007). These observations provide circumstantial evidence that large sulfide oxidizers may promote phosphogenesis. Schulz & Schulz (2005) recently suggested a mechanism by which *Thiomargarita namibiensis* induces the accumulation of phosphorus leading to phosphorite formation. These bacteria have been found to be able to store polyphosphate under oxic conditions. When redox conditions episodically switch from oxic to anoxic, polyphosphate is used as an additional energy source, and phosphate is released. To date, the study by Schulz & Schulz (2005) is the only one that provides evidence for a mechanism by which large sulfide-oxidizing bacteria are linked to phosphogenesis. A follow-up study on phosphogenic sediments from upwelling regions off Namibia, Peru, and Chile revealed a close relationship between sulfide-oxidizing bacteria and sulfate-reducing bacteria (Arning *et al.*, 2008).

The aim of this work is to decipher the relevance of microbial processes, especially sulfate reduction and sulfide oxidation, in the formation of authigenic phosphorite crusts. A useful tool to extract such information from authigenic minerals and rocks are molecular fossils (i.e. lipid biomarkers), which represent fingerprints of the dominant microorganisms involved in authigenesis. In addition, stable sulfur isotopic compositions of sulfide minerals and of CFA-bound sulfate are used to obtain constraints on sulfur cycling and on environmental conditions during precipitation of CFA.

REGIONAL SETTING AND SAMPLE DESCRIPTION

Phosphatic crusts were obtained during SONNE cruise SO-147 with a TV-Grab and a box corer (Kudrass, 2000). According to the nomenclature of Garrison & Kastner (1990) the crusts represent D-phosphorites, which display well-lithified, often dark and dense nodules, gravels, and hardgrounds of carbonate fluorapatite (CFA). Samples investigated in this study are from the Chimbote Platform of the shelf of Peru (sites A54, 10°01.89S/79°04.33W and A84, 10°24.57S/78°48.9W). The sampling sites are within the present day oxygen minimum zone extending from 50 to 650 m water depth (Emeis *et al.*, 1991; Lückge & Reinhardt, 2000). Abundant large sulfide-oxidizing bacteria of the genera *Beggiatoa* and *Thioploca* have been found in the area at 9°41.47S/78°40.99W, somewhat closer to the coast compared to the sampling sites (cf. Wieringa & Riechmann, 2002).

The Peru Undercurrent accelerates over the broad, shallow Chimbote platform leading to erosion and hence development of hardgrounds on this topographic height. Sediment accumulates in regions that are protected from the bottom currents. Perennial upwelling off Peru is driven by persistently blowing southerly winds. Recent major upwelling cells are located at 7° to 8°S, 11° to 12°S, and 14° to 16°S (Suess *et al.*, 1986).

Phosphatic laminites (Fig. 1) represent one facies of composite phosphorite crusts (Arning *et al.*, submitted). The laminites superpose a phosphooid facies composed of phosphooids, phosphatic coated siliceous grains, fish bone fragments, and phosphatic peloids. Phosphatic laminites consist of irregular light brown and dark phosphatic layers of CFA, which alternate irregularly with light grey organic-rich phosphatic layers and lenses. Sedimentary components, like detrital quartz grains, phosphatic peloids or fish bone fragments have been trapped and bound by the layers. Sulfide minerals are abundant in some horizons of the laminite (Fig. 1B). Strontium isotopes indicate a Pleistocene age of the laminite facies between 1.1 and 0.9 Ma (Arning *et al.*, submitted).

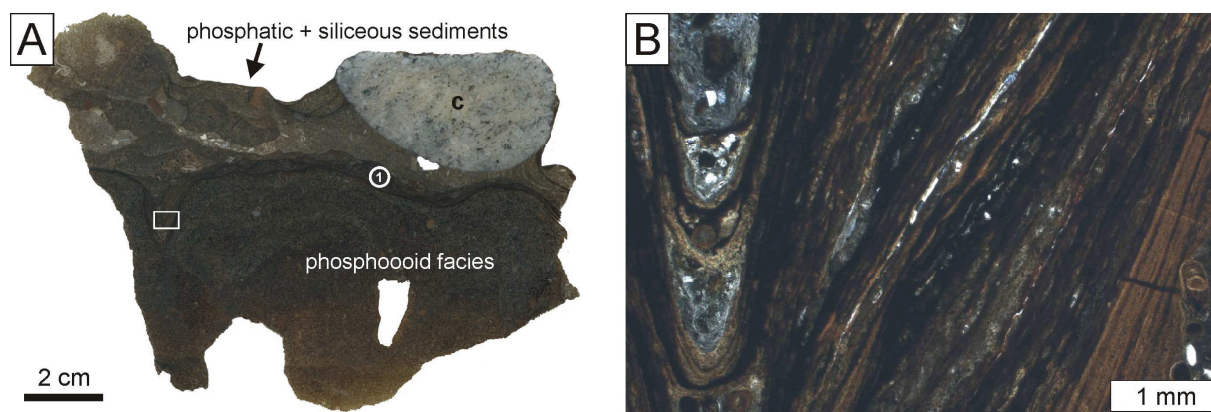


Fig 1 Peruvian phosphorite crust. (A) Scanned thin section. 1 = phosphatic laminite. Box enlarged in (B). (B) Photomicrograph of the phosphatic laminite; plane polarized light.

METHODS

Petrography and element contents

Standard petrographic and fluorescence microscopy were performed on thin sections with a Zeiss Axioskop 40 A Pol equipped with an Axio-Cam MRc digital camera (MARUM Bremen, Germany). Element contents of individual mineral phases were determined with a JXA 8900 R electron microprobe (University of Kiel, Germany). The electron microprobe is equipped with five WD spectrometers and an EDX system.

Sulfur isotopes

Extraction of CFA-bound sulfates and sulfides of the phosphatic laminite was done with a combined (3-step) method on two microdrilled samples (0.09 g, each). One sample was taken from the lower part, the other from the upper part of the laminite. In addition, a powdered bulk sample (0.54 g) of the laminite was also extracted with this method.

Step (1): Samples were pre-treated with 1M sodium chloride (NaCl) solution (24 h) to extract easily soluble sulfates, e.g. gypsum. Sample and reagent solutions were flushed with nitrogen. Ascorbic acid (1M) was added to NaCl solution to avoid oxidation of sulfides. The NaCl-solution was pipetted off and filtered. The filtrate was acidified with hydrochloric acid (HCl) and sulfate from the NaCl-leach was precipitated with barium chloride (BaCl_2) as barium sulfate (BaSO_4). After 24 h the BaSO_4 precipitate was filtered off and dried. Step (2): The extraction of the sulfides was performed after the standard method of Canfield *et al.* (1986) and Fossing & Jørgensen (1989). Samples were covered with 50% ethanol. Under nitrogen atmosphere, 16 ml 6M HCl were added and samples were distilled under nitrogen

atmosphere for 1h. Acid volatile sulfides (AVS) were precipitated in 0.1 M silver nitrate (AgNO_3) traps as silver sulfide (Ag_2S). The Ag_2S precipitate was filtered off and dried. Following AVS extraction, 16 ml of reduced 1M chromium chloride (CrCl_2) solution was added. Samples were heated and distilled for 1.5 h. Chromium reducible sulfur (CRS), mainly pyrite, was precipitated in 0.5 M AgNO_3 traps as Ag_2S . The silver sulfide precipitate was filtered off and dried. Step (3): Finally, the $\text{HCl} + \text{CrCl}_2$ solution was filtered to collect the sulfate leached from the CFA by the HCl . Barium chloride was added to the filtrate to precipitate barium sulfate. After 24 h the BaSO_4 precipitate was filtered off and dried.

CFA-bound sulfate and sulfide extractions have also been performed separately on two powdered samples of bulk laminite (0.31 g for CFA-bound SO_4 extraction, 0.67 g for sulfide extraction). Easily extractable sulfates were removed following step (1) in the combined method above. CFA-bound sulfate of the sample was extracted with 2M $\text{HCl} + 1\text{M}$ ascorbic acid for 24 h. All sample and reagent solutions were flushed with nitrogen. Afterwards, the HCl -solution was filtered and BaCl_2 was added to the filtrate to precipitate dissolved sulfate as BaSO_4 . After 24 h BaSO_4 precipitate was filtered off and dried. Sulfides were extracted in the same manner as described in step two of the combined method.

The sulfur isotopic composition is reported with respect to the standard Vienna Canñon Diablo Troilite (VCDT). Measurements were performed with a gas source stable isotope ratio mass spectrometer (GS-IRMS) model Delta V (Finnigan) at the Max-Planck-Institute for Marine Microbiology in Bremen, Germany. For sulfur isotope analysis, samples and 1 mg V_2O_5 were weighed into a tin capsule and combusted at 1060°C in an elemental analyzer (Hekatech[®]) to produce SO_2 . The sample weight was 0.4 to 0.6 mg for BaSO_4 and 0.2 to 0.4 mg for Ag_2S . The evolved SO_2 was carried by a helium stream through a GC column, Finnigan Conflo III[®], and into a Finnigan Delta V[®] stable isotope ratio mass spectrometer to determine $\delta^{34}\text{S}$. The sulfur isotope measurements were calibrated with reference materials NBS 127 ($\delta^{34}\text{S} = +20.3\text{‰}$) and IAEA-SO-6 ($\delta^{34}\text{S} = -34.1\text{‰}$). The standard errors (σ_1) of the measurements were less than 0.2‰ for $\delta^{34}\text{S}$.

Molecular biomarkers

For lipid biomarker analyses, phosphatic laminites were separated carefully from the entire crust. Then, the laminites were crushed to small pieces and cleaned by repeated washing with acetone. Afterwards the sample (8 g) was powdered and extracted three times with 60 ml

dichlormethane (DCM):methanol 3:1 by microwave-extraction (CEM, MARS X[®]) at 80°C and 600 W. Four internal standards (*n*-hexatriacontane, behenic acid methylester, 1-nonadecanol, 2-Me-octadecanoic acid) were added to the samples prior to extraction. The resulting total lipid extracts (TLEs) were purified by separation in DCM soluble asphaltenes and in hexane soluble maltenes. The maltenes were desulfurized with activated copper powder and subsequently separated by column chromatography (supelco LC-NH₂[®] glass cartridges; 500 g sorbed). Maltenes were separated into four fractions of increasing polarity (1. alkanes, 2. ketones/esters, 3. alcohols, and 4. free fatty acids). Fatty acid methyl esters (FAMES) were derivatized from free fatty acids by adding 1 ml of 12 % BF₃ in methanol to the dried fatty acid fraction. Reaction time was 1 h at 70°C. The alcohols were reacted to trimethylsilyl- (TMS-) derivatives with 100 µl BSTFA and 100 µl pyridine (1 h at 70°C). Fractions 1 and 2 are not discussed.

After the first extraction, the residue of the extracted sample was dissolved in DCM-washed HCl (24 h, pH 3-4). After HCl-dissolution, the residual sediment was extracted again and analyzed with the same extraction method and analytical procedure described above.

Fractions of all samples were examined with coupled gas chromatography-mass spectrometry (GC-MS) using a DSQ Trace GC-MS[®] equipped with a 30-m RTX-5MS fused silica capillary column at the MARUM in Bremen, Germany. The carrier gas was helium. For quantification, the samples were run on a Thermo Electron Trace GC[®] coupled with a flame ionization detector (FID) and equipped with a 30-m RTX-5MS fused silica capillary column at the MARUM in Bremen, Germany. Contents are given in µg g⁻¹ laminite independent of the extraction procedure.

Compound specific carbon isotope analyses were done for fractions 3 and 4 of the extract after HCl-dissolution. Compound specific carbon isotope analyses were performed with a Thermo Electron Trace GC coupled via a Thermo Electron GC-combustion-III-interface[®] to a Thermo Electron Delta^{plus}XP[®] mass spectrometer at the MARUM in Bremen, Germany. The measured carbon isotope data are given as δ values in per mil (‰) relative to Vienna Pee Dee Belemnite (V-PDB) and are corrected for addition of carbon during preparation of TMS- and methyl-derivatives.

RESULTS

Element contents and inferred mineralogy

Microprobe analyses reveal that phosphatic laminites consist of CFA layers, some of which contain abundant small elongated sphalerite (ZnS) crystals (Fig. 2A,B,D). Aggregates of pyrite (FeS₂) framboids are abundant in defined horizons as well (Fig. 2A,B). Pyrite is also common in depressions within the laminite (Fig. 2C).

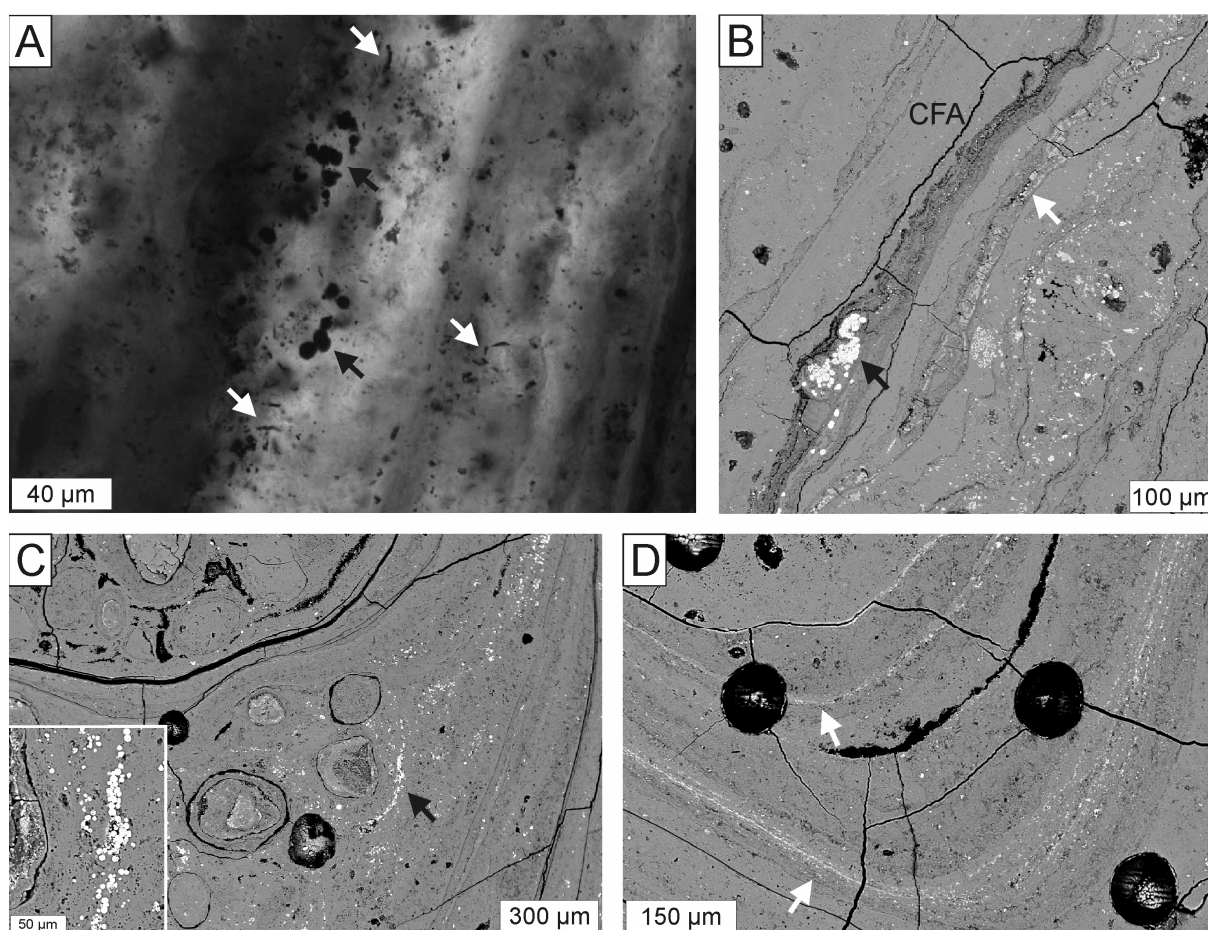


Fig 2 Photomicrographs of sulfide minerals within phosphatic laminites. See Figure 3 for S, Zn, and Fe contents. (A) Phosphatic laminite, sample A54; plane polarized light. Black arrows point to pyrite framboids, white arrows point to small elongated sphalerite crystals. (B) Phosphatic laminite, sample A54. Black arrows point to pyrite framboids, white arrow points to a sphalerite layer. CFA: carbonate fluorapatite; back scatter image. (C) Pyrite aggregations in sample A84. Black arrow points to pyrite framboids within organic rich CFA matrix (enlarged in inset); back scatter image. (D) Sphalerite layers (white arrows) within laminite, sample A84; back scatter image.

The dominant elements of the laminites are listed in Table 1. P:Ca ratios are in agreement with CFA after the empiric formula $\text{Ca}_5(\text{PO}_4)_{2.5}(\text{CO}_3)_{0.5}\text{F}$ (corresponding to Ca = 41.16 weight%, P = 15.91 weight%, O = 37.79 weight%, F = 3.90 weight%, and C = 1.23

weight%; cf. Roberts *et al.*, 1990). The detection of sulfur in pure CFA layers indicates that CFA contains sulfate. CFA is thought to incorporate sulfate in proportion to its concentration in ambient pore fluids (Jarvis *et al.*, 1994).

In the sphalerite layer from sample A54, the remaining sulfur after subtraction of CFA-bound sulfate is in a ratio of 2:1 to Zn (Fig. 3A). Furthermore, abundant Fe was detected in the sphalerite layer, clearly more than can be bond to the excess sulfur. Presumably iron is also present as iron oxides/hydroxides. In the sphalerite layer from sample A84, the remaining sulfur after subtraction of CFA-bound sulfate is in a ratio of approximately 1:1 to Zn (Fig. 3B). Less iron than in the sphalerite layer from sample A54 was detected and all iron probably occurs as sulfide. Pyrite is generally very pure, with a ratio of S:Fe of 2:1 (Fig. 3C,D).

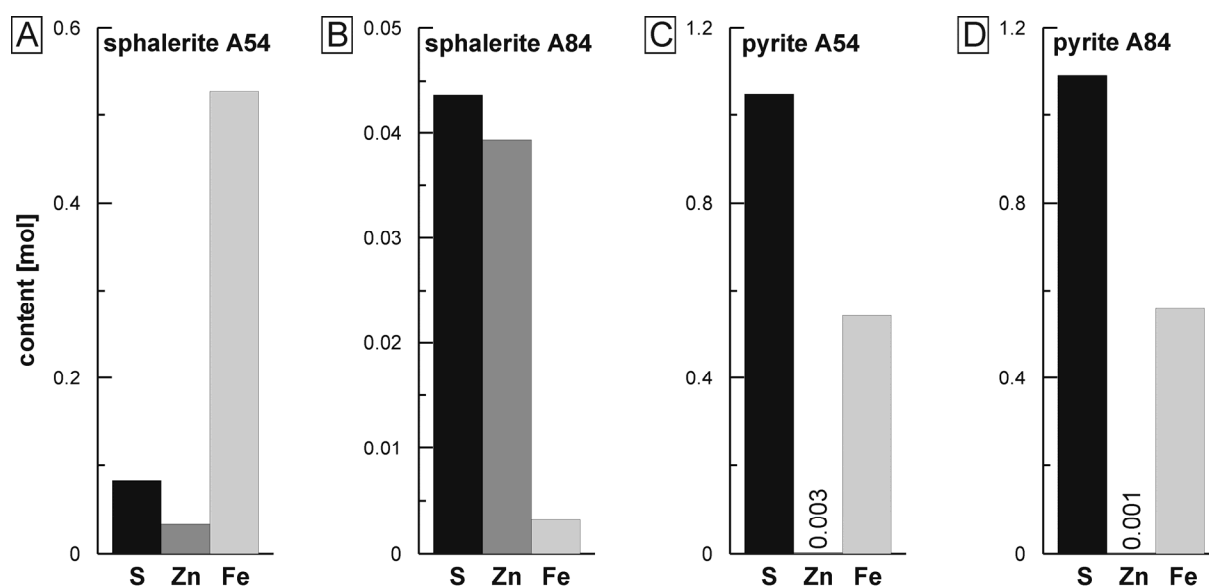


Fig 3 Content of sulfur (present as sulfide), zinc, and iron (mol) detected with electron microprobe in sphalerite layers from sample A54 (A) and A84 (B) as well as in pyrite framboids from sample A54 (C) and A84 (D). Note that resolution of beam size was not sufficient to analyze individual phases.

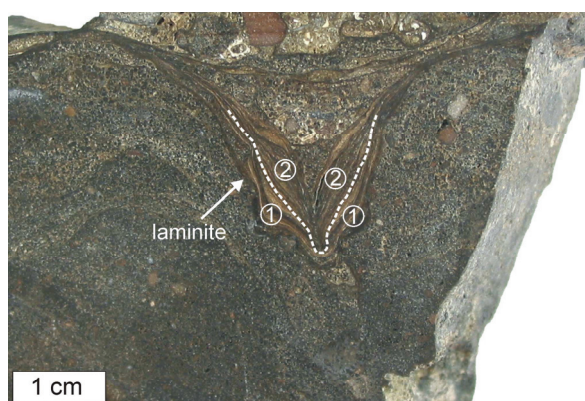
Table 1 Results of microprobe analyses. Given are contents (in weight % and in mol) of the most abundant and relevant elements (sulfur, zinc, iron, calcium, and phosphorus) in sphalerite layers, pyrite minerals, and carbonate fluorapatite (CFA) layers of samples A54 and A84. Compare Figure 2 for mineral distribution within the laminites.

		S		Zn		Fe		Ca		P	
		[wt. %]	[mol]	[wt. %]	[mol]	[wt. %]	[mol]	[wt. %]	[mol]	[wt. %]	[mol]
Sphalerite^a											
A54	1	2.45	0.077	1.06	0.016	17.03	0.305	21.68	0.541	7.41	0.239
A54	2	2.82	0.088	1.34	0.021	14.78	0.265	22.43	0.560	7.45	0.241
A54	3	2.77	0.086	2.55	0.039	37.69	0.675	4.89	0.122	1.28	0.041
A54	4	4.04	0.126	1.99	0.030	20.16	0.361	18.34	0.457	6.68	0.216
A54	5	2.68	0.083	2.46	0.038	31.81	0.570	12.29	0.307	3.59	0.116
A54	6	3.40	0.106	2.57	0.039	33.85	0.606	10.77	0.269	3.91	0.126
A54	7	2.58	0.080	1.87	0.029	25.74	0.461	15.08	0.376	5.09	0.164
A54	8	2.78	0.087	2.46	0.038	34.81	0.623	9.68	0.241	3.67	0.119
A54	9	2.58	0.081	1.92	0.029	26.26	0.470	17.43	0.435	7.69	0.248
A54	10	3.20	0.100	2.41	0.037	37.16	0.665	7.97	0.199	3.19	0.103
A54	11	4.04	0.126	2.15	0.033	36.54	0.654	9.22	0.230	3.50	0.113
A54	12	6.24	0.194	2.98	0.046	37.04	0.663	8.63	0.215	3.20	0.103
A84	13	3.21	0.100	2.82	0.043	0.21	0.004	34.40	0.858	13.12	0.424
A84	14	3.57	0.111	3.52	0.054	0.22	0.004	33.93	0.847	13.30	0.429
A84	15	4.28	0.134	4.91	0.075	0.31	0.006	32.88	0.820	12.81	0.413
A84	16	3.36	0.105	2.82	0.043	0.22	0.004	33.86	0.845	13.10	0.423
A84	17	5.01	0.156	5.53	0.085	0.30	0.005	31.53	0.787	12.44	0.402
A84	18	4.06	0.126	3.55	0.054	0.22	0.004	33.59	0.838	13.18	0.425
A84	19	2.17	0.068	1.29	0.020	0.13	0.002	35.24	0.879	13.79	0.445
A84	20	4.60	0.143	5.07	0.078	0.16	0.003	33.03	0.824	12.75	0.412
A84	21	3.23	0.101	2.54	0.039	0.17	0.003	34.84	0.869	13.11	0.423
A84	22	3.22	0.101	2.52	0.039	0.17	0.003	33.92	0.846	12.81	0.414
A84	23	2.17	0.068	1.49	0.023	0.16	0.003	35.98	0.898	13.61	0.439
A84	24	3.14	0.098	2.51	0.038	0.16	0.003	34.65	0.864	13.34	0.431
A84	25	1.97	0.061	0.73	0.011	0.09	0.002	36.15	0.902	13.61	0.440
A84	26	2.10	0.065	1.21	0.018	0.11	0.002	36.08	0.900	13.48	0.435
A84	27	2.32	0.072	1.39	0.021	0.10	0.002	35.75	0.892	13.36	0.431
A84	28	1.82	0.057	1.03	0.016	0.11	0.002	36.48	0.910	13.31	0.430
A84	29	1.87	0.058	0.80	0.012	0.11	0.002	35.54	0.887	12.91	0.417
Pyrite											
A54	1	39.50	1.232	0.09	0.001	34.86	0.624	9.02	0.225	3.72	0.120
A54	2	31.81	0.992	0.25	0.004	27.68	0.496	14.46	0.361	5.15	0.166
A54	3	41.08	1.281	0.16	0.002	35.62	0.638	8.13	0.203	3.13	0.101
A54	4	24.30	0.758	0.19	0.003	22.75	0.407	18.44	0.460	7.01	0.226
A84	5	25.50	0.795	0.07	0.001	22.53	0.403	18.13	0.452	7.43	0.240
A84	6	52.11	1.625	0.02	<0.001	45.69	0.818	0.56	0.014	0.13	0.004
A84	7	18.41	0.574	0.08	0.001	15.33	0.274	24.86	0.620	9.55	0.308
A84	8	14.80	0.462	0.06	0.001	11.76	0.211	27.12	0.677	8.42	0.272
A84	9	51.45	1.605	0.09	0.001	45.33	0.812	0.93	0.023	0.22	0.007
A84	10	21.63	0.675	0.03	<0.001	20.19	0.362	19.82	0.495	9.23	0.298
A84	11	52.24	1.629	0.04	0.001	44.89	0.804	0.71	0.018	0.16	0.005
A84	12	52.00	1.622	0.05	0.001	45.35	0.812	0.76	0.019	0.17	0.005
A84	13	33.03	1.030	0.01	<0.001	28.88	0.517	14.39	0.359	5.99	0.193
CFA											
A54	1	1.57	0.049	0.24	0.004	0.33	0.006	36.61	0.913	13.42	0.433
A54	2	2.02	0.063	0.44	0.007	1.91	0.034	34.54	0.862	12.49	0.403
A54	3	1.83	0.057	0.22	0.003	0.24	0.004	35.56	0.888	12.92	0.417

^a: sphalerite layer, no pure sphalerite, abundant iron as iron oxides/hydroxides in this layer, sphalerite minerals are too small to avoid analysis of surrounding phases.

Sulfur isotopes

Sulfur isotope data ($\delta^{34}\text{S}$) for CFA-bound sulfate ($\text{SO}_{4\text{-CFA}}$) and sulfides obtained from chromium reduction (S_{pyrite}) are shown in Fig. 4. The CFA-bound sulfate yields $\delta^{34}\text{S}$ values of 7.4‰ and 5.9‰ for the laminite samples 1 and 2, respectively. The bulk sample of the laminite from the combined extraction method has a $\delta^{34}\text{S}_{\text{SO}_4\text{-CFA}}$ value of 14.7‰, similar to the bulk sample from the separate extraction method (12.5‰). The two S_{pyrite} laminite samples have $\delta^{34}\text{S}$ values of −31.0‰ and −29.9‰. $\delta^{34}\text{S}_{\text{pyrite}}$ values of bulk laminite samples are slightly higher (−26.9‰ and −27.3‰). Contents of extracted AVS were too low in all samples to determine their S isotopic composition. Easily extractable sulfates have $\delta^{34}\text{S}$ values of −1.6‰ (laminite 1), −6.2‰ (laminite 2), −1.2‰ (bulk sample, combined method), and −3.3‰ (bulk sample, separate method).



	$\delta^{34}\text{S}$ [‰]			
	bulk laminite-sep.	bulk laminite-com.	①	②
$\text{SO}_{4\text{-CFA}}$	14.7	12.5	7.4	5.9
S_{pyrite}	−26.9	−27.3	−31.0	−29.9

Fig 4 Sulfur isotopic composition (‰) of carbonate fluorapatite (CFA)-bound sulfate ($\text{SO}_{4\text{-CFA}}$) and pyrite within the laminite (S_{pyrite}); bulk laminite-sep. = two separate samples were used for extraction of CFA-bound sulfate and pyrite, bulk laminite-com. = the combined (3-step) method was used on one sample for extraction of CFA-bound sulfate and pyrite. (1) and (2) represent microdrilled samples.

Molecular biomarker inventory

Alcohols

Contents of lipid biomarkers from the alcohol fraction are given in Table 2. Saturated *n*-alcohols with even chain length of C_{16} to C_{26} are present. While contents of *n*- $\text{C}_{16:0}$ are almost equal before HCl-dissolution ($0.30 \mu\text{g g}^{-1}$) and in the pre-extracted residue following

dissolution ($0.31 \mu\text{g g}^{-1}$), other *n*-alcohols are slightly enriched in the first extract compared to the extract after dissolution, with highest contents for *n*-C_{18:0} (0.16 and $0.12 \mu\text{g g}^{-1}$). Long-chain *n*-alcohols are only present in minor amounts, as for example *n*-C_{24:0} (0.05 and $0.02 \mu\text{g g}^{-1}$) and *n*-C_{26:0} (0.09 and $0.05 \mu\text{g g}^{-1}$).

C₂₇ to C₃₀ sterols are common. Overall contents of sterols are significantly higher in the extract after dissolution. Cholesterol (C₂₇) is most abundant (0.25 and $1.40 \mu\text{g g}^{-1}$) followed by brassicasterol (C₂₈; 0.14 and $0.59 \mu\text{g g}^{-1}$) and β -sitosterol (C₂₉; 0.09 and $0.30 \mu\text{g g}^{-1}$). A cluster of *sn*-1-mono-*O*-alkyl glycerol ethers (MAGEs) containing alkyl side chains of C_{14:0}, *i/ai*-C_{15:0}, C_{15:0}, *ai*-C_{16:0}, C_{16:0}, *i/ai*-C_{17:0}, and C_{18:0} are present in the alcohol fraction. They are significantly higher concentrated in the extract after dissolution. MAGE C_{16:0} is also more abundant with $0.14 \mu\text{g g}^{-1}$ in the second extract compared to $0.03 \mu\text{g g}^{-1}$ in the first extract. MAGE *ai*-C_{17:0} shows low contents, but is also enriched in the extract following dissolution ($0.06 \mu\text{g g}^{-1}$ compared to $0.02 \mu\text{g g}^{-1}$). MAGE *ai*-C_{17:0} could not be quantified due to co-elution. Other *sn*-1-MAGEs were only detected in trace amounts. Besides MAGEs with *sn*-1 moieties, trace amounts of *sn*-2 MAGEs C_{16:1} and C_{16:0} were identified. Furthermore non-isoprenoidal di-*O*-alkyl glycerol ethers (DAGEs) with alkyl side chains of *i/ai*-C_{15:0}, C_{15:0}, *i/ai*-C_{16:0}, C_{16:0}, *i/ai*-C_{17:0}, and C_{17:0} are present. DAGEs are also significantly more abundant after dissolution (Table 2). The most abundant DAGE is *i*-C_{15:0}/*i*-C_{15:0} with $0.36 \mu\text{g g}^{-1}$. Contents of other DAGEs after dissolution range from $0.17 \mu\text{g g}^{-1}$ (DAGE *ai*-C_{16:0}/*ai*-C_{16:0}) to $0.26 \mu\text{g g}^{-1}$ (DAGE *i*-C_{15:0}/*ai*-C_{15:0}). Before dissolution, DAGE *ai*-C_{16:0}/*ai*-C_{16:0} were measured only in trace amounts, other DAGEs show contents of 0.10 to $0.16 \mu\text{g g}^{-1}$ (Table 2). Hopanol and *bis*-homohopanol show higher contents after dissolution (0.18 and $0.19 \mu\text{g g}^{-1}$, respectively, compared to hopanol: $0.08 \mu\text{g g}^{-1}$; content of *bis*-homohopanol is too low for quantification).

The $\delta^{13}\text{C}$ value of *n*-alcohol C_{18:0} is -27‰ and the sterols cholesterol and brassicasterol reveal $\delta^{13}\text{C}$ values of -24‰ and -23‰ , respectively (Table 2). MAGE C_{16:0} shows a significantly lower $\delta^{13}\text{C}$ value of -31‰ . $\delta^{13}\text{C}$ values of DAGEs (-30‰ to -35‰) and *bis*-homohopanol (-33‰) are in the same range as MAGEs.

Table 2 Contents ($\mu\text{g g}^{-1}$ laminite) and stable carbon isotopic compositions ($\delta^{13}\text{C}$ [‰]) of molecular biomarkers after dissolution. (MAGE: *sn*-1-mono-*O*-alkyl glycerol ether, DAGE: di-*O*-alkyl glycerol ether).

Compound	Source	Biomarker content [$\mu\text{g g}^{-1}$]		$\delta^{13}\text{C}$ [‰]
		non-dissolved	HCl-dissolved	
MAGE $\text{C}_{16:0}$	sulfate-reducing bacteria	0.03	0.14	−31
MAGE <i>ai</i> - $\text{C}_{17:0}$	sulfate-reducing bacteria	0.02	0.06	nd
DAGE <i>i</i> - $\text{C}_{15:0}$ / <i>i</i> - $\text{C}_{15:0}$	sulfate-reducing bacteria	0.12	0.36	−34 ^a
DAGE <i>i</i> - $\text{C}_{15:0}$ / <i>ai</i> - $\text{C}_{15:0}$	sulfate-reducing bacteria	0.16	0.26	nd
DAGE $\text{C}_{15:0}$ / $\text{C}_{15:0}$	sulfate-reducing bacteria	0.10	0.13	−35
DAGE <i>ai</i> - $\text{C}_{16:0}$ / <i>ai</i> - $\text{C}_{16:0}$	sulfate-reducing bacteria	nq	0.17	−30 ^b
<i>i</i> - $\text{C}_{15:0}$ fatty acid	sulfate-reducing bacteria	0.03	0.13	−33
<i>ai</i> - $\text{C}_{15:0}$ fatty acid	sulfate-reducing bacteria	0.05	0.18	−33
<i>i</i> - $\text{C}_{17:0}$ fatty acid	sulfate-reducing bacteria	0.06	0.31	−29
<i>ai</i> - $\text{C}_{17:0}$ fatty acid	sulfate-reducing bacteria	0.05	0.31	−29
10MeC $_{16:0}$ fatty acid	sulfate- and iron-reducing bacteria	0.08	0.32	−35
hopanol	bacteria	0.08	0.18	nd
<i>bis</i> -homohopanol	bacteria	nq	0.19	−33
C_{32} hopanoic acid	bacteria	0.15	0.69	−24
cholesterol	eukaryotic organisms (e.g. diatoms, dinoflagellates, algae)	0.25	1.40	−24
brassicasterol	diatoms, microalgae, higher plants	0.14	0.59	−23
β -sitosterol	diatoms, green algae, cyanobacteria	0.09	0.30	nd
$\text{C}_{18:0}$ <i>n</i> -alcohol	widespread, e.g. bacteria, phytoplankton	0.16	0.12	−27
$\text{C}_{26:0}$ <i>n</i> -alcohol	terrestrial higher plants	0.09	0.05	nd
$\text{C}_{15:0}$ <i>n</i> -fatty acid	widespread, bacteria, phytoplankton	0.15	0.28	−32
$\text{C}_{16:0}$ <i>n</i> -fatty acid	widespread, bacteria (e.g. sulfate reducers, sulfide oxidizers), marine phytoplankton	1.14	2.47	−30
$\text{C}_{17:0}$ <i>n</i> -fatty acid	widespread, bacteria, phytoplankton	0.10	0.37	−31
$\text{C}_{18:0}$ <i>n</i> -fatty acid	widespread, bacteria (e.g. sulfate reducers, sulfide oxidizers), phytoplankton	0.87	1.87	−31
$\text{C}_{22:0}$ <i>n</i> -fatty acid	terrestrial higher plants, phytoplankton	0.22	0.70	−25
$\text{C}_{23:0}$ <i>n</i> -fatty acid	terrestrial higher plants, phytoplankton	0.10	0.24	−22
$\text{C}_{24:0}$ <i>n</i> -fatty acid	terrestrial higher plants, phytoplankton	0.37	0.84	−23

nq: not quantifiable

nd: not determined, due to low contents or co-elution

^a: mixed with DAGE *i*- $\text{C}_{15:0}$ /*ai*- $\text{C}_{15:0}$

^b: mixed with DAGE *i*- $\text{C}_{16:0}$ /*ai*- $\text{C}_{16:0}$

Fatty acids

Contents of lipids from the fatty acid fraction are given in Table 2. *n*-Fatty acids with chain lengths of C_{14} to C_{32} were detected as well as short chain branched fatty acids with chain lengths of C_{15} to C_{17} . Higher contents of fatty acids are found in the extract after dissolution. While *n*-fatty acids are enriched by a factor of two to three, short chain branched fatty acids are enriched by a factor of four to six after dissolution. Most abundant are *n*- $\text{C}_{16:0}$ (1.14 and $2.47 \mu\text{g g}^{-1}$) and *n*- $\text{C}_{18:0}$ (0.87 and $1.87 \mu\text{g g}^{-1}$). Long chain *n*-fatty acids (C_{19} to C_{32}) show an even over odd predominance with highest contents for *n*- $\text{C}_{24:0}$ fatty acid (0.37 and $0.84 \mu\text{g g}^{-1}$). Among short chain branched fatty acids, *i*- $\text{C}_{17:0}$ (0.06 and $0.31 \mu\text{g g}^{-1}$), *ai*- $\text{C}_{17:0}$ (0.05 and $0.31 \mu\text{g g}^{-1}$), and 10MeC $_{16:0}$ (0.08 and $0.32 \mu\text{g g}^{-1}$) dominate.

Hopanoic acids (C₃₁ to C₃₃) are also more abundant after dissolution. Hopanoic acids are peaking at 17 β (H),21 β (H)-C₃₂-hopanoic acid with contents of 0.15 $\mu\text{g g}^{-1}$ (before dissolution) and 0.69 $\mu\text{g g}^{-1}$ (after dissolution), whereas the other hopanoic acids occur only in trace amounts.

$\delta^{13}\text{C}$ values (Table 2) of short chain *n*-fatty acids C_{15:0} to C_{18:0} fall between -30‰ (C_{16:0}) and -32‰ (C_{15:0}). Long chain *n*-fatty acids C_{22:0}, C_{23:0}, and C_{24:0} show values of -25‰ , -25‰ , and -23‰ , respectively. $\delta^{13}\text{C}$ values of *n*-C_{26:0} (-29‰) and *n*-C_{28:0} (-30‰) are slightly lower. Short chain branched fatty acids *i*-C_{15:0} and *ai*-C_{15:0} have a $\delta^{13}\text{C}$ value of -33‰ . While *i*-C_{17:0} and *ai*-C_{17:0} are less depleted in ^{13}C (both -29‰), 10MeC_{16:0} fatty acid shows the lowest $\delta^{13}\text{C}$ value (-35‰).

DISCUSSION

Sulfate-reducing bacteria and sulfide-oxidizing bacteria as key players in phosphorite formation

Based on lipid biomarker patterns of modern phosphogenic sediments of upwelling regions, the interaction of sulfate-reducing bacteria and sulfide-oxidizing bacteria has been suggested to be crucial for phosphate enrichment and precipitation (Arning *et al.*, 2008). Unfortunately, the supposed role of sulfide-oxidizing bacteria in phosphogenesis (Schulz & Schulz, 2005) cannot be traced easily by lipid biomarkers, because the signatures of these organisms like *Thioploca*, *Beggiatoa*, or *Thiomargarita* are rather unspecific (monounsaturated *n*-C₁₆ and *n*-C₁₈ fatty acids) and unstable (see Arning *et al.*, 2008 and references therein). Sulfate-reducing bacteria, on the other hand, synthesize more specific biomarkers, which are also more persistent. Short-chain branched fatty acids are prominent biomarkers of sulfate-reducing bacteria including *i/ai*-C_{15:0} synthesized by *Desulfosarcina* and *Desulfococcus* (Perry *et al.*, 1979; Taylor & Parkes, 1983; Dowling *et al.*, 1986; Kaneda, 1991; Wakeham & Beier, 1991). 10MeC_{16:0} fatty acid is characteristic for the genera *Desulfobacter* and *Desulfobacula*, as well as iron-reducing bacteria of the genus *Geobacter* (Taylor & Parkes, 1983; Dowling *et al.*, 1986; Kuever *et al.*, 2001; Zhang *et al.*, 2003; Londry *et al.*, 2004). *i/ai*-C_{17:0} fatty acids typify *Desulfovibrio*, which are also known to be able to reduce ferric iron (Coleman *et al.*, 1993; Lovley *et al.*, 1993; Londry *et al.*, 2004). Non-isoprenoidal MAGEs and DAGEs have also commonly been attributed to sulfate-reducing bacteria (Langworthy *et al.*, 1983; Huber *et al.*, 1992; Rütters *et al.*, 2001).

Unusually high contents of lipid biomarkers of sulfate-reducing bacteria were found in the phosphatic laminite (see Table 2). The preferred liberation of these lipids only after dissolution of the phosphatic matrix reveals that the molecular fossils of sulfate reducers are tightly bound to the CFA mineral lattice. This observation agrees with a direct involvement of sulfate-reducing bacteria in phosphogenesis. Interestingly, the highest contents of all fatty acids were identified for *n*-C₁₆ and *n*-C₁₈ fatty acids, which may partially represent breakdown products of monounsaturated fatty acids derived from large sulfide-oxidizing bacteria. Lipids derived from sulfate-reducing bacteria show on average lower $\delta^{13}\text{C}$ values (–35‰ to –29‰; Table 2), than lipids of marine phototrophs and terrestrial sources (short-chain fatty acids, sterols, long-chain fatty acids –32‰ to –23‰). The $\delta^{13}\text{C}$ values of sulfate-reducing bacteria agree with heterotrophic growth, although autotrophy cannot be excluded, since the isotope fractionation of both growth modes is very similar (see Londry *et al.*, 2004 for details).

Prominent sulfate-reduction is not only reflected by the presence of molecular fossils, but also by sulfide minerals such as pyrite and sphalerite enclosed in CFA layers (Fig. 2). The bacterial origin of pyrite is strongly supported by $\delta^{34}\text{S}_{\text{pyrite}}$ values as low as –31‰ (cf. Canfield, 2001). Insight for the importance of sulfate reduction in phosphogenesis also stems from the temporal sequence of CFA, sphalerite, and pyrite formation. The occurrence of framboidal aggregates of pyrite in CFA layers and low $\delta^{34}\text{S}_{\text{pyrite}}$ values clearly point to an open system during sulfate reduction (e.g. Jørgensen, 1979; Canfield, 2001). Consequently, CFA layers were not yet lithified when pyrite formed.

Accordingly, the enclosure of sphalerite within CFA layers indicates more or less contemporaneous precipitation. Remarkably, formation of sphalerite has been observed in biofilms of sulfate-reducing bacteria including *Desulfovibrio*, *Desulfobacter*, and *Desulfobacterium* spp. (Labrenz *et al.*, 2000). Molecular fossils most likely derived from *Desulfovibrio* and *Desulfobacter* (*i*/*ai*-C_{17:0} and 10MeC_{16:0} fatty acids, respectively) are the most abundant bacterial compounds in the phosphatic laminite (Table 2). Some of these bacteria can live microaerophilic and are able to grow in close proximity to the oxic zone under only moderately reducing conditions (Minz *et al.*, 1999a; Minz *et al.*, 1999b). This is in agreement with sphalerite formation supposedly proceeding under moderately reducing conditions (cf. Labrenz *et al.*, 2000).

Hopanols in the phosphatic laminite (Table 2) may derive from anaerobic or microaerophilic sulfate-reducing bacteria (*Desulfovibrio*; Blumenberg *et al.*, 2006), or iron-reducing bacteria (*Geobacter*; Fischer *et al.*, 2005; Härtner *et al.*, 2005), although the majority

of these compounds is believed to derive from aerobic bacteria (e.g. Ourisson *et al.*, 1987; Rohmer *et al.*, 1992; Summons *et al.*, 1999). Both *Desulfovibrio* and *Geobacter* are known to synthesize hopanoids, especially tetrafunctionalized bacteriohopanepolyols (BHPs). *Bis-homohopanol* identified in the extract after dissolution may represent a breakdown product of tetrafunctionalized BHPs. However, because of the uncertainty regarding the sources of hopanols, they are of little specificity for environmental conditions.

Based on the line of evidence provided here and in accord with petrographic observations and patterns of redox-sensitive elements (Arning *et al.*, submitted), we propose that phosphatic laminites formed under suboxic conditions close to the sediment-water interface. Suboxic zones of sediments underlying upwelling areas represent habitats for large sulfide-oxidizing bacteria (Gallardo, 1977; Fossing *et al.*, 1995; Schulz *et al.*, 1999). These bacteria follow concentration gradients of sulfide and oxygen or nitrate (Schulz & Jørgensen, 2001). Sulfide-oxidizing bacteria are locally abundant in the study area on the Peruvian shelf (Wieringa & Riechmann, 2002). Although we are unable to verify the involvement of these bacteria by molecular fossils, the stable sulfur isotopic composition of CFA-bound sulfate strongly argues for bacterial sulfide oxidation. The obtained $\delta^{34}\text{S}_{\text{SO}_4\text{-CFA}}$ values (+5.9 to +14.7‰, Fig. 4) are significantly lower than those of sea water (about +21 to +22‰; see Paytan *et al.*, 1998), indicating the admixture of sulfate derived from the reoxidation of sulfide by sulfide-oxidizing bacteria. As a note of caution, the $\delta^{34}\text{S}_{\text{SO}_4}$ values of CFA-bound sulfate should be taken as minimum values, because reoxidation of pyrite with low $\delta^{34}\text{S}$ values during extraction cannot be completely excluded (cf. Mazumdar *et al.*, 2008). However, Benmore *et al.* (1983) observed similar $\delta^{34}\text{S}_{\text{SO}_4}$ values (+10‰) in phosphorites from the shelves of Peru, Chile, and Namibia, which confirms the reliability of our data.

Feasibility of bacterial phosphogenesis

It is still a matter of debate whether sufficient phosphate can be provided by bacterial degradation of organic matter to form large phosphorite deposits. For the Monterey Formation it has been proposed that degradation of organic matter would not provide enough phosphate for phosphorite formation (Föllmi & Garrison, 1991; Föllmi *et al.*, 2005). Here, we introduce a new model calculation to elucidate this problem. In the study area, organic matter is mainly derived from marine phytoplankton and terrestrial inputs as indicated by abundant sterols (e.g. cholesterol, brassicasterol, β -sitosterol) and *n*-fatty acids (Table 2). We estimate the amount of phosphorous which could be released by remineralization of the organic matter in two

different ways: (1) taking primary productivity (Fig. 5A) or (2) known sulfate reduction rates as starting point (Fig. 5B).

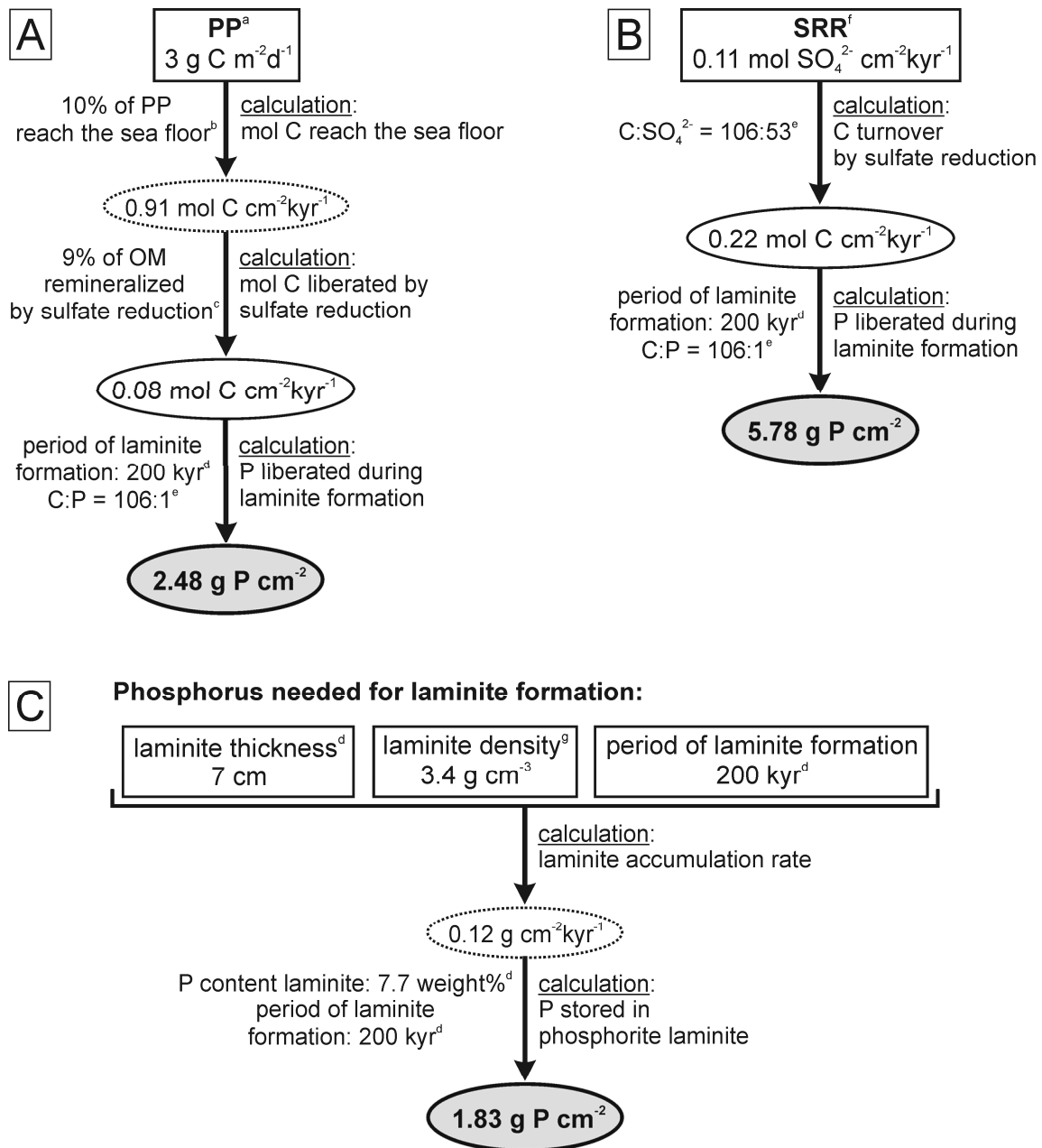


Fig 5 Model calculations. (A) and (B) Calculations of the amount of liberated phosphorus (g P cm⁻²) from remineralization of organic matter by sulfate reduction during the time of laminite formation. (A) Starting point for the calculation is the known primary productivity (PP) from the upwelling region off Peru. (B) Starting point for the calculation is the known sulfate reduction rate (SRR) in Peruvian shelf sediments. (C) Calculation of the amount of phosphorus (g P cm⁻²) needed for laminite formation. ^a: from Fossing (1990), primary productivity between 1 and 10 g C m⁻²d⁻¹, ^b: from Fossing (1990), ^c: from Fossing (1990), remineralization of organic matter from primary production that reaches the sea floor is between 9 and 29%, ^d: from Arning et al. (submitted), ^e: according to the reaction (CH₂O)₁₀₆(NH₃)₁₆(H₃PO₄) + 53SO₄²⁻ → 106HCO₃⁻ + 53H₂S + 16NH₃ + H₃PO₄ (e.g. Jørgensen, 2005), ^f: from Niggemann (2005), ^g: approximate value.

The time period of laminite formation (200 kyr) is estimated from calculated Sr ages, of Pleistocene age, between 1.1 and 0.9 Ma (Arning *et al.*, submitted). Due to the small gradient in the Sr isotope curve of sea water during the Pleistocene, the estimated period of 200 kyr is considered as an approximation.

(1) For primary productivity an average value is assumed, whereas a minimum value for the estimated remineralization of organic matter by sulfate reduction in the upwelling region off Peru is used (9%; cf. Fossing, 1990). This calculation suggests that 2.48 g P cm^{-2} could have been released from organic matter remineralization during the period of laminite formation (Fig. 5A). Based on a calculated phosphorous aggregation rate of 1.83 g P cm^{-2} required for laminite formation (Fig. 5C), the bacterial phosphogenesis scenario appears to be feasible. (2) The calculation via sulfate reduction rates (Fig. 5B) indicates even higher potential phosphorus liberation (5.78 g P cm^{-2}), suggesting that the calculated values using a mean primary productivity of $3 \text{ g C m}^{-2}\text{d}^{-1}$ and only minimum remineralization rates by sulfate reduction (9%) are an underestimation.

Although our age model for laminite formation is rather crude, the otherwise conservative calculations indicate that degradation of organic matter by sulfate reduction could have liberated sufficient amounts of phosphate to form the Peruvian phosphatic laminites. Similar calculations should be made for other autochthonous, ideally laminated or banded phosphorites for which good age models exist to test, if bacterial remineralization of organic matter can explain phosphogenesis at other sites as well.

CONCLUSIONS

Sulfate-reducing bacteria are involved in the formation of authigenic phosphatic laminites from the upwelling region off Peru. Lipid biomarkers of these bacteria such as short chain branched fatty acids, mono-*O*-alkyl glycerol ethers (MAGEs), and di-*O*-alkyl glycerol ether (DAGEs) are not only highly concentrated in the laminites, but also tightly bound to the CFA mineral lattice. More bacterial lipids are extracted after acid dissolution of the phosphorite than in a preceding extraction step. This observation indicates a close link between the activity of sulfate-reducing bacteria and carbonate fluorapatite (CFA) precipitation. The sulfide minerals pyrite and sphalerite, which are known to be produced by sulfate-reducing bacteria, formed contemporaneously with CFA. Low $\delta^{34}\text{S}_{\text{pyrite}}$ values are consistent with a bacterial origin. Model calculations indicate that remineralization of organic matter by sulfate reduction could have liberated enough phosphate for the formation of the Peruvian laminites.

Recent studies corroborate the idea that the Peruvian laminites formed under suboxic conditions (Arning *et al.*, submitted). This is further supported by the occurrence of sphalerite, which is thought to form under suboxic conditions and the dominance of lipid biomarkers typifying sulfate-reducing bacteria adapted to only moderately reducing conditions. Large sulfide-oxidizing bacteria populate the suboxic zone close to the sediment-water interface in sediments of upwelling areas and are present in the study area today. $\delta^{34}\text{S}$ values of CFA-bound sulfate (+5.9 to +14.7‰) are significantly lower than those of seawater sulfate, suggesting that bacterial reoxidation of sulfide by large sulfide-oxidizing bacteria occurred. Our results reinforce the scenario that the combined activities of closely associated sulfide-oxidizing bacteria, known to be capable to liberate phosphate (Schulz & Schulz, 2005), and sulfate-reducing bacteria have the potential to drive phosphogenesis in marine sediments below high productivity zones.

ACKNOWLEDGEMENTS

Special thanks to Andreas Lückge and Hermann Kudraß (both BGR, Hannover, Germany) for providing the Peruvian phosphorite crusts. We thank Sebastian Flotow for preparation of thin sections and Xavier Prieto Mollar (both University of Bremen) for his support in the lab. Further thanks go to Barbara Mader (University of Kiel) and Wolfgang Bach (University of Bremen) for help with microprobe measurements as well as to Enno Schefuß for some GC-irMS measurements. Patrick Meister and Thomas Max (both MPI Bremen) are acknowledged for support during sulfur extraction and sulfur isotope measurements. Gail Lee Arnold and Heide Schulz-Vogt (both MPI Bremen) made helpful comments. Financial support was provided by the “Deutsche Forschungsgemeinschaft” through the DFG-Excellence Cluster MARUM, Bremen.

REFERENCES

- Arning ET, Birgel D, Schulz-Vogt HN, Holmkvist L, Jørgensen BB, Larson A, Peckmann J (2008) Lipid biomarker patterns of phosphogenic sediments from upwelling regions. *Geomicrobiology Journal* **25**, 69-82.
- Arning ET, Lückge A, Breuer C, Gussone N, Birgel D, Peckmann J (submitted) Genesis of phosphorite crusts off Peru. *Marine Geology*.

- Bailey JV, Joye SB, Kalanetra KM, Flood BE, Corsetti FA (2007) Evidence of giant sulphur bacteria in Neoproterozoic phosphorites. *Nature* **445**, 198-201.
- Baturin GN (2000) Formation and evolution of phosphorite grains and nodules on the Namibian shelf, from recent to Pleistocene. In: *Marine Authigenesis: from Global to Microbial. SEPM Special Publication No. 66* (eds. Glenn CR, Prévôt-Lucas L, Lucas J). SEPM, Tulsa, OK, pp. 185-199.
- Benmore RA, Coleman ML, McArthur JM (1983) Origin of sedimentary francolite from its sulfur and carbon isotope composition. *Nature* **302**, 516-518.
- Blumenberg M, Krüger M, Nauhaus K, Talbot HM, Oppermann BI, Seifert R, Pape T, Michaelis W (2006) Biosynthesis of hopanoids by sulfate-reducing bacteria (genus *Desulfovibrio*). *Environmental Microbiology* **8**, 1220-1227.
- Canfield DE (2001) Biogeochemistry of sulfur isotopes. *Reviews in Mineralogy & Geochemistry* **43**, 607-636.
- Canfield DE, Raiswell R, Westrich JT, Reaves CM, Berner RA (1986) The use of chromium reduction in the analysis of reduced inorganic sulfur in sediments and shales. *Chemical Geology* **54**, 149-155.
- Coleman ML, Hedrick DB, Lovley DR, White DC, Pye K (1993) Reduction of Fe(III) in sediments by sulfate-reducing bacteria. *Nature* **361**, 436-438.
- Dowling NJE, Widdel F, White DC (1986) Phospholipid ester-linked fatty-acid biomarkers of acetate-oxidizing sulfate-reducers and other sulfide-forming bacteria. *Journal of General Microbiology* **132**, 1815-1825.
- Emeis K-C, Whelan JK, Tarafa M (1991) Sedimentary and geochemical expressions of oxic and anoxic conditions on the Peru shelf. In: *Modern and Ancient Continental Shelf Anoxia* (eds. Tyson RV, Pearson TH). Geological Society Special Publications, London, pp. 155-170.
- Ferdelman TG, Fossing H, Neumann K, Schulz HD (1999) Sulfate reduction in surface sediments of the southeast Atlantic continental margin between 15 degrees 38'S and 27 degrees 57'S (Angola and Namibia). *Limnology and Oceanography* **44**, 650-661.
- Ferdelman TG, Lee C, Pantoja S, Harder J, Bebout BM, Fossing H (1997) Sulfate reduction and methanogenesis in a *Thioploca*-dominated sediment off the coast of Chile. *Geochimica et Cosmochimica Acta* **61**, 3065-3079.
- Fischer WW, Summons RE, Pearson A (2005) Targeted genomic detection of biosynthetic pathways: anaerobic production of hopanoid biomarkers by a common sedimentary microbe. *Geobiology* **3**, 33-40.

- Föllmi KB (1996) The phosphorus cycle, phosphogenesis and marine phosphate-rich deposits. *Earth-Science Reviews* **40**, 55-124.
- Föllmi KB, Badertscher C, de Kaenel E, Stille P, John CM, Adatte T, Steinmann P (2005) Phosphogenesis and organic-carbon preservation in the Miocene Monterey Formation at Naples Beach, California - The Monterey Hypothesis revisited. *Geological Society of America Bulletin* **117**, 589-619.
- Föllmi KB, Garrison RE (1991) Phosphatic sediments, ordinary or extraordinary deposits? The example of the Miocene Monterey Formation (California). In: *Controversies in Modern Geology: Evolution of Geological Theories in Sedimentology, Earth History and Tectonics* (eds. Müller DW, McKenzie JA, Weissert H). Academic Press, London, pp. 55-84.
- Fossing H (1990) Sulfate reduction in shelf sediments in the upwelling region off Central Peru. *Continental Shelf Research* **10**, 355-367.
- Fossing H, Gallardo VA, Jørgensen BB, Hüttel M, Nielsen LP, Schulz HN, Canfield DE, Forster S, Glud RN, Gundersen JK, Küver J, Ramsing NB, Teske A, Thamdrup B, Ulloa O (1995) Concentration and transport of nitrate by the mat-forming sulfur bacterium *Thioploca*. *Nature* **374**, 713-715.
- Fossing H, Jørgensen BB (1989) Measurement of bacterial sulfate reduction in sediments - evaluation of a single-step chromium reduction method. *Biogeochemistry* **8**, 205-222.
- Froelich PN, Arthur MA, Burnett WC, Deakin M, Hensley V, Jahnke R, Kaul L, Kim KH, Roe K, Soutar A, Vathakanon C (1988) Early diagenesis of organic matter in Peru continental-margin sediments - phosphorite precipitation. *Marine Geology* **80**, 309-343.
- Gallardo VA (1977) Large benthic microbial communities in sulfide biota under Peru-Chile Subsurface Countercurrent. *Nature* **268**, 331-332.
- Garrison RE, Kastner M (1990) Phosphatic sediments and rocks recovered from the Peru margin during ODP LEG 112. In: *Proceedings of the Ocean Drilling Program, Scientific Results, Vol. 112* (eds. Suess E, von Huene R, et al.). ODP, College Station, TX, pp. 111-134.
- Glenn CR, Arthur MA (1988) Petrology and major element geochemistry of Peru margin phosphorites and associated diagenetic minerals - authigenesis in modern organic-rich sediments. *Marine Geology* **80**, 231-267.
- Glenn CR, Arthur MA, Resig JM, Burnett WC, Dean WE, Jahnke RA (1994) Are modern and ancient phosphorites really so different? In: *Siliceous, Phosphatic and Glauconitic*

- Sediments of the Tertiary and Mesozoic* (eds. Iijima A, Abed AM, Garrison RE). VSP Publishers, Utrecht, pp. 159-188.
- Glenn CR, Arthur MA, Yeh HW, Burnett WC (1988) Carbon isotopic composition and lattice-bound carbonate of Peru-Chile margin phosphorites. *Marine Geology* **80**, 287-307.
- Härtner T, Straub KL, Kannenberg E (2005) Occurrence of hopanoid lipids in anaerobic *Geobacter* species. *FEMS Microbiology Letters* **243**, 59-64.
- Huber R, Wilharm T, Huber D, Trincone A, Burggraf S, König H, Rachel R, Rockinger I, Fricke H, Stetter KO (1992) *Aquifex-Pyrophilus* gen-nov sp-nov represents a novel group of marine hyperthermophilic hydrogen-oxidizing bacteria. *Systematic and Applied Microbiology* **15**, 340-351.
- Ingall E, Jahnke R (1994) Evidence for enhanced phosphorus regeneration from marine-sediments overlain by oxygen depleted waters. *Geochimica et Cosmochimica Acta* **58**, 2571-2575.
- Jarvis I, Burnett WC, Nathan Y, Almbaydin FSM, Attia AKM, Castro LN, Flicoteaux R, Hilmy ME, Husain V, Qutawnah AA, Serjani A, Zanin YN (1994) Phosphorite geochemistry: state-of-the-art and environmental concerns. *Eclogae Geologicae Helvetiae* **87**, 643-700.
- Jørgensen BB (1982) Mineralization of organic matter in the sea bed - the role of sulfate reduction. *Nature* **296**, 643-645.
- Jørgensen BB (2005) Bacteria and marine biogeochemistry. In: *Marine Geochemistry* (eds. Schulz HD, Zabel M). Springer, Berlin, Heidelberg, pp. 169-206.
- Jørgensen BB (1979) Theoretical model of the stable sulfur isotope distribution in marine sediments. *Geochimica et Cosmochimica Acta* **43**, 363-374.
- Jørgensen BB, Gallardo VA (1999) *Thioploca* spp: filamentous sulfur bacteria with nitrate vacuoles. *FEMS Microbiology Ecology* **28**, 301-313.
- Kaneda T (1991) *Iso*- and *anteiso*-fatty acids in bacteria - biosynthesis, function, and taxonomic significance. *Microbiological Reviews* **55**, 288-302.
- Krajewski KP, van Cappellen P, Trichet J, Kuhn O, Lucas J, Martín-Algarra A., Prévôt L, Tewari VC, Gaspar L, Knight RI, Lamboy M (1994) Biological processes and apatite formation in sedimentary environments. *Eclogae Geologicae Helvetiae* **87**, 701-745.
- Kudrass HR (2000) *Cruise Report SO-147 Peru-Upwelling: Valparaiso-Callao, 29.05.-03.07.2000*. BGR Hannover, Germany.

- Küver J, Konneke M, Galushko A, Drzyzga O (2001) Reclassification of *Desulfobacterium phenolicum* as *Desulfobacula phenolica* comb. nov and description of strain Sax(T) as *Desulfotignum balticum* gen. nov., sp nov. *International Journal of Systematic and Evolutionary Microbiology* **51**, 171-177.
- Labrenz M, Druschel GK, Thomsen-Ebert T, Gilbert B, Welch SA, Kemner KM, Logan GA, Summons RE, de Stasio G, Bond PL, Lai B, Kelly SD, Banfield JF (2000) Formation of sphalerite (ZnS) deposits in natural biofilms of sulfate-reducing bacteria. *Science* **290**, 1744-1747.
- Langworthy TA, Holzer G, Zeikus JG, Tornabene TG (1983) Iso-branched and anteiso-branched glycerol diethers of the thermophilic anaerobe *Thermodesulfotobacterium commune*. *Systematic and Applied Microbiology* **4**, 1-17.
- Londry KL, Jahnke LL, Marais DJD (2004) Stable carbon isotope ratios of lipid biomarkers of sulfate-reducing bacteria. *Applied and Environmental Microbiology* **70**, 745-751.
- Lovley DR, Roden EE, Phillips EJP, Woodward JC (1993) Enzymatic iron and uranium reduction by sulfate-reducing bacteria. *Marine Geology* **113**, 41-53.
- Lückge A, Reinhardt L (2000) CTD measurements in the water column off Peru. In: *Cruise Report SO147 Peru-Upwelling: Valparaiso-Callao, 29.05.-03.07.2000* (ed. Kudrass HR). BGR, Hannover, pp. 35-37.
- Malone PHG, Towe KM (1970) Microbial carbonate and phosphate precipitates from seawater cultures. *Marine Geology* **9**, 301-309.
- Mazumdar A, Goldberg T, Strauss H (2008) Abiotic oxidation of pyrite by Fe(III) in acidic media and its implications for sulfur isotope measurements of lattice-bound sulfate in sediments. *Chemical Geology* **253**, 30-37.
- Minz D, Fishbain S, Green SJ, Muyzer G, Cohen Y, Rittmann BE, Stahl DA (1999a) Unexpected population distribution in a microbial mat community: sulfate-reducing bacteria localized to the highly oxic chemocline in contrast to a eukaryotic preference for anoxia. *Applied and Environmental Microbiology* **65**, 4659-4665.
- Minz D, Flax JL, Green SJ, Muyzer G, Cohen Y, Wagner M, Rittmann BE, Stahl DA (1999b) Diversity of sulfate-reducing bacteria in oxic and anoxic regions of a microbial mat characterized by comparative analysis of dissimilatory sulfite reductase genes. *Applied and Environmental Microbiology* **65**, 4666-4671.
- Nathan Y, Bremner JM, Lowenthal RE, Monteiro P (1993) Role of bacteria in phosphorite genesis. *Geomicrobiology Journal* **11**, 69-76.

- Niggemann J. (2005) *Composition and degradation of organic matter in sediments from the Peru-Chile upwelling region*. PhD thesis, Bremen.
- Otte S, Kuenen JG, Nielsen L, Paerl HW, Zopfi J, Schulz HN, Teske A, Strotmann B, Gallardo VA, Jørgensen BB (1999) Nitrogen, carbon, and sulfur metabolism in natural *Thioploca* samples. *Applied and Environmental Microbiology* **65**, 3148-3157.
- Ourisson G, Rohmer M, Poralla K (1987) Prokaryotic hopanoids and other polyterpenoid sterol surrogates. *Annual Review of Microbiology* **41**, 301-333.
- Paytan A, Kastner M, Campbell D, Thiemens MH (1998) Sulfur isotopic composition of Cenozoic seawater sulfate. *Science* **282**, 1459-1462.
- Perry GJ, Volkman JK, Johns RB, Bavor HJ (1979) Fatty acids of bacterial origin in contemporary marine-sediments. *Geochimica et Cosmochimica Acta* **43**, 1715-1725.
- Reimers CE, Kastner M, Garrison RE (1990) The role of bacterial mats in phosphate mineralization with particular reference to the Monterey Formation. In: *Phosphate Deposits of the World: Neogene to Modern Phosphorites* (eds. Burnett WC, Riggs SR). Cambridge University Press, Cambridge, pp. 300-311.
- Roberts WL, Campbell TJ, Rapp GR (1990) *Encyclopedia of Minerals*. Van Nostrand Reinhold, New York.
- Rohmer M, Bissere P, Neunlist S (1992) The hopanoids, prokaryotic triterpenoids and precursors of ubiquitous molecular fossils. In: *Biological Markers in Sediments and Petroleum* (eds. Moldowan JM, Albrecht P, Philp RP). Prentice-Hall, New York, pp. 1-17.
- Rütters H, Sass H, Cypionka H, Rullkötter J (2001) Monoalkylether phospholipids in the sulfate-reducing bacteria *Desulfosarcina variabilis* and *Desulforhabdus amnigenus*. *Archives of Microbiology* **176**, 435-442.
- Schenau SJ, Slomp CP, de Lange GJ (2000) Phosphogenesis and active phosphorite formation in sediments from the Arabian Sea oxygen minimum zone. *Marine Geology* **169**, 1-20.
- Schuffert JD, Kastner M, Jahnke RA (1998) Carbon and phosphorus burial associated with modern phosphorite formation. *Marine Geology* **146**, 21-31.
- Schulz HN, Brinkhoff T, Ferdelman TG, Marine MH, Teske A, Jørgensen BB (1999) Dense populations of a giant sulfur bacterium in Namibian shelf sediments. *Science* **284**, 493-495.
- Schulz HN, Jørgensen BB (2001) Big bacteria. *Annual Reviews of Microbiology* **55**, 105-137.
- Schulz HN, Schulz HD (2005) Large sulfur bacteria and the formation of phosphorite. *Science* **307**, 416-418.

- Suess E, Kulm LD, Killingley JS (1986) Coastal upwelling and a history of organic-rich mudstone deposition off Peru. In: *Marine Petroleum Source Rocks* (eds. Brooks J, Fleet AJ). The Geological Society, London, pp. 181-197.
- Summons RE, Jahnke LL, Hope JM, Logan GA (1999) 2-methylhopanoids as biomarkers for cyanobacterial oxygenic photosynthesis. *Nature* **400**, 554-557.
- Taylor J, Parkes RJ (1983) The cellular fatty acids of the sulfate-reducing bacteria, *Desulfobacter* sp, *Desulfobulbus* sp and *Desulfovibrio-desulfuricans*. *Journal of General Microbiology* **129**, 3303-3309.
- Thamdrup B, Canfield DE (1996) Pathways of carbon oxidation in continental margin sediments off central Chile. *Limnology and Oceanography* **41**, 1629-1650.
- van Cappellen P, Berner RA (1988) A mathematical model for the early diagenesis of phosphorus and fluorine in marine Sediments - apatite precipitation. *American Journal of Science* **288**, 289-333.
- van Cappellen P, Ingall ED (1996) Redox stabilization of the atmosphere and oceans by phosphorus-limited marine productivity. *Science* **271**, 493-496.
- van Cappellen P, Berner RA (1991) Fluorapatite crystal growth from modified seawater solutions. *Geochimica et Cosmochimica Acta* **55**, 1219-1234.
- Wakeham SG, Beier JA (1991) Fatty acid and sterol biomarkers as indicators of particulate organic matter source and alteration processes in the Black Sea. *Deep Sea Research* **38**, 943-968.
- Watkins RT, Nathan Y, Bremner JM (1995) Rare earth elements in phosphorite and associated sediment from the Namibian and South African continental shelves. *Marine Geology* **129**, 111-128.
- Wieringa EBA, Riechmann D (2002) Abundance of nitrate-storing sulfur bacteria (*Thioploca* spp., *Beggiatoa* spp.) along the coast of Peru and microsensor profiling. In: *Peru upwelling, SONNE-cruise SO147, Final report* (ed. Kudrass HR). BGR, Hannover.
- Williams LA, Reimers C (1983) Role of bacterial mats in oxygen-deficient marine basins and coastal upwelling regimes - preliminary-report. *Geology* **11**, 267-269.
- Zhang CLL, Li YL, Ye Q, Fong J, Peacock AD, Blunt E, Fang JS, Lovley DR, White DC (2003) Carbon isotope signatures of fatty acids in *Geobacter metallireducens* and *Shewanella algae*. *Chemical Geology* **195**, 17-28.

PAPER 4

Methanogenic archaea involved in dolomite formation in phosphorite dominated strata

Esther T. Arning¹, Daniel Birgel¹, Karl Föllmi², Jörn Peckmann^{1,*}

¹ MARUM, University of Bremen, D-28334 Bremen, Germany

² Institut de Géologie et Paléontologie, University of Lausanne, CH-1015 Lausanne, Switzerland

* Corresponding author: J. Peckmann, Tel.: 0049 421 218 65740; fax: 0049 421 218 65715; e-mail: peckmann@uni-bremen.de

RRH: METHANOGENIC DOLOMITE FORMATION

LLH: ARNING ET AL.

Keywords: archaea, dolomite formation, methanogenesis, Monterey Formation, lipid biomarkers, sulfate reduction, stable isotopes

in preparation for submission to PALAIOS as a research note

ABSTRACT

The occurrence of dolomites of the Miocene Monterey Formation is related to organic carbon-rich sediments. This suggests an involvement of microorganisms in their formation, which should be traced by means of lipid biomarker and stable carbon isotopic analyses. The broad range of the $\delta^{13}\text{C}$ values of the dolomites (between -15‰ and $+10\text{‰}$) indicates organogenic dolomite formation in the zones of bacterial sulfate reduction and methanogenesis. The contribution of methanogenic archaea in the formation of dolomites with relatively high $\delta^{13}\text{C}_{\text{dol}}$ values (around $+10\text{‰}$) is unequivocally proven by the discovery of the lipid biomarker *sn*-2-hydroxyarchaeol with a stable carbon isotopic composition of -25‰ within these dolomites. *sn*-2-hydroxyarchaeol is thought to be a product of methanogenic archaea belonging to the *Methanosarcinales* and *Methanococcales* order. This is the first time that the molecular signal of methanogenesis has been identified in dolomites. The presence of sulfate-reducing bacteria in dolomites with low $\delta^{13}\text{C}_{\text{dol}}$ values (around -15‰) is indicated by the bacterial lipid biomarker *i*-C_{17:0} fatty acid extracted from these rocks. However, the concurrent appearance of *sn*-2-hydroxyarchaeol together with *i*-C_{17:0} fatty acid suggests a later deeper burial of dolomites into the methanogenic zone. However, intermediate $\delta^{13}\text{C}_{\text{dol}}$ values between -1 and $+1\text{‰}$ of some of the analyzed dolomites suggest that some dolomites presumably formed at the transition between the zones of sulfate reduction and methanogenesis.

INTRODUCTION

Dolomites are commonly associated with organic carbon-rich continental margin sediments. This relationship has been observed on the California Margin (Pisciotta and Mahoney, 1981), in the Gulf of California (Kelts and McKenzie, 1982) and on the Peru Margin (e.g., Suess and von Huene, 1988). In the geological record, the occurrence of dolomites is also related to organic carbon-rich sediments. One prominent example is the Miocene Monterey Formation in California (e.g., Friedman and Murata, 1979; Kablanow et al., 1984; Compton and Siever, 1984; Burns and Baker, 1987; Compton, 1988; Baker and Allen, 1990). These observations led to the assumption that the major part of the inorganic carbon for dolomite formation originates from organic matter degradation. However, mechanisms to overcome kinetically barriers of initial dolomite formation at earth-surface temperatures are still not known with certainty. Variable carbon isotopic composition ($\delta^{13}\text{C}$) of the dolomite indicates different diagenetic conditions of organogenic dolomite precipitation (e.g., Claypool and Kaplan,

1974). In the zone of sulfate reduction, dolomites with negative $\delta^{13}\text{C}$ values formed, while dolomites precipitated in the methanogenic zone show positive $\delta^{13}\text{C}$ values (see in Warren, 2000; Mazzullo, 2000). A recent study by Meister et al. (2007) shows that dolomites at the Peru shelf formed at the sulfate-methane interface, where microbial activity is very high. Accordingly, alkalinity production by microbial degradation of organic matter is the driving mechanism for the dolomite precipitation. Overall, there seems to be growing evidence that sulfate reduction and methanogenesis may be the key to initial dolomitization (Mazzullo, 2000).

Dolomites in the Miocene Monterey Formation occur as layers or nodules and have been described by several authors (e.g., Kushnir and Kastner, 1984; Kablanow et al., 1984; Compton and Siever, 1984; Burns and Baker, 1987; Kastner et al., 1990). They are closely associated with the organic-rich sediments of the Monterey Formation. Burns and Baker (1987) suggested an early diagenetic formation of the dolomites within the upper meters of the sediment column. Stable carbon isotopic compositions ($\delta^{13}\text{C}$) of dolomites from the Monterey Formation show a great variety ranging from distinctly negative values (approximately -11‰) to distinct positive ones (approximately $+15\text{‰}$) (Murata et al., 1969; Kastner et al., 1984; Kushnir and Kastner, 1984; Kablanow et al., 1984; Burns and Baker, 1987; Malone et al., 1994). These values indicate organogenic dolomite formation in the zone of sulfate reduction and in the methanogenic zone.

The aim of this work is to decipher the involvement of microorganisms in the formation of dolomites of the Monterey Formation. Useful to reveal microbial involvement are lipid biomarkers, which are preserved as molecular fossils in authigenic rocks and represent fingerprints of the dominant microorganisms involved in authigenesis. Additionally, stable carbon and oxygen isotopes of the dolomites will be used to define the diagenetic environment of dolomite formation.

GEOLOGICAL SETTING AND SAMPLE LOCATION

The organic-rich and siliceous deposit of the Monterey Formation is composed primarily of siliceous and calcareous microfossils, organic matter, and terrigenous clay and contains a variety of calcareous and phosphatic rocks. The Monterey Formation is said to be the product of a high productivity upwelling system (Garrison et al., 1987; Garrison et al., 1990). The sediments deposited in small, fault-bounded and sediment-starved basins, which formed

during late Oligocene and Miocene along the San Andreas transform system (Blake et al., 1978; Crouch, 1979; Howell et al., 1980; Graham, 1987).

Sedimentation in the basins changed from calcareous-siliceous in the lower Monterey Formation during generally weak upwelling to dominantly siliceous sedimentation in the upper part during intense upwelling in Middle Miocene. Particularly in more distal basins (e.g. Santa Barbara Basin, Santa Maria Basin, and Pismo and Huasna Basin) a distinctive phosphatic marlstone facies occurs between the calcareous-siliceous and siliceous facies (see in Garrison et al., 1990). This led to the general division of the Monterey Formation into three facies: a lower calcareous or calcareous-siliceous facies, a middle phosphatic facies, and an upper siliceous facies (e.g., Isaacs, 1980; Pisciotto and Garrison, 1981). Periodic anoxia during formation of the Monterey Formation led to widespread laminated sediments and preservation of organic carbon. The diatomaceous Sisquoc Formation is overlying the Monterey Formation and contains generally more detrital clay and silt (Compton and Siever, 1984).

Dolomites were sampled from the sections Mussel Rock, Shell Beach (e.g., Filippelli et al., 1994), and Naples Beach (e.g., Föllmi et al., 2005), which are located in the Santa Maria Basin, the Pismo and Huasna Basin, and the Santa Barbara Basin, respectively (Fig. 1).

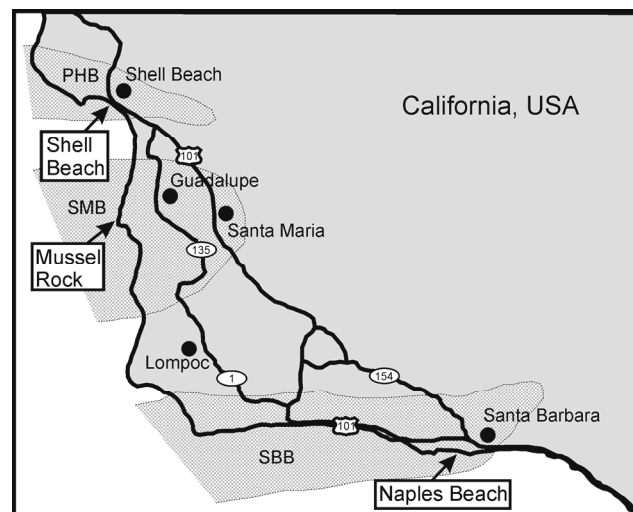


FIGURE 1 – Location map of the sampled sections from the Miocene Monterey Formation in California, USA. Outlined are the major Neogene Basins of this area. PHB: Pismo and Huasna Basin, SMB: Santa Maria Basin, SBB: Santa Barbara Basin.

In total, seven dolomite samples from the middle phosphatic facies of the Monterey Formation have been analyzed: two from Mussel Rock, two from Shell Beach, and three from

Naples Beach. In addition, one dolomite sample from the Sisquoc Formation at Mussel Rock has been examined (Table 1).

TABLE 1 – Location, stratigraphy, and description of habitat and background sediments of the analyzed dolomite samples.

Name	Sample location¹	Stratigraphy	Background sediment²
G02B	Mussel Rock	middle phosphatic Monterey Formation	C _{org} -rich, no PO ₄
G02C	Mussel Rock	middle phosphatic Monterey Formation	C _{org} -rich, no PO ₄
G05	Mussel Rock	Sisquoc Formation	diatomite, no PO ₄
S01	Shell Beach	lower phosphatic Monterey Formation	C _{org} and PO ₄ -rich
S03	Shell Beach	middle phosphatic Monterey Formation	C _{org} and PO ₄ -rich
N03B	Naples Beach	middle phosphatic Monterey Formation	C _{org} and PO ₄ -rich
N01	Naples Beach	middle phosphatic Monterey Formation	C _{org} and PO ₄ -rich
N06	Naples Beach	middle phosphatic Monterey Formation	C _{org} and PO ₄ -rich

¹: compare Figure 1

²: from field observations

METHODS

Standard petrographic and fluorescence microscopy were performed on thin sections of dolomites with a Zeiss Axioskop 40 A Pol equipped with a Axio-Cam MRc digital camera (University of Bremen).

Stable carbon ($\delta^{13}\text{C}$) and oxygen ($\delta^{18}\text{O}$) isotope measurements of eight dolomite samples (three from Mussel Rock, three from Naples Beach, and two from Shell Beach) were performed with a Finnigan MAT 252 mass spectrometer using the "Kiel" carbonate device type "Bremen" (MARUM, University of Bremen). Carbonates are converted into CO₂ and measured regarding their 45/44 and 46/44 relation against a standard gas (Burgbrohl CO₂ gas). A Solnhofen limestone is used as standard, which is calibrated against NBS 19 as an internal standard. Analytical standard deviation is about $\pm 0.02\text{‰}$ for $\delta^{13}\text{C}$ and $\pm 0.03\text{‰}$ for $\delta^{18}\text{O}$. Results for $\delta^{13}\text{C}$ and $\delta^{18}\text{O}$ are given in ‰ relative to Pee Dee belemnite (PDB).

Lipid biomarker analyses were done on three different dolomite samples from different regional and stratigraphical locations (one sample from Mussel Rock (G02B), Naples Beach (N03B), and Shell Beach (S01), respectively). Preparation and decalcification of three dolomite samples was performed after Birgel et al. (2006). Dolomites were crushed in small pieces and cleaned by washing with 10% HCl and acetone. Water, cleaned with dichlormethane was added to the sample and approximately 80% of the carbonate matrix was slowly dissolved with 10% HCl. Remaining carbonate pieces were removed and the residue was centrifuged and subsequently saponified in 6% KOH in methanol. The supernatants were

decanted and the residues were extracted three times with 60 ml dichloromethane (DCM):methanol 3:1 by microwave-extraction (CEM, MARS X) at 80°C and 600 W. Four internal standards (hexatriacontane, behenic acid methylester, 1-nonadecanol, 2-Me-octadecanoic acid) were added to the samples prior to extraction. The resulting total lipid extracts (TLEs) were purified by separation in DCM soluble asphaltenes and in hexane soluble maltenes. The maltenes were desulfurized with activated copper powder and subsequently separated by column chromatography (supelco LC-NH₂ glass cartridges; 500 g sorbed). Maltenes were separated into four fractions of increasing polarity (1. hydrocarbons, 2. ketones/esters, 3. alcohols, and 4. free fatty acids). Fatty acid methyl esters (FAMEs) were derivatized from free fatty acids by adding 1 ml of 12 % BF₃ in methanol to the dried fatty acid fraction. Reaction time was 1 h at 70°C. The alcohols were reacted to trimethylsilyl- (TMS-) derivatives with 100 µl BSTFA and 100 µl pyridine (1 h at 70°C). Fractions of all samples were examined with coupled gas chromatography-mass spectrometry (GC-MS) using a DSQ Trace GC-MS equipped with a 30-m RTX-5MS fused silica capillary column at the MARUM in Bremen, Germany. The carrier gas was helium. For quantification, the samples were run on a Thermo Electron Trace GC coupled with a flame ionization detector (FID) and equipped with a 30-m RTX-5MS fused silica capillary column at the MARUM in Bremen, Germany. We quantitatively analyzed fractions 3. and 4. Contents are given in µg g⁻¹ rock.

Compound specific carbon isotope analyses were performed with a Thermo Electron Trace GC coupled via a Thermo Electron GC-combustion-III-interface to a Thermo Electron Delta^{plus}XP mass spectrometer at the MARUM in Bremen, Germany. The measured carbon isotope data are given as δ values in per mil (‰) relative to Vienna Pee Dee Belemnite (V-PDB) and are corrected for addition of carbon during preparation of TMS- and methyl-derivatives.

RESULTS

Description of dolomites

Dolomites occur as very hard and dense nodules and layers in the Monterey Formation (Table 1). Samples G02B and G02C were collected from a dolomite nodule of Mussel Rock. The nodule is located in the middle Monterey Formation in siliceous, non-phosphatic, and organic carbon-rich sediments. Sample N01 was taken from a dolomite layer from siliceous, phosphate-rich, and organic carbon-rich sediments of the Naples Beach section. From the same setting, samples N03B and N06 were collected from dolomite nodules. Samples S01 and

S03 were taken from dolomite layers in siliceous, phosphate-rich, and organic carbon-rich sediments of the Shell Beach section.

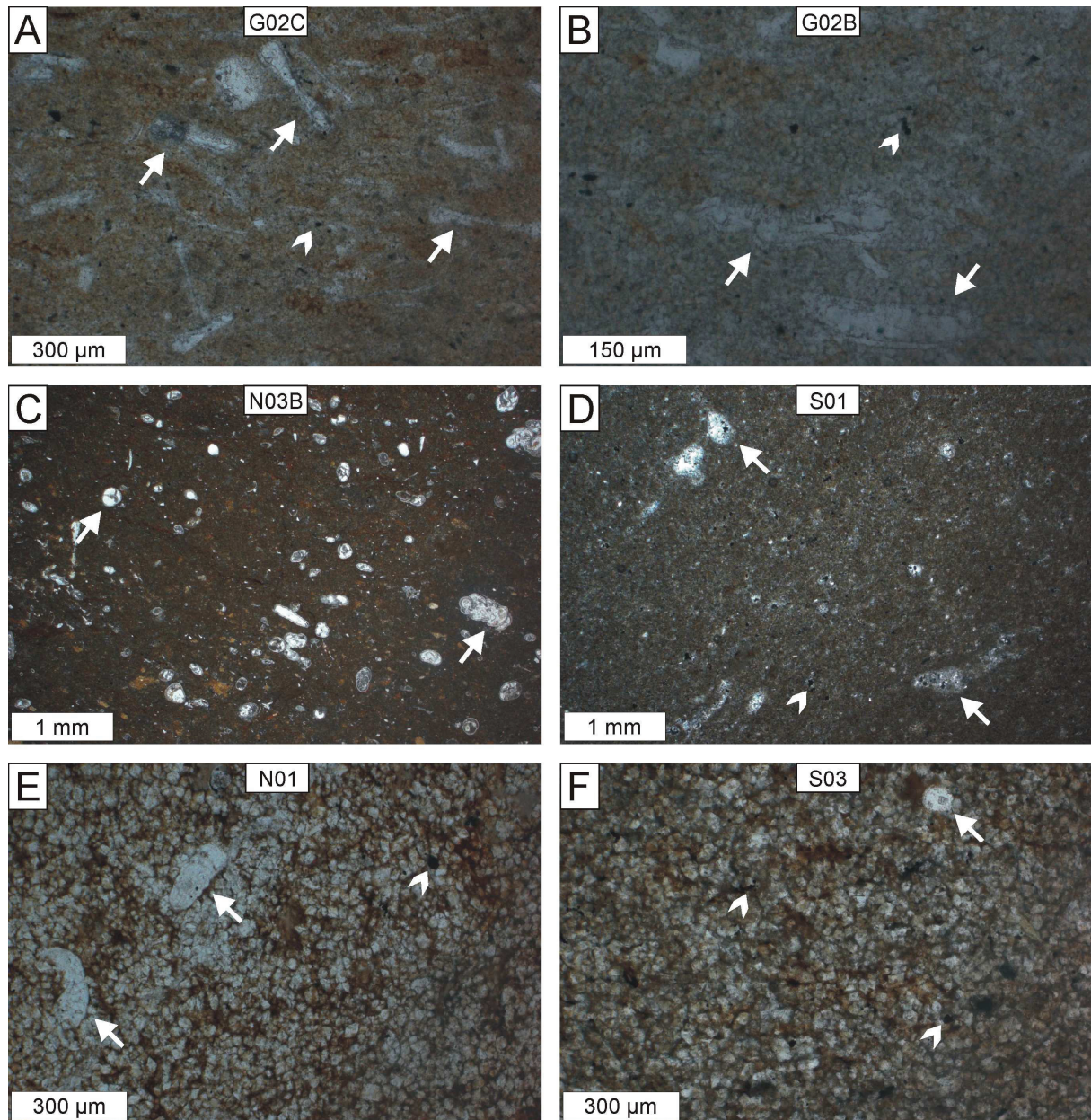


FIGURE 2 – Photomicrographs of dolomites from the Monterey Formation, plane polarized light. A) and B) Dolomites G02C and G02B from Mussel Rock with abundant remains of diatoms (arrows) and small framboidal pyrite aggregates (arrow heads). Interiors of diatoms are filled with sparry calcite. C) Fine grained dolomite N03B from Naples Beach with abundant foraminiferal tests (white arrows), partly filled with sparry calcite. D) Fine grained dolomite S01 from Shell Beach with partly dolomitized foraminiferal tests (arrows) and small framboidal pyrite aggregates (arrow head). E) Coarse grained dolomite N01 from Naples Beach with partly dolomitized foraminiferal tests (arrows) and small framboidal pyrite aggregates (arrow head). F) Coarse grained dolomite S03 from Shell Beach with small framboidal pyrite aggregates (arrow heads) and a dolomitized relict of a foraminiferal test (arrow).

Dolomite samples of the Monterey Formation show differences in texture and incorporated components (Fig. 2). Dolomites G02B and G02C from Mussel Rock are laminated and reveal a fine-grained matrix. They are rich in remains of diatoms whose interiors are filled with sparry calcite (Figs. 2A–B; see in Murata et al., 1969 for comparison). Furthermore, some remains of agglutinated foraminifera are present and small framboidal pyrite aggregates are abundant. Samples N03B and N06 from Naples Beach are identical in their petrography. They have a fine-grained matrix and contain abundant calcareous foraminiferal tests (Fig. 2C). Framboidal pyrite aggregates are present randomly in the matrix and sometimes fill the interior of foraminiferal tests, which is otherwise filled with sparry calcite. Dolomite S01 (Fig. 2D) consists of a fine-grained matrix, containing abundant small framboidal pyrite aggregates and remains of calcareous foraminiferal tests, which are partly dolomitized. Rarely, remains of diatoms can be found. Samples N01 (Fig. 2E) from Naples Beach and S03 from Shell Beach (Fig. 2F) are coarse-grained secondary dolomites, which are recrystallized. They contain framboidal pyrite aggregates and rarely tests of calcareous foraminifera, which are partly dolomitized.

The dolomite sample from the Sisquoc Formation (G05) is softer compared to the dolomites from the Monterey Formation and has a fine-grained matrix. The sample contains tests of agglutinated as well as of calcareous foraminifera and abundant remains of diatoms. Also small framboidal pyrite aggregates are present.

Carbon and oxygen isotopes

The analyzed dolomite samples reveal a broad range of their stable carbon isotopic composition ($\delta^{13}\text{C}_{\text{dol}}$, Fig. 3). Samples G02B and G02C from Mussel Rock show relatively high $\delta^{13}\text{C}$ values between +7.40 and +10.28‰. The same accounts for the dolomite from the Sisquoc Formation (G05) with $\delta^{13}\text{C}$ of +11.15 to +12.85‰. Dolomites obtained from Naples Beach show significant variations in their $\delta^{13}\text{C}$. While $\delta^{13}\text{C}$ values of samples N03B (–11.09 to –11.98‰) and N06 (–12.79 to –14.59‰) are relatively low, sample N01 reveal higher $\delta^{13}\text{C}$ values (–1.00 to +1.38‰). Both dolomites from Shell Beach are relatively similar in their carbon isotopic composition, with intermediate $\delta^{13}\text{C}$ values of –6.36 to –6.85‰ (S01) and –3.06 to –5.16‰ (S03).

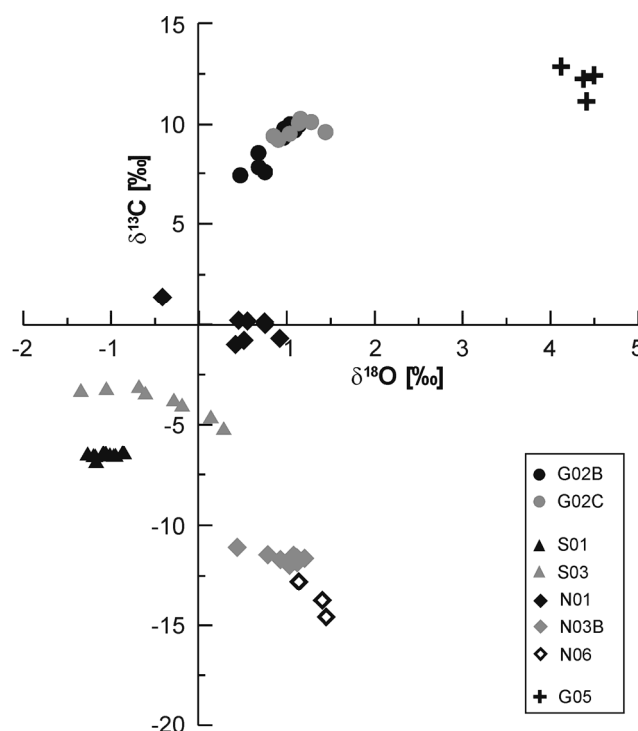


FIGURE 3 – Carbon and oxygen stable isotope plot of dolomites from the Monterey and the Siquoc Formation.

Stable oxygen isotopic compositions ($\delta^{18}\text{O}_{\text{dol}}$) of the analyzed dolomites from the Monterey Formation plot in a narrow range between -1.34‰ and $+1.45\text{‰}$ (Fig. 3). In samples G02B and G02C from Mussel Rock, $\delta^{18}\text{O}_{\text{dol}}$ values are between $+0.47$ and $+1.44\text{‰}$. Dolomites from Naples Beach (N01, N03B, and N06) reveal $\delta^{18}\text{O}$ of -0.42 to $+1.45\text{‰}$ and Shell Beach dolomites (S01 and S03) plot between -1.34 and $+0.28\text{‰}$. Clearly higher $\delta^{18}\text{O}_{\text{dol}}$ values ($+4.12$ to $+4.50\text{‰}$) were measured in dolomite G05 from the Siquoc Formation.

Lipid biomarker inventory

Lipid biomarker studies were performed on the primary dolomites of the Monterey Formation G02B, N03B, and S01. The secondary dolomites N01 and S03 were excluded. Lipid biomarkers extracted from the dolomites from Mussel Rock (G02B) and Naples Beach (N03B) indicate the presence of *sn*-2-hydroxyarchaeol (0.02 and $0.10 \mu\text{g g}^{-1}$, respectively) and archaeol, which was too low in concentration to be quantified (Fig. 4, Table 2). In sample S01 *sn*-2-hydroxyarchaeol and archaeol are absent. Further compounds present in the alcohol fraction of samples G02B and N03B are *n*-alcohols with chain length between $\text{C}_{12:0}$ (0.04 and $0.06 \mu\text{g g}^{-1}$) and $\text{C}_{26:0}$, with dominating $\text{C}_{16:0}$ (0.21 and $0.24 \mu\text{g g}^{-1}$) and $\text{C}_{18:0}$ *n*-alcohols (0.19 and $0.18 \mu\text{g g}^{-1}$). C_{27} to C_{30} sterols were detected, with β -sitosterol being most abundant in

sample G02B ($0.04 \mu\text{g g}^{-1}$) while in sample N03B only cholesterol could be quantified ($0.02 \mu\text{g g}^{-1}$). C_{30} hopanol is present in both samples in trace amounts. In sample S01 the alcohol fraction is relatively small, only $\text{C}_{12:0}$, $\text{C}_{14:0}$, $\text{C}_{16:0}$ and $\text{C}_{18:0}$ n -alcohols (0.02 to $0.04 \mu\text{g g}^{-1}$) could be identified (Table 2).

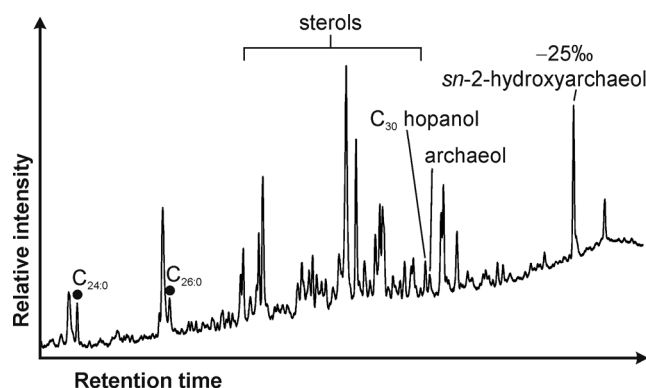


FIGURE 4 – Detail of the gas chromatogram (FID) of the alcohol fraction of dolomite G02B from Mussel Rock. The carbon isotopic composition ($\delta^{13}\text{C}$) of *sn*-2-hydroxyarchaeol is indicated; black circles: n -alcohols.

In the fatty acid fraction of sample G02B n -fatty acids with chain lengths between $\text{C}_{16:0}$ and $\text{C}_{22:0}$ could be identified, with dominating $\text{C}_{16:0}$ and $\text{C}_{18:0}$ fatty acids ($2.73 \mu\text{g g}^{-1}$, respectively; Table 2). In sample N03B n -fatty acids with chain lengths between $\text{C}_{14:0}$ (too low for quantification) and $\text{C}_{34:0}$ ($0.08 \mu\text{g g}^{-1}$), with dominating $\text{C}_{18:0}$ fatty acid ($2.19 \mu\text{g g}^{-1}$), were found. Additionally, the short chain branched fatty acid *i*- $\text{C}_{17:0}$ ($0.14 \mu\text{g g}^{-1}$) was detected. In sample S01 n -fatty acids with chain length between $\text{C}_{14:0}$ (too low for quantification) and $\text{C}_{34:0}$ ($0.12 \mu\text{g g}^{-1}$), with dominating long chain fatty acids $\text{C}_{22:0}$ ($0.27 \mu\text{g g}^{-1}$) and $\text{C}_{24:0}$ ($1.01 \mu\text{g g}^{-1}$), were found. Among the long chain fatty acids a strong predominance of even-numbered carbon chains is apparent. In addition, the short chain branched fatty acid *i*- $\text{C}_{17:0}$ ($0.08 \mu\text{g g}^{-1}$) was detected. Hopanoic acids are present only in the Shell Beach dolomite (S01) with dominating C_{32} hopanoic acid ($0.20 \mu\text{g g}^{-1}$).

$\delta^{13}\text{C}$ values of hydroxyarchaeol are -25‰ in dolomites G02B and N03B, while n -alcohols $\text{C}_{12:0}$ to $\text{C}_{20:0}$ show $\delta^{13}\text{C}$ values between -28‰ and -31‰ (Table 2). The sterols β -sitosterol (G02B) and cholesterol (N03B) reveal $\delta^{13}\text{C}$ values of -27‰ and -24‰ , respectively. Due to low concentrations and co-elutions, $\delta^{13}\text{C}$ values of the alcohol fraction of sample S01 were not measured. Short chain n -fatty acids $\text{C}_{16:0}$ (-24‰) and $\text{C}_{17:0}$ (-25‰) of sample S01 reveal $\delta^{13}\text{C}$ values, which are slightly higher than $\delta^{13}\text{C}$ values of n -fatty acids

with chain length C₁₈ to C₃₄ (between −28‰ and −32‰) and of C₃₂ hopanoic acid (−28‰). The $\delta^{13}\text{C}$ value of the branched *i*-C_{17:0} fatty acid of sample S01 is −27‰. Due to low concentrations and co-elutions, $\delta^{13}\text{C}$ values of the fatty acid fractions of samples G02B and N03B were not measured.

TABLE 2 – Contents ($\mu\text{g g}^{-1}$ rock) and stable carbon isotopic compositions ($\delta^{13}\text{C}$ [‰]) of molecular biomarkers.

Compound	G02B		N03B		S01	
	concentration [$\mu\text{g g}^{-1}$]	$\delta^{13}\text{C}$ [‰]	concentration [$\mu\text{g g}^{-1}$]	$\delta^{13}\text{C}$ [‰]	concentration [$\mu\text{g g}^{-1}$]	$\delta^{13}\text{C}$ [‰]
<i>sn</i> -2-hydroxyarchaeol	0.02	−25	0.10	−25	nd	-
C _{12:0} <i>n</i> -alcohol	0.04	nq	0.06	nq	0.04	nq
C _{14:0} <i>n</i> -alcohol	0.04	nq	0.05	nq	0.02	nq
C _{16:0} <i>n</i> -alcohol	0.21	−28	0.24	−29	0.04	nq
C _{18:0} <i>n</i> -alcohol	0.19	−28	0.18	−29	0.04	nq
C _{16:0} <i>n</i> -fatty acid	2.73	nq	0.92	nq	0.15	−24
<i>i</i> -C _{17:0} <i>n</i> -fatty acid	nd	-	0.14	nq	0.08	−27
C _{18:0} <i>n</i> -fatty acid	2.67	nq	2.19	nq	0.24	−28
C _{22:0} <i>n</i> -fatty acid	nd	-	0.11	nq	0.27	−28
C _{24:0} <i>n</i> -fatty acid	nd	-	0.36	nq	1.01	−25

nd: not detected

nq: not determined, due to low concentrations or co-elution

DISCUSSION

Sulfate reduction and methanogenesis have been proposed to enable early dolomite formation in modern and ancient shallow marine settings (see in Mazzullo, 2000 and references therein). The broad range of $\delta^{13}\text{C}_{\text{dol}}$ values between −15‰ and +10‰ (Fig. 3) of the different dolomites obtained from the Monterey Formation indicates organogenic dolomite formation within the zone of sulfate reduction as well as in the methanogenic zone. The facies dependence of $\delta^{13}\text{C}_{\text{dol}}$ values is conspicuous. Dolomites, containing relicts of diatoms and no foraminifera from non-phosphatic sections (G02B, G02C, and G05; Figs. 2A–B) exhibit high $\delta^{13}\text{C}_{\text{dol}}$ values, while dolomite with low $\delta^{13}\text{C}_{\text{dol}}$ values from phosphatic sections contain abundant foraminifera and no diatoms (Figs. 2C–F). This result is in accordance with observations by Burns and Baker (1987) who also observed dolomites with higher $\delta^{13}\text{C}$ values in sections of the Monterey Formation, characterized by lower biogenic carbonate and higher detrital contents and a higher sedimentation rate. A higher content of detrital clay minerals in the Sisquoc Formation (Compton and Siever, 1984) may also explain the relatively high $\delta^{18}\text{O}_{\text{dol}}$ values (around +4‰) of sample G05, as clay dehydration produces an increase in pore water $\delta^{18}\text{O}$ values (Savin and Epstein, 1970). Low $\delta^{13}\text{C}_{\text{dol}}$ values were observed in sections

with higher original biogenic calcite, lower detrital mineral content and a lower sedimentation rate (Burns and Baker, 1987). Therefore, the sedimentation rate is suggested to be the controlling factor of determining the diagenetic zone of dolomite formation (c.f., Kelts and McKenzie, 1982).

The positive $\delta^{13}\text{C}_{\text{dol}}$ values of dolomites G02B and G02C from the Monterey Formation as well as of dolomite G05 from the Sisquoc Formation of the Mussel Rock section indicate their precipitation in the methanogenic zone as the process of methanogenesis results in ^{13}C -enriched bicarbonate in pore water (e.g., Mazzullo, 2000 and references therein). Unequivocal evidence for the importance of methanogenic archaea in dolomite formation is provided by the presence of the lipid biomarker *sn*-2-hydroxyarchaeol with a $\delta^{13}\text{C}$ value of -25‰ in these dolomites (Fig.4, Table 2). It has been shown that *sn*-2-hydroxyarchaeol is synthesized by methanogenic archaea belonging to the *Methanosarcinales* and *Methanococcales* order (Sprott et al., 1993; Koga et al., 1998). The discovery of ^{13}C enriched *sn*-2-hydroxyarchaeol in these dolomites is the first molecular evidence of archaeal participation in methanogenic dolomite formation. Ahmed et al. (2001) found biphytanyl dicarboxylic acids, which are attributed to planktonic archaea in organic-rich sediments of the Naples Beach section. However, the absence of these lipids in the dolomites excludes an input of planktonic archaea to the lipids, which are extracted from the dolomites.

The dolomites N03B and S01 formed in the zone of sulfate reduction (low $\delta^{13}\text{C}_{\text{dol}}$ values, Fig. 3). Here, bacterial sulfate reduction results in ^{12}C -enriched bicarbonate in pore water (e.g., Mazzullo, 2000 and references therein). The detection of *i*-C_{17:0} fatty acid, a lipid biomarker for sulfate-reducing bacteria (Kaneda, 1991; Londry et al., 2004), in organic extracts of the dolomites corroborate the activity of sulfate reducing bacteria during dolomite precipitation. Furthermore, Ahmed et al. (2001) identified the presence of sulfate-reducing bacteria in the sediments from the Naples Beach by means of the bacterial biomarkers *i*-C_{17:0} and 10MeC_{16:0} fatty acids. However, the detection of *sn*-2-hydroxyarchaeol with a $\delta^{13}\text{C}$ value of -25‰ , the molecular signal of methanogenic archaea, in dolomite N03B may indicate a deeper burial of the dolomites in the methanogenic zone during later diagenesis. It is also possible that the dolomite formation took place at the sulfate-methane interface, where microbial activity is very high, as has been shown for dolomites at the Peru shelf (Meister et al., 2007). Furthermore, the less depleted $\delta^{13}\text{C}_{\text{dol}}$ values of sample N01 (Fig. 3) suggest a formation during the transition of sulfate reduction to methanogenesis. However, also dolomite formation during early sulfate reduction prior to maximum ^{12}C enrichment in pore water also can explain intermediate $\delta^{13}\text{C}_{\text{dol}}$ values (Mazzullo, 2000).

CONCLUSIONS

Methanogenic archaea are involved in the formation of dolomites of the Miocene Monterey Formation. The discovery of the lipid biomarker *sn*-2-hydroxyarchaeol with a $\delta^{13}\text{C}$ value of -25‰ in these dolomites is the first molecular evidence of archaeal participation in methanogenic dolomite formation. For the first time, a molecular signal of methanogenesis could be traced in dolomites. Relatively high $\delta^{13}\text{C}_{\text{dol}}$ values corroborate the formation of these dolomites in the methanogenic zone. Furthermore, other dolomites with low $\delta^{13}\text{C}_{\text{dol}}$ values (-15‰) were formed in the zone of sulfate reduction. The lipid biomarker *i*-C_{17:0} fatty acid, which was extracted from these dolomites, provide the molecular evidence for the presence of sulfate-reducing bacteria during dolomite precipitation. The presence of *sn*-2-hydroxyarchaeol in dolomites with low $\delta^{13}\text{C}_{\text{dol}}$ values suggests their later burial in the methanogenic zone. However, not all analyzed dolomites can be attributed unequivocally to the zone of sulfate reduction or methanogenesis according to their stable carbon isotopic compositions. Dolomites with intermediate $\delta^{13}\text{C}_{\text{dol}}$ values formed presumably at the transition between sulfate reduction and methanogenesis.

ACKNOWLEDGEMENTS

We thank Sebastian Flotow for preparation of thin sections and Xavier Prieto Mollar for his support in the lab (both University of Bremen). Further thanks go to Monika Segl (University of Bremen) for stable carbon and oxygen isotope measurements. Financial support was provided by the “Deutsche Forschungsgemeinschaft” through the DFG-Excellence Cluster MARUM, Bremen.

REFERENCES

- AHMED, M., SCHOUTEN, S., BAAS, M., and DE LEEUW, J.W., 2001, Bound lipids in kerogen from the Monterey Formation, Naples Beach, California, *in* Isaacs, C.M., and Rullkötter, J., eds., The Monterey Formation - From Rocks to Molecules: Columbia University Press, New York, p. 189–205.
- BAKER, P., and ALLEN, M., 1990, Occurrence of dolomite in Neogene phosphatic sediments, *in* Burnett, W.C., and Riggs, S.R., eds., Phosphate Deposits of the World - Neogene to Modern Phosphorites, v. 3: Cambridge University Press, Cambridge, p. 75–86.

- BIRGEL, D., THIEL, V., HINRICHS, K.-U., ELVERT, M., CAMPBELL, K.A., REITNER J., FARMER, J.D., and PECKMANN, J., 2006, Lipid biomarker patterns of methane-seep microbialites from the Mesozoic convergent margin of California: *Organic Geochemistry*, v. 37, p. 1289–1302.
- BLAKE, M.C., CAMPBELL, R.H., DIBBLEE, T.W., HOWELL, D.G., NILSEN, T.H., NORMARK, W.R., VEDDER, J.C., and SILVER, E.A., 1978, Neogene basin formation in relation to plate tectonic evolution of San Andreas fault system: *American Association of Petroleum Geologists Bulletin*, v. 62, p. 344–372.
- BURNS, S.J., and BAKER, P.A., 1987, A geochemical study of dolomite in the Monterey Formation, California: *Journal of Sedimentary Petrology*, v. 57, p. 128–139.
- CLAYPOOL, C.E., and KAPLAN, I.R., 1974, The origin and distribution of methane in marine sediments, *in* Kaplan, I.R., ed., *Natural Gases in Marine Sediments*: Plenum Press, New York, p. 99–140.
- COMPTON, J., 1988, Sediment composition and precipitation of dolomite and pyrite in the Neogene Monterey and Sisquoc Formations, Santa Maria area, California, *in* Shukla, V., and Baker, P.A., eds., *Sedimentology and Geochemistry of Dolostones*: SEPM Special Publications, Tulsa, p. 53–64.
- COMPTON, J.S., and SIEVER, R., 1984, Stratigraphy and dolostone occurrence in the Miocene Monterey Formation, Santa Maria Basin area, California, *in* Garrison, R.E., Kastner, M., and Zenger, D.H., eds., *Dolomites of the Monterey Formation and Other Organic-Rich Units*: Pacific Section SEPM, Los Angeles, p. 141–153.
- CROUCH, J.K., 1979, Neogene tectonic evolution of the California continental borderland and western Transverse Ranges: *Geological Society of America Bulletin*, v. 90, p. 338–345.
- FILIPPELLI, G.M., DELANEY, M.L., GARRISON, R.E., OMARZAI, S.K., and BEHL, R.J., 1994, Phosphorus accumulation rates in a Miocene low-oxygen basin - the Monterey Formation (Pismo Basin), California: *Marine Geology*, v. 116, p. 419–430.
- FÖLLMI, K.B., BADERTSCHER, C., DE KAENEL, E., STILLE, P., JOHN, C.M., ADATTE, T., and STEINMANN, P., 2005, Phosphogenesis and organic-carbon preservation in the Miocene Monterey Formation at Naples Beach, California - The Monterey hypothesis revisited: *Geological Society of America Bulletin*, v. 117, p. 589–619.
- FRIEDMAN, I., and MURATA, K.J., 1979, Origin of dolomite in Miocene Monterey shale and related formations in the Temblor Range, California: *Geochimica et Cosmochimica Acta*, v. 43, p. 1357–1365.

- GARRISON, R.E., KASTNER, M., and KOLODNY, Y., 1987, Phosphorites and phosphatic rocks in the Monterey Formation and related Miocene units, coastal California, *in* Ingersoll, R.V., and Ernst, W.G., eds., *Cenozoic Basin Development of Coastal California*, Rubey, v. 6: Prentice Hall, Englewood Cliffs, p. 349–381.
- GARRISON, R.E., KASTNER, M., and REIMERS, C.E., 1990, Miocene phosphogenesis in California, *in* Burnett, W.C., and Riggs, S.R., eds., *Phosphate Deposits of the World: Neogene to Modern Phosphorites*: Cambridge University Press, Cambridge, p. 285–299.
- GRAHAM, S.A., 1987, Tectonic controls on petroleum occurrence in central California. *in* Ingersoll, R.V., and Ernst, W.G., eds., *Cenozoic Basin Development in Coastal California*, Rubey, v. 6: Prentice Hall, Englewood Cliffs, p. 47–63.
- HOWELL, D.G., CROUCH, J.K., GREENE, H.G., MCCULLOCH, D.S., and VEDDER, J.C., 1980, Basin development along the late Mesozoic and Cenozoic California margin: a plate tectonic margin of subduction, oblique subduction and transform tectonics, *in* Ballance, P.F., and Reading, H.G., eds., *Sedimentation in Oblique Slip Mobile Zones*: International Association of Sedimentologists, Los Angeles, p. 43–62.
- ISAACS, C.M., 1980, Diagenesis in the Monterey Formation examined laterally along the coast near Santa Barbara, California: Unpublished Ph.D. thesis, Stanford University, Stanford, 329 p.
- KABLANOW, R.I., SURDAM, R.C., and PREZBINDOWSKI, D., 1984, Origin of dolomites in the Monterey Formation: Pismo and Huasna Basins, California, *in* Garrison, R.E., Kastner, M., and Zenger, D.H., eds., *Dolomites of the Monterey Formation and Other Organic-Rich Units*: Pacific Section SEPM, Los Angeles, p. 103–114.
- KANEDA T., 1991, *Iso-* and *anteiso* fatty acids in bacteria - biosynthesis, function, and taxonomic significance: *Microbiological Reviews*, v. 55, p. 288–302.
- KASTNER, M., GARRISON, R.E., KOLLODNY, Y., REIMERS, C.E., and SHEMESH, A., 1990, Coupled changes of oxygen isotopes in PO_4^{3-} and CO_3^{2-} in apatite, with emphasis on the Monterey Formation, California, *in* Burnett, W.C., and Riggs, S.R., eds., *Phosphate Deposits of the World: Neogene to Modern Phosphorites*: Cambridge University Press, Cambridge, p. 312–324.
- KASTNER, M., MERZ, K., HOLLANDER, D., and GARRISON, R.E., 1984, The association of dolomite-phosphorite-chert: causes and possible diagenetic consequences, *in* Garrison, R.E., Kastner, M., and Zenger, D.H., eds., *Dolomites of the Monterey Formation and Other Organic-Rich Units*: Pacific Section SEPM, Los Angeles, p. 75–86.

- KELTS, K., and MCKENZIE, J.A., 1982, Diagenetic dolomite formation in Quaternary anoxic diatomaceous muds of Deep Sea Drilling Project Leg 64, *in* Curray, J.R., Moore, D.G., and cruise participants, eds., Initial Reports of the Deep Sea Drilling Project, v. 46: Government Printing Office, Washington, DC, p. 553–569.
- KOGA, Y., MORII, H., KAGAWA-MATSUSHITA, M., and OHGA, I., 1998, Correlation of polar lipid composition with 16S rRNA phylogeny in methanogens. Further analysis of lipid component parts: *Bioscience Biotechnology and Biochemistry*, v. 62, p. 230–236.
- KUSHNIR, J., and KASTNER, M., 1984, Two forms of dolomite occurrences in the Monterey Formation, California: concretions and layers - a comparative mineralogical, geochemical and isotopic study: *in* Garrison, R.E., Kastner, M., and Zenger, D.H., eds., Dolomites of the Monterey Formation and Other Organic-Rich Units: Pacific Section SEPM, Los Angeles, p. 171–184.
- LONDY, K.L., JAHNKE, L.L., and MARAIS, D.J.D., 2004, Stable carbon isotope ratios of lipid biomarkers of sulfate-reducing bacteria: *Applied and Environmental Microbiology*, v. 70, p. 745–751.
- MALONE, M.J., BAKER, P.A., and BURNS, S.J., 1994, Recrystallization of dolomite - evidence from the Monterey Formation (Miocene), California: *Sedimentology*, v. 41, p. 1223–1239.
- MAZZULLO, S.J., 2000, Organogenic dolomitization in peritidal to deep-sea sediments: *Journal of Sedimentary Research*, v. 70, p. 10–23.
- MEISTER, P., MCKENZIE, J.A., VASCONCELOS, C., BERNASCONI, S., FRANK, M., GUTJAHR, M., and SCHRAG, D.P., 2007, Dolomite formation in the dynamic deep biosphere: results from the Peru Margin: *Sedimentology*, v. 54, p. 1007–1031.
- MURATA, K.J., FRIEDMAN, I., and MADSEN, B.M., 1969, Isotopic composition of diagenetic carbonates in marine Miocene formations of California and Oregon: Geological Survey Professional Paper, v. 614, p. B1–B24.
- PISCIOOTTO, K.A., and GARRISON, R.E., 1981, Lithofacies and depositional environments of the Monterey Formation, California, *in* Garrison, R.E., and Douglas, R.G., eds., The Monterey Formation and Related Siliceous Rocks of California: Pacific Section SEPM, Los Angeles, p. 97–122.
- PISCIOOTTO, K.A., and MAHONEY, J.J., 1981, Isotopic survey of diagenetic carbonates, *in* Yeats, R.S., Haq, B.U., and cruise participants, eds., Initial Reports of the Deep Sea Drilling Project Leg 63: Government Printing Office, Washington, p. 595–609.

- SAVIN, S.M., and EPSTEIN, S., 1970, Oxygen and hydrogen isotope geochemistry of clay minerals: *Geochimica et Cosmochimica Acta*, v. 34, p. 25–42.
- SPROTT, G.D., DICAIRE, C.J., CHOQUET, C.G., PATEL, G.B., and EKIEL, I., 1993, Hydroxydiether lipid structures in *Methanosarcina* spp. and *Methanococcus voltae*: *Applied and Environmental Microbiology*, v. 59, p. 912–914.
- SUESS, E., and VON HUENE, R., 1988, Ocean Drilling Program Leg-112, Peru Continental Margin 2, sedimentary history and diagenesis in a coastal upwelling environment: *Geology*, v. 16, p. 939–943.
- WARREN J., 2000, Dolomite: occurrence, evolution, and economically important associations: *Earth-Science Reviews*, v. 25, p. 1–81.

CONCLUDING REMARKS AND PERSPECTIVES

Even though phosphorites have been intensively studied, most data on phosphorites are descriptive and data, which provide information on biogeochemical processes involved in phosphogenesis are uncommon. This thesis represents the first molecular biomarker study on phosphorites. It is the first approach that combines biochemical, geochemical, and geological methods and consequently provides insights into biogeochemical processes crucial for phosphorite formation. The data presented here resulted in a new and better understanding of biological processes that are important for phosphogenesis in upwelling areas.

The presented results reveal for the first time the extraordinary importance of sulfate-reducing bacteria in the formation of phosphorites in upwelling areas. sediments sulfate-reducing bacteria are critical for organic matter remineralization in recent phosphogenic sediments of upwelling regions, which are populated by large sulfide-oxidizing bacteria. This has been indicated by the dominance of molecular biomarkers for sulfate-reducing bacteria (mono-*O*-alkyl glycerol ethers (MAGEs), 10MeC_{16:0} fatty acid, and *ai*-C_{15:0} fatty acid). High abundances in the biomarker content of the sediments correlate with high concentrations in pore water phosphate. This suggests a connection between sulfate-reducing bacteria and phosphate enrichment in the sediments.

Sulfate-reducing bacteria are also definitely involved in the formation of authigenic phosphatic laminites from the upwelling region off Peru. Geochemical analyses of major, trace, and rare earth elements showed that the Peruvian phosphorites were formed under suboxic conditions in sediments near the sediment-water interface. They consist of a reworked and transported Miocene phosphooid facies and Pleistocene authigenic phosphatic laminites. These observations provide the basis for the following biochemical analyses because primary bacterial signals are only preserved in autochthonous formed phosphorites.

The molecular biomarker pattern of the laminite resembles the molecular biomarker patterns of recent phosphogenic sediments, with high contents of biomarkers attributed to sulfate-reducing bacteria, (short chain branched fatty acids, MAGEs, and DAGEs). However, these bacterial biomarkers are not only highly concentrated in the laminite, but also tightly bound to the mineral lattice. Furthermore, model calculations highlight that organic matter degradation by sulfate-reducing bacteria could have liberated sufficient amounts of phosphate to form the Peruvian phosphatic laminite. A significant role in the process of phosphogenesis may be also attributed to the interaction between sulfate-reducing bacteria and large sulfide-oxidizing bacteria like *Thioploca*, *Beggiatoa*, or *Thiomargarita*. Unfortunately, the supposed

role of sulfide-oxidizing bacteria in phosphogenesis (Schulz & Schulz, 2005) cannot be traced easily by lipid biomarkers, since the signatures of these organisms are rather unspecific (monounsaturated $n\text{-C}_{16}$ and $n\text{-C}_{18}$ fatty acids) and unstable. For this reason, other approaches are necessary to prove the involvement of these bacteria in the formation of ancient phosphorites.

In this thesis, an involvement of large sulfide-oxidizing bacteria in the formation of phosphorites off the coast of Peru has been identified by means of stable sulfur isotopes. $\delta^{34}\text{S}$ values of carbonate fluorapatite-bound sulfate are significantly lower than those of seawater sulfate, suggesting a bacterial reoxidation of sulfide by large sulfide-oxidizing bacteria. The successful detection of bacterial activity in phosphorites by means of stable sulfur isotope analyses provides a promising tool for future studies about the involvement of large sulfide-oxidizing bacteria in phosphogenesis. Additionally, the analyses of oxygen isotopes in phosphorites may give some further insights. During this thesis, single measurements of stable oxygen isotopes of sulfate bound to carbonate fluorapatite as well as of phosphate (kindly measured by Michael Joachimski, University of Erlangen) from the Peruvian phosphorites have been done. While the oxygen isotopes of phosphate do not differ from those of the apatite in shark teeth, which were found in the phosphorite crusts, the stable oxygen isotope values of carbonate fluorapatite-bound sulfate are lower than stable oxygen isotope values of sea water sulfate. This indicates a bacterial involvement in sulfate formation and consequently in carbonate fluorapatite precipitation. Although, these are only preliminary measurements, this approach is worthwhile to be developed and further expanded.

The utilization of molecular biomarkers for the identification of microbial processes involved in the formation of pristine phosphorites of the Miocene Monterey Formation proved to be problematic. These phosphorites do not display appropriate rocks to preserve molecular fossils because of their soft and porous texture. Furthermore, the flooding by sea water led to a strong weathering of these rocks. The investigation of dolomites from the Monterey Formation turned out to be more useful. In contrast to the pristine phosphorites of the Monterey Formation, the dolomites are appropriate for molecular biomarker analyses because they are hard, dense, and have a good preservation potential for the molecules. This study provides the first molecular proof that methanogenic archaea are involved in dolomite formation.

However, we are just at the beginning to understand the biological processes, which are important for the formation of authigenic phosphorites. This thesis focused on phosphorite

formation in recent as well as in ancient upwelling areas. It would be interesting to compare the results of this study with phosphorites from non-upwelling areas, like the phosphorites off the coast of Australia (*e.g.* O'Brien *et al.*, 1981; Cook & O'Brien, 1990) in order to see whether similar microbial signatures can be found or if these signals are unique to upwelling areas.

Lipid biomarkers show a good preservation potential in the hard and dense Peruvian phosphorites. Therefore, the lipid biomarker approach may be also tested on older phosphorites in the geological record, *e.g.* on Cretaceous phosphorites from Jordan (*e.g.* Pufahl *et al.*, 2003), on the Permian Phosphoria Formation (*e.g.* Sheldon, 1989), or even on Cambrian phosphorites (*e.g.* Shields *et al.*, 1999). However, a primary biomarker signal, reflecting bacterial activity during the time of carbonate fluorapatite precipitation will be only preserved in authigenic phosphorites that are not reworked. Therefore, other geochemical as well as petrographic studies should always accompany the biomarker analyses.

Old phosphorites from the Early Carboniferous of the “Rheinisches Schiefergebirge” in Germany were examined during this thesis in a side project in the Bachelor thesis of Matthias Gothieu. Phosphorite nodules within the organic-rich “Liegende Alaunschiefer” contain phosphatic stromatolites (Figure 1), which indicate a close association between microbes and phosphogenesis.

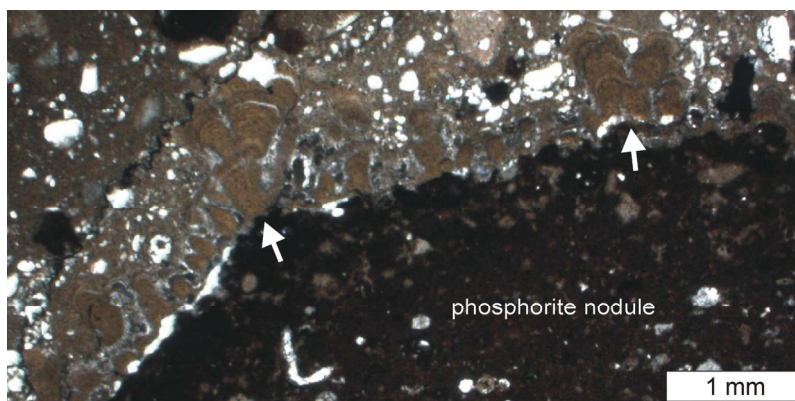


Figure 1 Phosphatic stromatolites (arrows) in phosphorites of the “Liegende Alaunschiefer” grow on an earlier formed phosphorite nodule; plane polarized light (courtesy of M. Gothieu).

The occurrence of phosphatic stromatolites has been observed by several other authors as well (*e.g.* Krajewski *et al.*, 1994; Martín-Algarra & Vera, 1994; Soudry & Panczer, 1994; Martín-Algarra & Sanchez-Navas, 1995; Bertrand-Sarfati *et al.*, 1997; Krajewski *et al.*, 2000; Lucas & Prevôt-Lucas, 2000; Schwennicke *et al.*, 2000; Chacón & Martín-Chivelet, 2008). However, so far a cause-effect relationship could not be deduced from the close association between phosphorites and preserved microbes. It would be interesting to compare molecular

biomarker patterns of stromatolitic phosphorites with non-stromatolitic ones of the same age. However, first measurements of lipid biomarkers in a phosphorite nodule from the “Liegende Alaunschiefer” did not reveal any results.

In summary, the results of this thesis reveal the huge potential of molecular biomarker analyses in combination with geochemical and petrographic methods as a tool to get deeper insights into microbial processes involved in phosphogenesis. With this thesis I was able to contribute significantly to a better understanding of the importance of bacteria in phosphorite formation. In particular, combined activities of closely associated sulfide-oxidizing bacteria and sulfate-reducing bacteria have the potential to drive phosphogenesis in marine sediments below high productivity zones.

REFERENCES

- Aller RC (1994) Bioturbation and remineralization of sedimentary organic matter - effects of redox oscillation. *Chemical Geology* **114**, 331-345.
- Bailey JV, Joye SB, Kalanetra KM, Flood BE., Corsetti FA (2007) Evidence of giant sulphur bacteria in Neoproterozoic phosphorites. *Nature* **445**, 198-201.
- Baturin GN (1982) *Phosphorites on the Sea Floor. Development in Sedimentology*. Elsevier, Amsterdam.
- Bentor YK (1980) Phosphorites - the unsolved problems. In *Marine Phosphorites-Geochemistry, Occurrence, Genesis* (ed. Bentor YK) Society of economic Paleontologists and Mineralogists, Tulsa, pp. 3-18.
- Berner EK, Berner RA (1996) *Global Environment*. Englewood Cliffs, Prentice Hall, New Jersey.
- Bertrand-Sarfati J, Flicoteaux R, Moussine-Pouchkine A, Ahmed AAK (1997) Lower Cambrian apatitic stromatolites and phospharenites related to the glacio-eustatic cratonic rebound (Sahara, Algeria). *Journal of Sedimentary Research* **67**, 957-974.
- Birch GF (1979) Phosphorite pellets and rock from the western continental margin and adjacent coastal terrace of South Africa. *Marine Geology* **33**, 91-116.
- Birch GF, Thomson J, McArthur JM, Burnett WC (1983) Pleistocene phosphorites off the west coast of South Africa. *Nature* **302**, 601-603.
- Brassel SC (1993) Application of biomarkers for delineating marine paleoclimatic fluctuations during the Pleistocene. In *Organic Geochemistry: Principles and Applications* (eds. Engel MH, Macko SA) Plenum Press, New York, pp. 699-738.
- Canfield DE (1994) Factors influencing organic carbon preservation in marine sediments. *Chemical Geology* **114**, 315-329.
- Canfield DE (2001) Biogeochemistry of sulfur isotopes. *Reviews in Mineralogy & Geochemistry* **43**, 607-636.
- Caraco NF, Cole JJ, Likens GE (1989) Evidence for sulfate-controlled phosphorus release from sediments of aquatic systems. *Nature* **341**, 316-318.
- Chacón B, Martín-Chivelet J (2008) Stratigraphy of Palaeocene phosphate pelagic stromatolites (Prebetic Zone, SE Spain). *Facies* **54**, 361-376.
- Colman AS, Holland HD (2000) The global diagenetic flux of phosphorous from marine sediments to the oceans: redox sensitivity and the control of atmospheric oxygen levels. In *Marine Authigenesis: from Global to Microbial* (eds. Glenn CR, Prevôt-Lucas L, Lucas J) SEPM, Tulsa, pp. 53-75.

- Compton J, Mallinson D, Glenn CR, Filippelli G, Föllmi K, Shields G, Zanin Y (2000) Variations in the global phosphorous cycle. In *Marine Authigenesis: from Global to Microbial* (eds. Glenn CR, Prevôt-Lucas L, Lucas J) SEPM, Tulsa, pp. 21-33.
- Cook PJ, McElhinny MW (1979) Re-evaluation of the spatial and temporal distribution of sedimentary phosphate deposits in the light of plate tectonics. *Economic Geology* **74**, 315-330.
- Cook PJ, O'Brien GW (1990) Neogene to Holocene phosphorites of Australia. In *Phosphate Deposits of the World: Neogene to Modern Phosphorites. Vol. 3* (eds. Burnett WC, Riggs SR) Cambridge University Press, Cambridge, pp. 98-115.
- Faul KL, Paytan A, Delaney ML (2005) Phosphorus distribution in sinking oceanic particulate matter. *Marine Chemistry* **97**, 307-333.
- Ferdelman TG, Fossing H, Neumann K, Schulz HD (1999) Sulfate reduction in surface sediments of the southeast Atlantic continental margin between 15 degrees 38'S and 27 degrees 57'S (Angola and Namibia). *Limnology and Oceanography* **44**, 650-661.
- Filippelli GM, Delaney ML (1996) Phosphorus geochemistry of equatorial Pacific sediments. *Geochimica et Cosmochimica Acta* **60**, 1479-1495.
- Föllmi KB, Garrison RE (1991) Phosphatic sediments, ordinary or extraordinary deposits? The example of the Miocene Monterey Formation (California). In *Controversies in Modern Geology: Evolution of Geological Theories in Sedimentology, Earth History and Tectonics* (eds. Müller DW, McKenzie JA, Weissert H) Academic Press, London, pp. 55-84.
- Föllmi KB (1996) The phosphorus cycle, phosphogenesis and marine phosphate-rich deposits. *Earth-Science Reviews* **40**, 55-124.
- Föllmi KB, Badertscher C, de Kaenel E, Stille P, John CM, Adatte T, Steinmann P (2005) Phosphogenesis and organic carbon preservation in the Miocene Monterey Formation at Naples Beach, California - the Monterey hypothesis revisited. *Geological Society of America Bulletin* **117**, 589-619.
- Froelich PN, Arthur MA, Burnett WC, Deakin M, Hensley V, Jahnke R, Kaul L, Kim KH, Roe K, Soutar A, Vathakanon C (1988) Early diagenesis of organic matter in Peru continental margin sediments - phosphorite precipitation. *Marine Geology* **80**, 309-343.
- Gächter R, Meyer JS, Mares A (1988) Contribution of bacteria to release and fixation of phosphorus in lake sediments. *Limnology and Oceanography* **33**, 1542-1558.
- Gallardo VA (1977) Large benthic microbial communities in sulfide biota under Peru-Chile subsurface countercurrent. *Nature* **268**, 331-332.

- Garrison RE, Kastner M (1990) Phosphatic sediments and rocks recovered from the Peru margin during ODP LEG 112. In *Proceedings of the Ocean Drilling Program, Scientific Results, Vol 112* (eds. Suess E, von Huene R, *et al.*) ODP, College Station, Texas, pp. 111-134.
- Glenn CR, Arthur MA (1988) Petrology and major element geochemistry of Peru margin phosphorites and associated diagenetic minerals - authigenesis in modern organic rich sediments. *Marine Geology* **80**, 231-267.
- Glenn CR, Föllmi KB, Riggs SR, Baturin GN, Grimm KA, Trappe J, Abed AM, Galli-Olivier C, Garrison RE, Ilyin AV, Jehl C, Rohrllich V, Sadaqah RMY, Schidlowski M, Sheldon RE, Siegmund H (1994) Phosphorus and phosphorites - sedimentology and environments of formation. *Eclogae Geologicae Helvetiae* **87**, 747-788.
- Hedges JI, Prahl FG (1993) Early diagenesis: consequences for application of molecular biomarkers. In *Organic Geochemistry: Principles and Applications* (eds. Engel MH, Macko SA) Plenum Press, New York, pp. 237-250.
- Hensen C, Zabel M, Schulz HN (2005) Benthic cycling of oxygen, nitrogen and phosphorus. In *Marine Geochemistry* (eds. Schulz HD, Zabel M). Springer, Berlin, Heidelberg, pp. 207-240.
- Jahnke RA, Emerson SR, Roe KK, Burnett WC (1983) The present-day formation of apatite in Mexican continental margin sediments. *Geochimica et Cosmochimica Acta* **47**, 259-266.
- Jahnke RA (1984) The synthesis and solubility of carbonate fluorapatite. *American Journal of Science* **284**, 58-78.
- Jarvis I, Burnett WC, Nathan Y, Almbaydin FSM, Attia AKM, Castro LN, Flicoteaux R, Hilmy ME, Husain V, Qutawnah AA, Serjani A, Zanin YN (1994) Phosphorite geochemistry: state-of-the-art and environmental concerns. *Eclogae Geologicae Helvetiae* **87**, 643-700.
- Jørgensen BB (1979) Theoretical model of the stable sulfur isotope distribution in marine sediments. *Geochimica et Cosmochimica Acta* **43**, 363-374.
- Jørgensen BB (1982) Mineralization of organic matter in the sea bed - the role of sulfate reduction. *Nature* **296**, 643-645.
- Jørgensen BB (2005) Bacteria and marine biogeochemistry. In *Marine Geochemistry* (eds. Schulz HD, Zabel M). Springer, Berlin, Heidelberg, pp. 169-206.
- Killops SD, Killops VJ (1993) *An Introduction to Organic Geochemistry*. Longman Scientific & Technical, Essex.

- Konhauser KO, Fyfe WS, Schultzelam S, Ferris FG, Beveridge TJ (1994) Iron phosphate precipitation by epilithic microbial biofilms in Arctic Canada. *Canadian Journal of Earth Sciences* **31**, 1320-1324.
- Krajewski KP, van Cappellen P, Trichet J, Kuhn O, Lucas J, Martín-Algarra A, Prevôt L, Tewari VC, Gaspar L, Knight RI, Lamboy M (1994) Biological processes and apatite formation in sedimentary environments. *Eclogae Geologicae Helvetiae* **87**, 701-745.
- Krajewski KP, Lesniak PM, Lacka B, Zawidzki P (2000) Origin of phosphatic stromatolites in the Upper Cretaceous condensed sequence of the Polish Jura Chain. *Sedimentary Geology* **136**, 89-112.
- Lucas J, Prevôt-Lucas L. (2000) Phosphorite and limestone, two independent end-member products of the range of bioproductivity in shallow marine environments. In *Marine Authigenesis: from Global to Microbial* (eds. Glenn CR, Prevôt-Lucas L, Lucas J) SEPM, Tulsa, pp. 117-125.
- Martín-Algarra A, Vera JA (1994) Mesozoic pelagic phosphate stromatolites from the Penibetic (Betic Cordillera, Southern Spain). In *Phanerozoic Stromatolites II* (eds. Bertrand-Sarfati J, Monty C) Kluwer Academic Publishers, pp. 345-391.
- Martín-Algarra A, Sánchez-Navas A (1995) Phosphate stromatolites from condensed cephalopod limestones, Upper Jurassic, Southern Spain. *Sedimentology* **42**, 893-919.
- McClellan GH (1980) Mineralogy of carbonate fluorapatites. *Journal of the Geological Society of London* **137**, 675-681.
- McClellan GH, van Kauwenbergh SJ (1990) Mineralogy of sedimentary apatites. In *Phosphorite Research and Development* (eds. Notholt AJG, Jarvis I) Geological Society Special Publications, London, pp. 23-31.
- Nathan Y (1984) The mineralogy and geochemistry of phosphorites. In *Phosphate Minerals* (eds. Nriagu JO, Moore PB) Springer, Berlin, Heidelberg, pp. 275-291.
- Nathan Y, Bremner JM, Lowenthal RE, Monteiro P (1993) Role of bacteria in phosphorite genesis. *Geomicrobiology Journal* **11**, 69-76.
- O'Brien GW, Harris JR, Milnes AR, Veeh HH (1981) Bacterial origin of East Australian continental margin phosphorites. *Nature* **294**, 442-444.
- Piper DZ (1994) Seawater as the source of minor elements in black shales, phosphorites and other sedimentary rocks. *Chemical Geology* **114**, 95-114.
- Pufahl PK, Grimm KA, Abed AM, Sadaqah RMY (2003) Upper Cretaceous (Campanian) phosphorites in Jordan: implications for the formation of a south tethyan phosphorite giant. *Sedimentary Geology* **161**, 175-205.

- Redfield AC (1958) The biological control of chemical factors in the environment. *American Scientist* **46**, 205-221.
- Reimers CE, Kastner M, Garrison RE (1990) The role of bacterial mats in phosphate mineralization with particular reference to the Monterey Formation. In *Phosphate Deposits of the World: Neogene to Modern Phosphorites* (eds. Burnett WC, Riggs SR) Cambridge University Press, Cambridge, pp. 300-311.
- Ruttenberg KC (1993) Reassessment of the oceanic residence time of phosphorus. *Chemical Geology* **107**, 405-409.
- Sandstrom MW (1986) Proterozoic and Cambrian phosphorites-specialist studies: geochemistry and organic matter in Middle Cambrian phosphorites from the Georgina Basin, Northern Australia. In *Phosphate Deposits of the World. Vol. 1. Proterozoic and Cambrian Phosphorites* (eds. Cook PJ, Shergold JH) Cambridge University Press, Cambridge, pp. 268-279.
- Sandstrom MW (1990) Organic matter in modern marine phosphatic sediments from the Peruvian continental margin. In *Phosphorite Deposits of the World. Vol. 3. Neogene to Modern Phosphorites* (eds. Burnett WC, Riggs SR) Cambridge University Press, Cambridge, pp. 33-45.
- Schulz HN, Jørgensen BB (2001) Big bacteria. *Annual Review of Microbiology* **55**, 105-137.
- Schulz HN, Schulz HD (2005) Large sulfur bacteria and the formation of phosphorite. *Science* **307**, 416-418.
- Schwennicke T, Siegmund H, Jehl C (2000) Marine phosphogenesis in shallow water environments: Cambrian, Tertiary, and Recent examples. In *Marine Authigenesis: from Global to Microbial* (eds. Glenn CR, Prevôt-Lucas L, J. Lucas J) SEPM, Tulsa, pp. 481-498.
- Sheldon RP (1981) Ancient marine phosphorites. *Annual Review of Earth and Planetary Sciences* **9**, 251-284.
- Sheldon RE (1989) Phosphorite deposits of the Phosphoria Formation, Western United States. In *Phosphate Deposits of the World. Phosphate Rock Resources, Vol. 2* (eds. Notholt AJG, Sheldon RE, Davidson DF) Cambridge University Press, Cambridge, pp. 53-61.
- Shields GA, Strauss H, Howe SS, Siegmund H (1999) Sulphur isotope compositions of sedimentary phosphorites from the basal Cambrian of China: implications for Neoproterozoic-Cambrian biogeochemical cycling. *Journal of the Geological Society* **156**, 943-955.

- Soudry D, Panczer G (1994) Stromatolitic phosphorites in the Eocene of the Negev (Southern Israel). In *Phanerozoic Stromatolites II* (eds. Bertrand-Sarfati J, Monty C) Kluwer Academic Publishers, Dordrecht, pp. 255-276.
- Soudry D (2000) Microbial phosphate sediment. In *Microbial Sediments* (eds. Riding RE, Awramik SM) Springer, Berlin, Heidelberg, pp. 127-136.
- Thamdrup B, Canfield DE (1996) Pathways of carbon oxidation in continental margin sediments off central Chile. *Limnology and Oceanography* **41**, 1629-1650.
- Trappe J (1998) *Phanerozoic phosphorite depositional systems - a dynamic model for a sedimentary resource system*. Springer, Berlin, Heidelberg.
- van Cappellen P, Berner RA (1988) A mathematical model for the early diagenesis of phosphorus and fluorine in marine sediments - apatite precipitation. *American Journal of Science* **288**, 289-333.
- van Cappellen P, Berner RA (1991) Fluorapatite crystal growth from modified seawater solutions. *Geochimica et Cosmochimica Acta* **55**, 1219-1234.
- Williams LA, Reimers C (1983) Role of bacterial mats in oxygen-deficient marine basins and coastal upwelling regimes - preliminary report. *Geology* **11**, 267-269.

DANKSAGUNG

In den letzten drei Jahren wurde ich von vielen großartigen, interessierten und hilfsbereiten Menschen unterstützt, ohne die diese Arbeit nicht zustande gekommen wäre und nur halb so viel Spaß gemacht hätte. Daher ist es schwer in einer solchen Danksagung alles in angemessene Worte zu fassen. Trotzdem will ich es hiermit versuchen:

Von ganzem Herzen danke ich:

- Prof. Dr. Jörn Peckmann für die hervorragende wissenschaftliche Betreuung der Arbeit, vor allem aber für die stetige Unterstützung, sein Vertrauen und die tolle Art die Arbeitsgruppe zu leiten, was nicht selbstverständlich ist. Dadurch konnte ich in den drei Jahren mit viel Freude eine Menge lernen.
- Prof. Dr. Heide Schulz-Vogt für die hervorragende Zusammenarbeit auf der „bakteriellen“ Seite des Projekts sowie für die Übernahme des Zweitgutachtens.
- Prof. Dr. Bo Barker Jørgensen für eine tolle „*Thioploca*-Expedition“ nach Chile, für viele hilfreiche Diskussionen und Anregungen die mich wissenschaftlich sehr voran gebracht haben.
- Prof. Kai-Uwe Hinrichs für wertvolle Kommentare und Anregungen aber besonders auch dafür, dass ich auch in der AG Geochemie stets willkommen war.
- der Deutschen Forschungsgemeinschaft für die Finanzierung meiner Arbeit im Rahmen des DFG-Excellence Cluster “MARUM – Marine Umweltwissenschaften”.
- Dr. Daniel Birgel für Anregungen, Unterstützung und Ideen aber besonders dafür, dass ich jederzeit mit Fragen und Problemen zu ihm kommen konnte Und er als mein „Co-Betreuer“ ein Engagement an den Tag gelegt hat, das außergewöhnlich ist.
- Dr. Markus Elvert der hilfreich bei technischen und wissenschaftlichen Problemen eingesprungen ist.
- Dr. Andreas Lückge und Prof. Dr. Hermann Kudrass und der BGR in Hannover für das hervorragende Probenmaterial sowie für die Durchführung von Analysen.
- Dr. Benjamin Brunner und Dr. Nikolaus Gussone für ihr großes Engagement bei diversen Isotopenmessungen.

- Prof. Dr. Karl Föllmi für tiefe Einblicke in die Phosphoritbildung und anregende Diskussionen, aber besonders für eine spannende und einzigartige Exkursion zu der „Monterey Formation“ in Kalifornien.
- allen Teilnehmern der „*Thioploca*-Expedition“ nach Chile für sehr interessante, erfahrungsreiche und schöne Wochen, wissenschaftlich sowie auch menschlich und kulturell.
- Xavier Prieto-Mollar, Sebastian Flotow und Birgit Schmincke ohne deren technische und administrative Unterstützung diese Arbeit gar nicht möglich gewesen wäre.
- Alyssa Larson, Suraiya Laloo und Matthias Gothieu die mit ihren Forschungs- und Laborarbeiten zum Gelingen dieser Arbeit beigetragen haben
- Simone Ziegenbalg, Benjamin Eickmann, Antonie Haas, Lars Hoffmann, Tobias Himmeler und Florian Brinkmann für diverse gemütliche und kommunikative Frühstücksrunden und viele andere fachliche und nicht-fachliche Unternehmungen.
- Stefanie Tille und Frauke Schmidt, die immer für mich da waren, und mit denen ich bei gemeinsamen Cocktailrunden entspannen konnte. Besonders danke ich auch Steffi für ihren Einsatz beim Korrekturlesen meiner Arbeit.
- allen Mitgliedern der AG Geochemie und auch noch mal allen Kollegen aus der Geobiologie für die tolle, freundschaftliche Arbeitsatmosphäre, dass ich nie alleine Mittagessen gehen oder Kaffee trinken musste und die vielen gemeinschaftlichen Unternehmungen.
- allen meinen Freunden, die immer für mich da sind und die somit wesentlich, wenn auch vielleicht unbewusst, zum Gelingen dieser Arbeit beigetragen haben, besonders Kirsten und ihr Lex und den „Volleyballern“ mit denen ich auf andere Gedanken kommen konnte.
- meinen Eltern Hannelore und Friedhelm sowie meinen Geschwistern Katrin und Jürgen die mich immer unterstützt und mir den nötigen Rückhalt, nicht nur bei dieser Arbeit sondern auch bei vielem mehr, gegeben haben.
- Malte für seine Liebe.

